Time-reversal Symmetry Breaking and Fragile Magnetic Superconductors

Warren E. Pickett[1]

[1] *Department of Physics and Astronomy, University of California Davis, Davis CA 95616*

(Dated: April 5, 2024)

Roughly a dozen reports of time-reversal-symmetry breaking (TRSB) states in superconducting (SC), otherwise conventional, Fermi liquid materials have been supported by muon spin relaxation (μSR) data. The detected fields inferred from the current interpretation of depolarization data, around 10^{-5}T = 0.1-1 G, correspond to magnetizations of the order of 10^{-3} μ_B/atom and lie near the limit of resolution of the experiment. [Note: for $B{\sim}1$ G, $\mu_B B{\sim}8{\times}10^{-8}$ eV.] These materials comprise a new class of *fragile moment superconductors*. The measured SC state parameters (excepting only μSR spontaneous fields) are representative of low T_c singlet BCS SCs, whereas proposed triplet phases possess highly unusual coherence lengths and critical fields, and strong sensitivity to disorder, properties that have not been observed. While construction of plausible order parameters has been a priority, possible origins of the magnetic fields have received little attention at the atomic level, being based on inert spins in a near-ideal crystal. While it is recognized that the muon does affect the sample by displacing somewhat nearby atoms, the measurement process, changing the system from sample $\rightarrow$ sample + μ^+, has not received full scrutiny. This report provides a survey of the environment of the muon from (say) 1 pm distance from the muon, where the dipolar magnetic field magnitude is of the order of 10^4T, to around 100 nm, typically the scale of the penetration depth. A progression of points can be stated. Deposition of the polarized muon, coupled to the solid by its vector potential, breaks TRS already in the normal state. Its magnetic field polarizes electron spins, whose vector potentials in turn impose a magnetic field at the muon site, *i.e.* a self-created magnetic field. Determination of the magnitude of this material-dependent field will be challenging, as it depends on some combination of (i) muon site asymmetry, (ii) quantum uncertainty of the muon position, (iii) non-linear susceptibility, and (iv) electron parallel-spin pair correlation near the muon site. Superconductivity introduces qualitative changes beyond the energy gap: (a) a quantum of magnetic flux with corresponding vortex centered on the muon, (b) associated toroidal supercurrents striving to shield the bulk of the superconductor from the muon's magnetic field, by creating an opposing magnetic field within the vortex with some non-zero value at the muon's site, and (c) bound Yu-Shiba-Rusinov states in the SC energy gap that may provide coupling of the muon to the order parameter, in addition to the muon-vortex coupling. Supposing that the μSR inference of a small field within the bulk of the SC obtains, broader scenarios than the current one of non-unitary triplet pairing are constructed. The unusual topological superconductor $LaNiGa_2$ is used as a case study, first for a BCS singlet phase, then for an exotic TRSB phase, with scenarios for the order parameter ranging from (i) possible singlet pairing with an anisotropic orbital pair state to (ii) triplet pairing based on valley symmetry breaking specific to the non-symmorphic crystal symmetry of $LaNiGa_2$.

CONTENTS

I. Introduction 3
- A. Roles of Symmetries 3
- B. Experimental constraints 3
- C. Previous overviews 4
- D. Purpose of this discussion 4

II. Organization of the paper 5

III. The muon dipolar magnetic field 6
- A. Charge effects, broadly 6
- B. Spin effects: magnetic polarization of the metal 7
- C. Orbital currents, fields, and polarization 7

IV. Normal state: crystal + μ^+ 7
- A. The induced spin polarization 7
- B. The induced magnetic field 7

V. Quantum effects near the muon 8
- A. Region of vanishing susceptibility 8
- B. Electronic pair correlation 9
- C. Summary of quantum effects 9

VI. Anisotropy 9
- A. Spatial anisotropy 9
- B. Magnetocrystalline anisotropy 9

VII. A case study: $LaNiGa_2$ 10
- A. Material parameters of $LaNiGa_2$ 10
- B. Non-symmorphic symmetry of $LaNiGa_2$ 10

VIII. Summary: normal state 11
- A. Magnetic polarization around the muon 11
- B. Experimental considerations relating to SC 11
  - 1. Origin of the magnetic field 11
  - 2. Magnitude of the induced field 12

IX. Superconducting state: a magnetic moment in a superconductor 12
- A. Reported instances of time reversal symmetry breaking at T_c 12

B. Organization of the following sections 12

X. Supercurrent, its field, and flux quantization 13
A. Supercurrent 13
B. Field at the muon site 14
C. Flux quantization 15

XI. Kondo physics; YSR states 15
A. Magnetic moment coupled to pairing 15
1. Kondo singlet versus Cooper singlet 16
2. Yu-Shiba-Rusinov states 17
3. μYSR states 17

XII. Implications for the pairing symmetry 17
A. Spin singlet scenarios 18
1. Ubiquitous electron-phonon coupling 18
2. Spin singlet pairing more generally 18
3. A degeneracy-inspired singlet order parameter 19
B. Spin triplet pairing 19
1. Challenges to triplet pairing 19
2. The INT model 20
C. Orbital magnetism scenario 20
D. FFLO possibility. 21

XIII. Discussion and Summary of the Paper 21
A. Normal state 21
B. Superconducting state 22
C. Compilation of loose ends 22

XIV. Appendices 23
A. The fundamental Hamiltonian 23
1. Electrons and a muon in a static lattice 23
2. The muon magnetic operator 24
B. Distance, moment, and magnetic field scales 25
C. The μSR experiment 25
1. The setup 25
2. The data and analysis 26
3. Experimental data of interest; $LaNiGa_2$ example 27
D. Symmetry of the dipolar field 27
E. Field at μ^+ site due to magnetic polarization 28
F. The small-r region in more detail 28
G. Induced magnetization; resulting B field 28
H. Operator representation for induced B-field 28
I. Quantum fluctuation of the muon 29
J. Pair correlation 29
K. μ^+ coupling to conduction electrons 30
L. Kondo impurity in an exotic superconductor 31
M. YSR states in real materials 31
N. $LaNiGa_2$ material parameters, energy scales 31
O. The triplet order parameter 32
1. Nonunitarity more generally 33
P. The order parameter for $LaNiGa_2$ 33
1. Basics of pairing 33
2. Electronic structure, Dirac points in $LaNiGa_2$ 33
3. Properties of $LaNiGa_2$ 34
4. Constructing an exotic order parameter 35
5. The INT model for the $LaNiGa_2$ order parameter 35
Q. Spin and magnetic aspects of pairing 36
1. Singlet spin scenario 36
2. Triplet spin scenario 36
3. Orbital moment scenario 36
R. Energetics relating to the superconducting state 37
S. Options for a mechanism for TRSB 37
1. Coulomb interaction: charge or spin 37
2. Orbital polarization 37

References 38

I. INTRODUCTION

A recent manuscript on *nanostructured superconductivity*[1] giving an overview of the various ways in which the superconducting state can be distorted when the bulk condensate is impeded by structural disruptions, begins with the sentence "the relevant length scales for superconductivity are of the order of nanometers." This statement is appropriate for the emphasis of that paper. Practically all of the theoretical characteristic description and the experimental interpretation of SC properties have been, and still are, done at the Ginzburg-Landau level of the coherence length ξ (several nanometers) and the penetration depth (usually hundreds of nanometers).

From another perspective, one observes that the materials-level theory of the SC gap Δ and critical temperature T_c is formulated at the atomic (sub-nm, Å) level and is accurate to any realistic expectation[2] for these properties for conventional bulk superconductors. While the study of unconventional superconductors has progressed considerably on the basis of symmetry requirements satisfying both theoretical constraints and experimental data, there are sub-nm electronic processes that need clarification for pairing and condensate formation, along with symmetry considerations.

A. Roles of Symmetries

Exotic superconductivity (SC), broadly characterized by symmetry-breaking order parameter(s) (OPs) beyond $U(1)$ symmetry breaking, *i.e.* beyond a spin-singlet, crystal-symmetric order parameter), has been attracting avid interest in solids for some decades.[3] There are an assortment of normal state symmetries that are available to be broken[4] along with unitary (particle conserving) $U(1)$ symmetry, its breaking giving Cooper pairing of electrons that disappear into the superconducting condensate, as long as the symmetries can be coupled. Symmetries include point group symmetry of the Brillouin zone and of the energy gap $\Delta(T)$ (viz. *s*-like, *d*-like, etc.), singlet spin pairing, spin rotation symmetry, atomic orbital/electron band indifference, translational symmetry, and perhaps more intricate types. [5–14]

One of the more elusive forms is that of time reversal symmetry breaking (TRSB) which, while alarming in name, is actually the simple appearance of a magnetic field and a magnetic component of the OP in an otherwise non-magnetic material, which breaks spin rotation symmetry. Several standard Fermi liquid type metals display spontaneous magnetic fields of 0.1-1 G, based on μSR depolarization data; a list is provided in Sec. **??**. The example of $LaNiGa_2$ will be given special attention in this article. This *superconductivity hosting fragile magnetism* raises many questions, several of which are addressed here, including some that are not discussed in the literature.

One issue is 'what broken symmetries?', based on the observation of broken TRS.[4] In the normal state the full symmetry group is $U(1)\otimes\mathcal{G}\otimes\mathcal{S}\otimes\mathcal{T}$ in terms of the space group $\mathcal{G}$ (comprised of translation and point group, giving equivalence of atoms on a given sublattice; often inversion is considered separately) spin rotation symmetry $\mathcal{S}$ (or its orbital magnetization analog), and time reversal $\mathcal{T}$. At T_c, pairing breaks $U(1)$ symmetry, *i.e.* two electrons form a bound pair and disappear into the condensate. If the magnetization causing a spontaneous field is spin in origin, $\mathcal{S}$ is broken. If it is orbital (currents) in nature, then crystal symmetry $\mathcal{G}$ of the electronic system is broken, such as two or more symmetry-related atoms or unit cells becoming inequivalent. Either breaks time reversal symmetry $\mathcal{T}$.

If the material involves transition metal atoms (especially in ionic materials), or $4f$ or $5f$ atoms, the appearance of some sort of magnetic order is not so unexpected, and there are various examples, viz. in heavy fermion superconductors.[15] There are numerous examples of proposed breaking of the space group symmetry, viz. *d*-wave character of the order parameter in some cuprates, and others for more enigmatic (viz. uranium) compounds.

B. Experimental constraints

In conventional *s-p* metals (standard non-magnetic Fermi liquids), however, spin polarization (TRS breaking) leading to an internal magnetic field, costs energy which occurs without obvious compensating gain in energy, and it is less clear how to recover that energy cost from violation of singlet pairing to parallel spin (triplet) pairing, which is commonly assumed to provide the magnetic signal as reported from several μSR (muon spin resonance, rotation, or relaxation) experiments.

An example that will be addressed in this paper is $LaNiGa_2$, which has recently been synthesized and characterized in single crystal form[16–21] with a space group ($Cmcm$) distinct from that reported on powder samples four decades earlier ($Cmmm$).[30] The electronic structures in these two space groups are similar, viz. the Ni $3d$ bands are filled in both. However, the multisheeted Fermi surfaces are different, and the differing space groups lead to an essential distinction. μSR experiments have detected spin relaxation characteristic of a small ($\sim$0.2 G) magnetic field[31] at the position of the muon, with onset at the superconducting transition at T_c=2 K: evident TRSB coupled to Cooper pairing. This magnitude of field is near to the stated detection limit of 10^{-5} T and corresponds to a a magnetic moment of no more than 10^{-2} μ_B/atom. A plausible resolution is that other superconductors also experience a spontaneous field but it is below the detectable limit, leading to misidentification as conventional BCS superconductors.

Full consideration of the properties of $LaNiGa_2$ point to a conventional singlet pairing, weak coupling Type II SC, so much of the published description and the language in this paper will rely on such an implication. On the other hand, the reported spontaneous field appearing

below T_c have led theorists to conclude it to be another example of the small class of probable superexotic SCs, being unique due to requiring TRSB hence triplet pairing, with an additional broken symmetry such as two orbital or two band character[32] to host the additional degree of freedom that encounters an additional hurdle: hosting a nonunitary spectrum of quasiparticles,[33] – all of this in spite of being quite typical normal state Fermi liquid metals. So far, the two topological diabolical Dirac points (DPs) pinned to the Fermi surface of $LaNiGa_2$[17,18] even when spin-orbit coupling (SOC) is included has not been included as a part of the picture. Regarding the latter, density functional theory (DFT) calculations for the *Cmcm* structure[17,18] revealed an extended planar zone boundary degeneracy (before including SOC) not previously encountered in TRSB materials. The pair of degenerate points provide a distinct platform for broken symmetry, as discussed toward the end of this article.

C. Previous overviews

A pedagogical and handbook-style monograph on muon spin rotation spectroscopy in solids was published by Schenck[22] in 1985, discussing several areas including the technique and applications in muons in metals. This introduction has been followed by a number of books, lecture notes, and reports on μSR spectroscopy.[23–29] The μSR experiment and analysis has been described by several authors associated with one of the present five muon facilities. Representatives include a description by Blundell[26], contrasting the pictures of the muon as a heavy position or alternatively as a light proton, a contemporary view of μSR theory and data on selected materials by Hillier *et al.*,[36], and a broad discussion provided in a recent monograph (an Introduction, for serious readers) by Blundell and co-authors.[29] For recent techniques, Blundell and Lancaster provided a description of 'DFT+μ' method for finding muon stopping position(s) in a crystal.[37] More on the package and an easy-to-use interface 'MuFinder' for the researcher is described by Huddart *et al.*[38] Calculation of the muon anharmonicity and zero point positional uncertainty for solid N_2 has been described by, for example, Gomilsek *et al.*[39]

After a few discoveries of heavy fermion compounds, Heffner reviewed in 1992 μSR studies of this class of quantum materials, with emphasis on uranium superconductors.[15] This class of highly unconventional materials, discovered in the early 1980s, have strongly renormalized properties in the normal state and are not the topic of this article. An extensive review of μSR data and theory was provided by Balatsky, Vekhter, and Zhu in 2006.[34]

Reviews on exotic order parameters moore generally are relevant to pasts of this paper. In 1991 Sigrist and Ueda[6] provided a review of the theory of unconventional superconductivity, extending from the generalization of BCS theory[35] to symmetry classification and its relation to Ginzburg-Landau theory, to symmetry-breaking including the non-unitary possibility for triplet superconductors, to crystal symmetry lowering effects (structural transformations, consequences of surfaces and interfaces, and more. Sigrist has provided following reviews in 1999 on broken time-reversal symmetry,[147], on unconventional SCs,[10] and on an extension specifically aimed at noncentrosymmetric SCs,[11]. Wysokinski provided in 2019 an overview[13] of time-reversal symmetry breaking with focus on Sr_2RuO_4.

An overview on the interplay between inhomogeneities and SC order parameters, especially TRSB ones, by Anderson, Kreisel, and Hirschfeld, addresses topics of relevance to μSR experiments.[40] They provide a brief but informative description of the zero field experiment that has provided evidence of TRSB SC phases in several otherwise conventional intermetallic compounds. Among the situations they discuss is that defects in a TRSB SC can produce local magnetic fields from spin disruption and from orbital currents. This article will provide some discussion of effects of magnetic impurities, viz. the muon, in a superconductor.

D. Purpose of this discussion

Electron pairing and related symmetries are fundamental to the formalism of the superconducting state and its excitations. OP character is intimately tied to the symmetry of the Cooper pair of fermions: the exchange of electron coordinates must lead to a π phase change. Surveying the symmetries in the μSR studies referenced above, one can notice that TRSB is observed in (i) cubic, tetragonal, octahedral, and hexagonal point groups, (ii) in centrosymmetric, or not, materials, (iii) in symmorphic, or non-symmorphic, crystal systems. A viable presumption could be to suppose there is some universal nature of, or proclivity toward, TRSB at T_c, with certain attribute(s) that determines whether it happens, or not. Since there are no identifiable similarities or distinctions in the group of *fragile magnetic superconductors*, allowable OP symmetries have been pursued case by case by theorists.

In this paper the focus is on surveying a more complete picture of the multiscale behavior (sub-atomic to coherence length $\xi(T)$) of the SC+μ^+ system, identifying properties that may either complicate analysis or contribute to a microscopic mechanism for coupling of an emergent magnetic moment to the pairing OP. It has been understood, and established by DFT studies,[42] that the μ^+ ion density disturbs the sample locally. Coming to rest at a favorable interstitial position away from positive atomic cores, its H-atom-like electron density causes, analogously to the proton, a relaxation of neighboring atoms by up to a few tenths of an Angstrom (nearly 0.6 Åin an ionic insulator).[38,43] The current understanding is that this charge disturbance, without any magnetic character, will not influence conclusions about TRS.[42]

An overview by Ghosh *et al.* mentions some of the microscopic complications of interest here.[44] These aspects arise from the realization that the muon is a significant

local perturbation of the sample beyond charge effects. These authors mention that (i) the inferred magnetization depends on the choice of presumed pairing symmetry, (ii) the field at the muon site in the SC state includes the possibility of a muon self-induced field, and (iii) the strong local perturbation changes the local crystal structure, the electronic structure, local symmetry, and induced magnetization. These features, yet to be understood, form some of the primary points of this article.

Late in this paper alternative possibilities to the present picture of this class of *fragile magnetic superconductors* are suggested. The present picture is that of a TRSB order parameter based on the detection of a magnetic depolarization onset below T_c characteristic of a (perpendicular component of) magnetic field of 0.1-1 G, just above the limit of detection. The other viewpoint – not specifically stated before, but indicating there is some other explanation for this signal – is based on (1) recognition that deposition of the polarized muon into the sample already breaks TRS of the coupled system, (2) the environment of the muon is already magnetically active in the normal state, (3) the superconducting properties such as coherence lengths, critical fields, etc. are characteristic of many low T_c BCS SCs whereas triplet SCs are likely to display quite different properties, and (4) one member of this class of fragile magnetic SCs, $LaNiGa_2$, has been found by Ghimire *et al.*[21] to be insensitive to disorder induced by electron irradiation, whereas triplet SCs are predicted to be highly sensitive to, even quickly destroyed by, disorder. The objective here is to review, and perhaps extend somewhat, the general behavior of a conventional metal with an implanted polarized muon, in both the normal and SC states.

II. ORGANIZATION OF THE PAPER

What has not been addressed in much detail is the effect of the μ^+ magnetic moment of the muon+sample system that enters through its vector potential, the kinetic aspect of a magnetic moment. Its free-space magnetic intensity $\vec{H}^{\mu}(\vec{r})$ is that of a point dipole, with distance dependence $1/r^3$ and the textbook angular dependence shown in Fig. 1. It will induce spin polarization as commonly treated in other contexts, as well as orbital currents of Fermi surface electrons that may give orbital-generated magnetic polarization. After some background information on the muon in Sec. III, magnetic field complications are introduced in Sec. IV. Subsection III A specifically addresses aspects of a model homogeneous electron gas+μ^+ (HEG+μ) system in the normal state, discovering complexities, including anomalies in the theory (a divergent integral in first approximation) that obviate precise quantification of the behavior in the vicinity of the muon.

Near-muon quantum effects – positional uncertainty, non-linear susceptibility, electron pair correlation – in Sec. V are shown to regularize the theory, but leave the big question as a highly numerical (and not yet well posed) challenge due to the r^{-3} increase of the field near the muon. Another essential aspect – anisotropy (versus the isotropic HEG) – that is material specific, is treated in Sec. VI. The unique case of the topological superconductor[46] $LaNiGa_2$ is the topic of Sec. VII, after which Sec. VIII provides a summary of the main points regarding the turbulent normal state.

Passing into the SC state is the topic of Sec. IX, with the strong magnetism-superconductivity conflict providing a complex picture of the system in the SC state. Detailed behavior is challenging to quantify because the length scale associated with the largest impact of the muon (say, the Bohr radius a_B, within which behavior becomes nonlinear) is much smaller than the length scale of the SC OP. The supercurrent as described by Ginzburg-Landau theory has a minimum scale of variation of the coherence length $\xi(T)$, with field variation on the scale of the (larger, in Type II SCs) London penetration depth $\lambda_L(T)$. (Type I SCs have these length scales in the opposite order.)

The possibility of Kondo screening of the muon moment is addressed in Sec. XI. For an isolated muon such screening might be extremely challenging to detect. However, study of a magnetic impurity in a SC initially by Yu, Shiba, and Rusinov and more recently using density functional methods in specific superconductors reveal that bound states within the SC gap form upon entering the SC state, and their character may provide clues to the coupling of the muon moment to the SC order parameter.

Specific aspects of pairing follow. Issues concerning pairing symmetry form the focus of Sec. XII, where possible OPs are contrasted with the current model (for $LaNiGa_2$). Sec. XIV S gives an overview of pairing mechanisms ("pairing glue") without finding any more likely candidate than the conventional, practically universal in such materials, phonon-exchange process of pair binding.

Section XIV S provides an overview on the implications of this paper to the underlying issues: the mechanism (the "glue") and the order parameter. The former centers on singlet versus triplet pairing. The latter gives an overview of much discussed but incompletely understood processes involving spin fluctuations or orbital polarization versus the conventional lattice polarization (phonons) in promoting the SC state, in possible TRSB materials. Any of these is difficult to prove or to definitely rule out, it is just a matter of deciding what picture accounts best for the available data.

Consideration of energetics of a few kinds[18] has not turned up any likely candidates for the mechanism behind the transition, viz. the SC condensation energy gain from superconductivity is much less than the cost of producing even a tiny magnetic polarization.[18] Having left several details to the plethora of Appendices A-S, a discussion and final summary is given in Sec. XIII.

III. THE MUON DIPOLAR MAGNETIC FIELD

Little attention has been given to the effect on the normal state of the magnetic moment of the muon (here denoted $\vec{\mu}$), whose dipolar magnetic field[47] extends to interatomic distances, polarizing the electron gas in its neighborhood as it diverges approaching the site of the muon. The characterization of Jackson[48] was
"Usually the books are a little vague about the nature of these intrinsic magnetic moments, letting the word 'intrinsic' imply that it is beyond the realms of present knowledge or none of your business, or both."
He went on in his CERN document to describe the theoretical description of intrinsic magnetic dipole moments, consistent with experimental data from elementary particle studies. The conclusion is included below.

The conventional dipole vector potential and magnetic intensity for an isolated muon is (some expressions following will incorporate $\vec{\mu} = \mu(0,0,1)$ defining the z-direction)

$$\begin{aligned}\vec{A}^{\mu}(\vec{r}) = &= \nabla \times \frac{\vec{\mu}}{r} = \frac{\vec{\mu}\times\hat{r}}{r^2} = \frac{\mu}{r^3}(-y,x,0)\\ \vec{H}^{\mu}_{tot}(\vec{r}) &= \nabla\times\vec{A}^{\mu}(\vec{r}) = \frac{3\hat{r}(\hat{r}\cdot\vec{\mu})-\vec{\mu}}{r^3} + \frac{8\pi}{3}\mu\delta(\vec{r})\\ &= \vec{H}^{\mu}_{dip} + \vec{H}^{\mu}_{con} \qquad (1)\end{aligned}$$

with dipole and contact terms. This form has amplitude μ/r^{-3} times an angular term of order unity; $\vec{A}\sim\mu/r^{-2}$. The field lines are pictured in Fig. 1 and more about its algebraic form and symmetry elements are provided in Appendix XIV D. Since only non-magnetic metals are discussed here, the choice of H versus B will be primarily conventional, except when both are used in a single equation with a distinction to be made.

It can readily be shown, and is intuitively clear, that in the midst of a electronic system, the contact will give rise to an interaction term

$$H^{\mu-el} = -\mu\cdot[\frac{8\pi}{3}\vec{m}(0)] \qquad (2)$$

in terms of the electronic magnetization density $m(\vec{r})$. Involving only an infinitesimal amount of electron density, this contact term will not affect the electronic density and induced magnetic field so it will be put aside for later consideration, and we drop the superscript *dip* and *tot* on $\vec{B}$. This contact term does enter proton NMR spectroscopy, which is not possible for isolated and short lifetime muons.

The factor $8\pi/3$ can be found, confusingly, in some literature to be replaced by $-4\pi/3$. Jackson has described[48] how the correct $8\pi/3$ factor for the muon (and any elementary particle now known) is consistent with experimental information that concludes that the point magnetic moment must be considered as the limit of a tiny circulating current. A $-4\pi/3$ factor instead arises if the dipole results from the limit of a bound pair of north-south monopoles (as could conceivably occur in an elementary particle, but apparently does not).

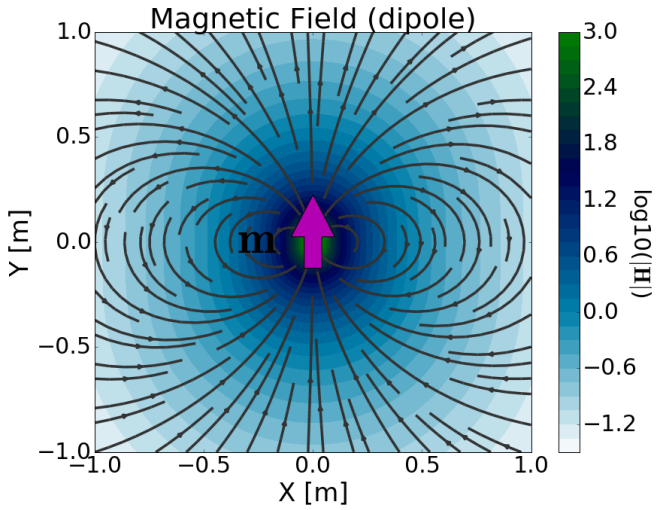

FIG. 1. Plot of constant magnetic field lines of a point dipole oriented in the $\hat{y}$ direction of this plot, plotted in the x-z plane; distances along the axes are in arbitrary units relative to the magnitude of the point dipole at the origin. The lines with arrows indicate the direction of the field at that point. The blue shading indicates lines of constant $|\vec{B}|$ field, which is an angular modulation of $1/r^3$ falloff.

The polarization of the electron density will in turn produce an additional magnetic field in the region arising from the dipolar vector potentials of the partially aligned electrons; see Sec. IV and Appendix. XIV E.

A. Charge effects, broadly

The immediate local environment of the muon is that of a positive charge in a slowly varying electron gas, where it attracts one unit charge of electron density to its vicinity. A first approximation is that of the constant electron density (jellium) plus the attracted density of the μ^+ effective $1s$ orbital, centered at the muon's site and spherically symmetric, is given approximately by $n(r)$=n_o+$n^{\mu}_{1s}(r)$, where n_o is the value of the uniform jellium density and n_{1s} is an effective $1s$ orbital density of the μ^+ attracted from the conduction electron reservoir. Neutrality apart from decaying Friedel oscillations will be achieved within a few times the Thomas-Fermi screening length. At interstitial densities of densely packed intermetallic compounds characteristic of most SCs, hybridization of the $1s$ orbital with itinerant metallic states will ensure that the muon "atomic density" will not be spin polarized due to electron gas exchange effects. (Some DFT studies indicate muon bound states below the bottom of the conduction band,[42] in which case single occupation and hence magnetic polarization effects might arise.) The self-consistent density will be somewhat more spread out than the atomic $1s$ density due to mixing with the itinerant planewave states.

Within a crystal, this effect is not as simple as for the proton, because the minima of the muon's potential in

the solid must account for the quantum uncertainty of the spatial position of the light mass muon, which expands the region over which the simple Hartree potential is sampled. This effect is structure- and material-dependent. The region of interest will first be considered to be a spherically symmetric system responding to the axial muon magnetic. At this level this discussion is identical to that of a proton in a HEG,[49] except that the proton's nuclear magnetic moment (traditionally neglected in defect studies) is smaller by a factor of nine and its local density and potential (and perhaps the muon's equilibrium site) has been modified by quantum corrections.

B. Spin effects: magnetic polarization of the metal

The dipole magnetic field intensity, from Appendix XIV D describing its origin in the vector potential and its symmetry properties, is

$$\vec{H}^{\mu}(\vec{r}) = \frac{3\hat{r}(\hat{r}\cdot\vec{\mu})-\vec{\mu}}{r^3} = \frac{3\mu}{r^3}(\frac{xz}{r^2},\frac{yz}{r^3},\frac{z^2}{r^2}-\frac{1}{3}), \quad (3)$$

arising from the muon's magnetization $\vec{M}^{\mu}(\vec{r}) = \vec{\mu}\delta(\vec{r})$. The contact term $(8\pi/3)\vec{\mu}\delta(\vec{r})$ affects only an infinitesimal a good description until high fields introduce nonlinear magnetization. Here $N(E)$ is the electron density of states per unit volume, and the Pauli spin susceptibility χ_{sp} has the symmetry of the density. The Stoner enhancement $S(n)$, typically between from 1.3 to below 2,[50] should not affect the physics for interstitial densities of metallic Fermi liquid compounds.

C. Orbital currents, fields, and polarization

The muon-induced electron currents will produce an orbital susceptibility χ_{orb}. For the HEG and a uniform magnetic field the value of this (Landau diamagnetic) susceptibility is $\chi_{orb} = -(1/3)\chi_{sp}$. In much of the following discussion a net paramagnetic susceptibility $\chi_p = \chi_{sp} + \chi_{orb}$ will be accounted for, with nonlinear effects and current contributions discussed separately. In normal density Fermi liquid metals χ_p is of the order of $10^{-3} - 10^{-4}$. This small polarization is relevant because the observed spontaneous field reported in these metals is extremely small.

For the muon's strongly non-uniform near-field, the orbital effect will be that given by Maxwell's equations, adapted for transport on periodic Fermi surfaces and subject to quantum conditions. Initially upon muon deposition, Maxwell's equation involves a displacement ($\vec{D}$) current and electric current $\vec{J}$ as

$$\nabla\times\vec{H}^{\mu} = \frac{4\pi}{c}\vec{J}^{\mu} + \frac{1}{c}\frac{\partial\vec{D}}{\partial t}$$

The displacement current term results as the system rapidly (on an electronic time scale) thermalizes to steady state, where the time derivative vanishes and the normal state electrical resistivity (not included in this equation) will damp the current density to a steady state zero value. Thus there will be no current contributions to a magnetic field in the normal state at low T. Thermally excited electrons will continue to experience the force $-e\vec{v}_k\times\vec{B}$, giving some circulating current around the muon which contribute to Hall effect-like physics. The change occurring in the SC state is addressed in Sec. X.

IV. NORMAL STATE: CRYSTAL + μ^+

A. The induced spin polarization

After deposition of the muon, the HEG+μ^+ system is a coupled system in which *TRS is broken by the muon magnetic field,* before lowering the temperature into the SC state. Why then is it that TRSB, *i.e.* a field at the μ^+ site, is not detected?

Away from the extremely strong (diverging but short range) field region near the muon, the induced magnetization at position $\vec{r}$ can be expressed as

$$\vec{M}^{ind}(\vec{r}) = \mu_B[n_{\uparrow}(\vec{r}) - n_{\downarrow}(\vec{r})] \rightarrow \chi_p(n(r))\vec{B}^{\mu}(\vec{r}). \quad (4)$$

where the last line is the textbook linear response of a metal, and is often realistic to multi-tesla-scale fields. [Recall that $\mu_B B$ at one tesla is 0.7 K in temperature units.] In this HEG approximation, which is formalized by density functional theory,[50,51] $\vec{M}^{ind}$ is parallel to $\vec{B}^{\mu}$ at each point, hence it and the entire system satisfies the same cylindrical and reflection symmetries given for $\vec{B}^{\mu}$ in Appendix XIV D. The induced field at the muon $\vec{B}^{ind}(0)$ will, by symmetry, align with the muon moment. It will then not provide any torque on the muon moment, hence be undetectable by depolarization studies. Discussion of the fact that the muon lies as a low symmetry position is discussed later.

B. The induced magnetic field

Each electron carries a magnetic moment of one μ_B, thus each volume element of induced magnetization $\vec{M}^{ind}(\vec{r})\Delta V$ will produce the same form of magnetic field intensity from the incremental moment $\vec{M}^{ind}\Delta V$ as given by the dipole expression in Appendix X B Eq. (43), except that the initial origin $\vec{0}$ will be assumed by $\vec{r}$ (the position of ΔV) and the position of a given field point will be $\vec{r'}$. Some details are presented in Appendix X B

The net result of the polarization is the magnetic flux density

$$\vec{B}(\vec{r}) = \vec{H}^{\mu}(\vec{r}) + 4\pi\vec{M}^{ind}(\vec{r}) = \vec{H}^{\mu}(\vec{r}) + 4\pi\chi_p\vec{H}^{\mu}(\vec{r}) = [1+4\pi\chi_p(\vec{r})]\vec{H}^{\mu}(\vec{r}), \quad (5)$$

The result is a textbook-like result, reminding again that this local linear response enhancement is good except within a very small volume surrounding the muon, to be addressed later. The polarization response is comparatively small, however, the muon does not experience its own field, and small magnetic fields are the topic of this paper.

The field seen by the muon will not include its own field H^{μ}, and that is the field of interest just now. Integrating the incremental moment over all space, the field intensity created by $\vec{M}^{ind}(\vec{r}')$ will be

$$\vec{H}^{ind}(\vec{r'}) = \int d^3r \frac{3\hat{R}[\vec{M}^{ind}(\vec{r}) \cdot \hat{R}] - \vec{M}^{ind}(\vec{R})}{|R|^3}. \quad (6)$$

where $\vec{R} \equiv \vec{r'} - \vec{r}$. Simplification occurs because we are only interested in the field at the muon site, *i.e.* at $\vec{r'} \to 0$, so $\hat{\vec{R}} \to -\hat{r}$, and that the source is a point (the muon). Renaming the integration variable to $\vec{r}$, substituting M^{ind} from Eq. (4), and simplifying as shown in Appendix XIV G, leads to the field at the muon site (in spherical coordinates r, θ, ϕ; $\nu = \cos\phi$)

$$H^{ind}(0) = 2\pi\mu \int_0^{\infty} \chi_p(n(r)) \frac{r^2 dr}{r^6} \int_{-1}^{1} d\nu (3\nu^2 + 1). \quad (7)$$

The angular integral gives a factor of two. The integrand, with r^{-3} factors entering twice, is badly infrared divergent as written. Incorporating an *ad hoc* cutoff from a muon effective radius would regularize the integral, but would leave a result sensitive to the choice of cutoff. Corrections inside this cutoff due to the finite muon radius and relativistic extensions of the theory are negligible for small Z point charges.[52] The following Sec. V will replace the *ad hoc* radius with additional processes from a non-linear susceptibility and a quantum many-body viewpoint that alleviate this divergence.

V. QUANTUM EFFECTS NEAR THE MUON

The infrared divergence of the integral for $H_z^{ind}(0)$ (Eq. 7) is daunting and obviously unphysical. Additional factors must be entering the physics. Three quantum factors serve to regularize point motion, contains information on how a confined quantum particle samples a region around the classical position. In its ground state the muon will sample a region around the minimum of the Coulomb potential, the minimum being the classical ground state position. For an ideal harmonic oscillator the shape of the region of the ground state wavefunction would be an (in orthorhombic symmetry, distorted) ellipsoid. This uncertainty is sometimes important for interstitial protons, and the effect will be larger for a muon with its order of magnitude smaller mass. With a lower symmetry environment the shape of the potential well will be less regular in shape,[42] and may even involve a quantum oscillation between two classically-preferred sites.[38]

Until recently, this QPU of the muon position had not become a mainstay of μSR analysis. Finding the classical muon position has been made more efficient, with a user-friendly platform, since the advent of the μSR analysis application MuFinder.[38] With only the underlying crystal structure as input, the algorithm chooses likely sites for the muon, calculates the energy of the system including relaxation (structural and electronic) of nearby atoms, and iterates to the minimum energy structure. The results can be used in the analysis of μSR data, especially for nuclear magnetic fields and for magnetic solids. QPU of the muon has now been realized as important for the interpretation of some specific μSR data.

The factor of 207 difference in muon and electron masses allows one to invoke the adiabatic approximation: for each point $\vec{R}$ within the muon ground state normalized wavefunction $\Psi(\vec{R})$, the electron density $n(\vec{r};\vec{R})$ and polarization (magnetization) $m(\vec{r};\vec{R})$ can be evaluated, and from it the magnetic intensity $H^{ind}(\vec{r};\vec{R})$. The physical magnetic intensity then is the expectation value:

$$\bar{H}^{ind}(\vec{r}) = \int d^3R \Psi(\vec{R})^* H^{ind}(\vec{r};\vec{R}) \Psi(\vec{R}). \quad (8)$$

Here $\vec{r}$ is measured from the classical muon position $\vec{R}_o$. This field is then evaluated at the muon minimum energy position. The precise description becomes involved, but because the muon will sample regions where the integrand is not divergent, the divergence at $\vec{r} = \vec{R}_o$ will be somewhat ameliorated. The effect will be to introduce into the integral something like an $r^2\ dr$ factor in the integrand that reduces the divergence by two powers of r. A more rigorous formulation of the phenomenon would be required for any numerical evaluation.

A. Region of vanishing susceptibility

The diverging magnetic field at the muon site will completely spin polarize the nearby conduction electrons along the lines of its dipolar field, modulo quantum restrictions. Specifically, inside some small radius the fractional spin polarization will become ± 1, with sign determined by the sign of the magnetic field at that point, and will vary rapidly from +1 to -1 with azimuthal angle When the polarization

$$P(\vec{r}) = \frac{n_{\uparrow}(\vec{r}) - n_{\downarrow}(\vec{r})}{n_{\uparrow}(\vec{r}) + n_{\downarrow}(\vec{r})} \quad (9)$$

approaches ± 1, any additional longitudinal field will produce no extra polarization. Specifically,

$$\chi_p(n(r)) \to \chi_p(n(r), m(r)) \to \chi(n(r), \pm 1) \quad (10)$$

and the fully polarized region $m \to \pm 1$ no longer can be further polarized, *i.e.* the longitudinal magnetic susceptibility goes to zero as some (probably even) power of the distance r from the muon site. This saturation of the polarization, hence vanishing of the susceptibility, will result in a reduction of the divergence, by (most probably) another factor of r^{-2}.

B. Electronic pair correlation

From variational[49,53,54] and quantum[55] Monte Carlo calculations on correlated wave functions (Gutzwiller-Slater determinants) at full polarization, the probability of parallel spin electrons (all electrons in this limit) being at the same point vanishes (Pauli repulsion). The pair correlation function in three dimensions increases from zero quadratically; a many-body treatment of the system thus further reduces the divergence of the integral by canceling a factor of r^{-2}, producing a convergent result. The magnitude seems not to be amenable to any simple estimate, as the various factors can vary considerably from material to material.

C. Summary of quantum effects

The conclusion from divergent Eq. 7 and recognition that these three quantum corrections renders it finite is that there is a self-field from magnetic polarization that is non-zero at the muon site. In the isotropic HEG model, the field aligns with the muon moment, leaving no perpendicular component to propel dynamics. Due to the low symmetry of the muon's environment, this field will no longer align with the muon's moment, with the deviation depending on the degree of anisotropy. There is no clear evidence from μSR of such a field in the normal state, which might be simply taken to be a part the background depolarization (90-97% of the signal in the SC state) that is ascribed to fields from randomly oriented nuclear and electron moments. (Given the 100% polarization of the muon moment, experiments on single crystals might reveal such an orientation-dependent depolarization.) This $-\mu \cdot \vec{B}^{ind}(0)$ interaction also provides a spin flip excitation, requiring energy of the order of $2\mu[B_z^{ind}(0) + B_z^{spon}(0)]$. For order of magnitude, this amounts to roughly 1 μeV for the ($LaNiGa_2$) 0.2 G field inferred from μSR. The rather involved theory of depolarization in a thermodynamic background is referenced in Sec. **??**. Such a small rotation energy should make the muon susceptible to thermalization at 1 K (k_BT $\sim$0.1 meV).

VI. ANISOTROPY

A. Spatial anisotropy

The detected spontaneous magnetic field (10% or less above the background) is near detection limits, making nominally second order effects of possible importance. In some cases the signal onset is identified as $\sim$20% below T_c, suggesting a transition within the SC state but possibly reflecting the weak signal. The muon sits in an interstitial site between a handful of atoms, at a local minimum in the Coulomb potential. In most of the preceding discussion we have taken the vicinity of the muon, before considering magnetic fields and crystallinity, as isotropic. This is a simplification, as the actual symmetry experienced by the muon will be low[38,43] with additional consequences. Moreover, DFT studies have established that the quantum zero-point uncertainty of the muon's position can be substantially larger[38,42,43] than that of a proton, where large anharmonicity and quantum uncertainty have been reported to be important in the muon's choice of site. Thus the quantum muon samples a region which has next to zero spatial symmetry, with near 100% likelihood.

The conclusion is that the net magnetic field of the muon will no longer have the symmetry of the point dipole. This result is relevant because the value of the inferred spontaneous magnetic field is small, quite close to the stated sensitivity of around 10^{-5} T for current μSR technology. This anisotropy field is present upon entering the SC state. Induced spin polarization or orbital currents will respond to the anisotropy, producing a field at the muon site that may become amenable to DFT studies.[56] The region is not limited by any symmetry, hence the field at the muon is almost certainly non-zero.

It may be premature to speculate further. What seems clear is that it is essential for quantitative studies to (i) determine the site, and symmetry if any, of the muon, (ii) calculate the quantum uncertainty of the muon position, then (iii) determine the resulting field at the muon given this uncertainty. Intuitively the field would be some smeared version of the standard DFT result, however intuition about such quantum effects can be incorrect,[57] and quantum corrections or perhaps formulations should be applied when necessary. This point along with several others raised here are left for further study.

B. Magnetocrystalline anisotropy

The spontaneous (presumed) uniform magnetic field $\vec{B}(0)$ extending at the muon site has been interpreted as the signature of a triplet OP. Verified triplet pairing in Fermi liquid metals is lacking, although promising candidates have been suggested. Neglecting for now the separate issue of how the supercurrent in a triplet SC copes with an intrinsic field, the spontaneous magnetization giving rise to the $\vec{B}$ field is a vector field and will have an easy axis, requiring energy to rotate it to another direction. This should be a clearer property in an orthorhombic structure such as that of $LaNiGa_2$ than in a cubic crystal, where symmetry limits effects of anisotropy.

Poling a "ferromagnetic superconductor" (aligning the magnetic domains) may be a new adventure in μSR studies for experimentalists, as there are no moments except in the SC state. One approach would be to reduce the applied field from above $H_{c2}(T)$ below T_c, a common procedure. Differences in magnetization for fields along each of the axes of a single crystal might reveal the magnetic anisotropy, and if so, provide clues into the microscopic origin: spin imbalance, orbital currents, or some more involved type of TRSB.

VII. A CASE STUDY: $LANIGA_2$

A. Material parameters of $LaNiGa_2$

The fully gapped superconducting state of $LaNiGa_2$, with critical fields $H_{c2}(0)$=0.27, 0.09, 0.24 T for uniform applied fields along the three crystal axes (Appendix XIV N), typical of singlet SCs, must accommodate the 'external' magnetic field from the muon via superconducting magnetic shielding currents, analogous to the simpler case of the Meissner effect at a surface. $LaNiGa_2$ is Type II,[17] – anisotropic Abrikosov indices κ=3.38,28.9,4.00 along the three crystal axes – like several other orthorhombic SCs. A straightforward accommodation in a singlet pairing system would occur by threading one flux quantum vortex centered on the muon at z=0, with supercurrents adjusting as necessary to provide screening of the bulk SC from the magnetic field within the vortex.

For the reported spontaneous field (at T=0) of 2×10^{-5}T for $LaNiGa_2$, the radius of a unit vortex is 10μm (see Appendix XIV B). The vortex would be pinched (narrow) at z=0 near the muon due to its relatively larger magnetic field will compress the flux density. A macroscopically large vortex area will occur at large $|z|$ where there is only the tiny emergent field to confine the flux quantum Φ_o. In simple sample geometry, the toroidal field lines would exit the sample at large $|z|$, wrap around the sample with miniscule flux density, and re-enter the vortex at the bottom of the sample to maintain continuous field lines.

Standard Meissner expulsion of magnetic fields applies to singlet pairing, where a magnetic field is pair-breaking, hence reducing T_c consistent with observation. The materials parameters of $LaNiGa_2$ seem to be in line with singlet pairing, with the exception of indications from μSR. In a triplet SC, a magnetic field will likely (i) tend to rotate any spontaneous SC magnetization into the applied field direction, thereby (ii) increasing $|\uparrow\uparrow>$ pairing versus $|\downarrow\downarrow>$ pairing, engendering a susceptibility process not available with singlet pairing, and (iii) also creating polarized supercurrents. Each of these effects may depend on the type of OP.[58] To quantify the energy cost of converting spin-down pairs to spin-up pairs would require a specific Hamiltonian. Studies of the properties of triplet phases are in early stages. One option is that coherence lengths can become unpredictable and the upper critical field can become arbitrarily large, which seem far from observations.

B. Non-symmorphic symmetry of $LaNiGa_2$

There are now ten or more superconducting Fermi liquid metals identified as displaying spontaneous magnetic fields, thus labeled as requiring TRSB OPs,[6] supported so far only by μSR data. We look more specifically at the case of the topological superconductor $LaNiGa_2$.

Recent studies of single crystals of $LaNiGa_2$ revealed[16–18] its space group to be $Cmcm$, with a non-symmorphic crystal symmetry, versus the 1982 assignment of symmorphic $Cmmm$ space group based on powder xray data.[30] The structural similarity and differences are pictured in Fig. 2. The non-symmorphic space group operation results in a double degeneracy (beyond spin symmetry) across an entire face of the Brillouin zone, a well known non-symmorphic symmetry consequence, but a full planar degeneracy is an unusual occurrence in an exotic SC, justifying characterization as an exotic topological superconductor.

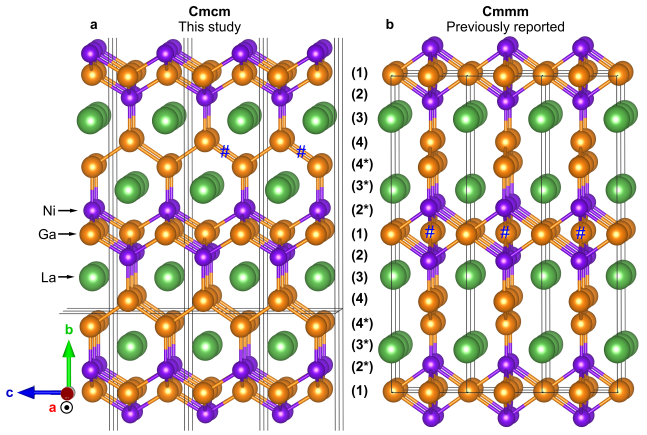

FIG. 2. (a) The structure of $LaNiGa_2$ from Badger *et al.*, determined from single crystal XRD. (b) The structure obtained in 1982 by Yarmolyuk and Grin[30] from powder XRD. The difference lies in (i) the Ni-Ga layer in the center (and top and bottom) layer of this plot, with Ni repositioning, and (ii) repositioning of Ga between the La layers, together resulting in a non-symmorphic operation and the $Cmcm$ space group.

Upon including spin-orbit coupling (SOC), this planar degeneracy is lifted throughout the zone *except along a single symmetry line* (the Z-T line).[17,18] Any pair of bands cutting the Fermi energy along this line has a Dirac point degeneracy in the normal state at that point, *on the Fermi surface, independent of doping, i.e.* independent of the position of E_F. It is highly unusual – almost an improbability – to have *diabolical points that remain pinned* to the Fermi surface as it varies due to external influences, doping, etc., remaining on the Fermi surface as long as the structural symmetry is retained. This symmetry-related pair of points has four-fold degeneracy and the topological character of anisotropic 3D Dirac points. The Fermi surfaces, symmetry point labelings, and Z-T line are shown in Fig. 3.

This degeneracy is only lifted finally by the opening of the SC gap.[17] Assuming a triplet OP, the bands that are involved open with two bandgaps, given by the expression (see Sec. XIV O, Eq. (65) for the BdG quasiparticle bands. This pair of bands, finally split only by pairing, form a basis for the discussion of a two-band system, however there is no extended two-band near-degeneracy. ["Two-orbital" language is also used, but two different but special, symmetry-related atomic orbitals are problematic to separate from the s-p orbitals

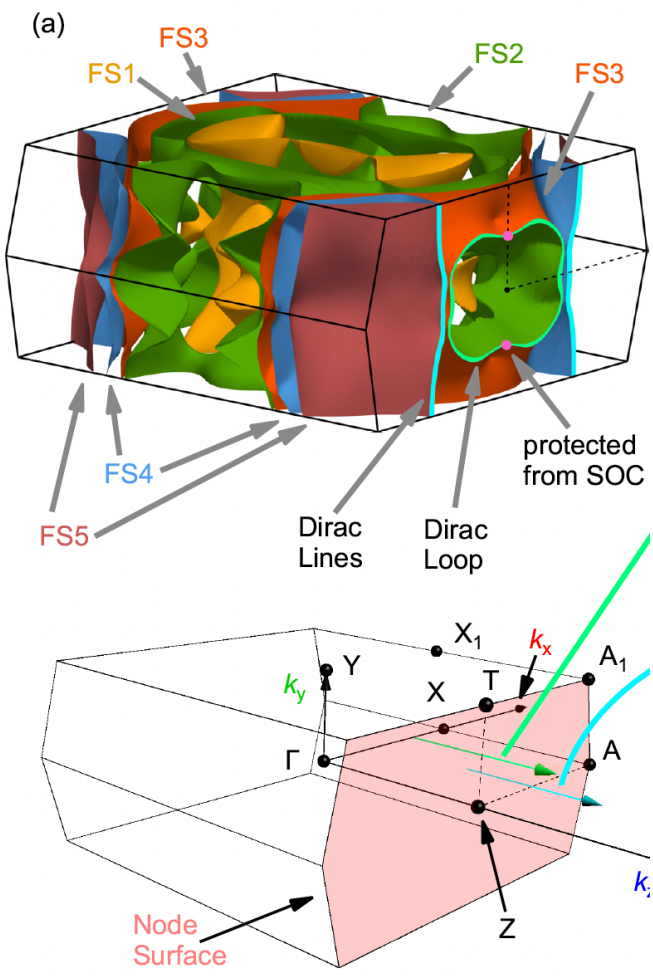

FIG. 3. Top panel: the five Fermi surfaces of *Cmcm* $LaNiGa_2$, illustrating the degeneracies on the node surface (the pink plane in the lower panel). The green and red Fermi surfaces (FS2 and FS3) merge together on the light green loop, while the blue and brown Fermi surfaces (FS4 and FS5) merge on the vertical blue line. The red dots pinpoint where the loop of degeneracies cross the *Z*-*T* lines, leading to 3D Dirac point character at those dots. Bottom panel: symmetry labels of *Cmcm* Brillouin zone, with the node surface shown in pink.

of La, Ni, Ga1, Ga2. (Point group symmetry guarantees in general degeneracy of atomic orbitals around each sublattice.) Ghosh *et al.* proposed Hund's coupling in the Ni 3*d* orbitals to account for triplet pairing,[33] but the density of states $N(E)$ indicates that the Ni *d* bands are rather narrow and fully occupied, lying in the -3 eV to -1.5 eV range and contributing only mildly at E_F through mixing with Ga *s*-*p* orbitals.

VIII. SUMMARY: NORMAL STATE

A. Magnetic polarization around the muon

In the initial HEG picture, the induced $\vec{B}$-field description is fixed to the direction of the muon's spin and is strongly local. Being aligned with the muon moment, the induced field produces no torque on the muon's magnetic moment. The pinning of the electronic (spin+orbital, in principle) magnetization to the μ^+ spin direction leads to a slightly renormalized value of the total moment μ^{eff} in the vicinity of the muon, a change that might be detectable in an appropriate spectroscopic study. The magnitude of this renormalization of the local moment is implicit in the formalism in this section, but has not been estimated quantitatively.

Anisotropy of the muon site and the electron density will engender a self-induced magnetic field that is not pinned to the direction of the muon moment, thus providing a mechanism for muon polarization decay. The first-pass (classical) expression is infrared divergent, and will be regularized by a radius cutoff within which quantum and high magnetic fields will replace the divergent integral. This may simply to the background depolarization that is not quantified or particularly relevant in a ZF experiment.

B. Experimental considerations relating to SC

The focus falls on a few central items. The TRSB magnetic field (following sections), whose origin may be the muon itself, has been the main subject of the preceding section. Now the theoretical foundations can give way to experimental aspects of the sample+muon system.

1. *Origin of the magnetic field*

The scale of measured values (typically a few tenths of gauss, see the listing in Sec. IX A), unusually small and near the limit of detection of a spontaneous field, has been noted in several reports. In $LaNiGa_2$ this measured value corresponds to a moment of the order of $10^{-2}\mu_B$ per f.u. This is a uniquely small value for spin polarization, one that would not be expected to appear spontaneously on its own, as for a ferromagnetic (Stoner) instability nor for any other known origin. Orbital polarization can be characterized similarly; a recent model of orbital polarization will be mentioned later. For reference, the internal field in ferromagnetic bcc Fe is around 2 T – in essence, 2 T per Fe atom with a moment per atom of $\sim 2\mu_B$, versus the 4-5 orders of magnitude smaller value for $LaNiGa_2$, which has no magnetic tendencies in the normal state.[21] In terms of the inferred spontaneous TRSB field, $LaNiGa_2$ is fairly typical of the other identified TRSB SCs while having one of the smallest reported fields.

Moments of orbital-loop origin in non-magnetic compounds have been suggested from a variety of models[59,60] directed at cuprates[59] initially and later to a variety of models, particularly to kagome materials.[61,62] Experiments on cuprates have put stringent limits on orbital loop currents. They are expected to be small in magnitude, thus challenging to detect as well as being mysteri-

ous in origin, and suggestions have been directed only to quantum materials, specifically strongly correlated metals. Any self-generated field experienced by a muon will be only a local field, not necessarily the uniform field that is pursued in the study of SC OPs. Some of these questions will be addressed in the following sections.

2. Magnitude of the induced field

While it seems reasonable to expect the miniscule spontaneous fields of the order of 10^{-5}T to provide an essential clue to the underlying physics, the reality has some similarity to the search for dark matter – proceeding with little guidance and focus. The electromagnetic environment and spin density distribution near the muon appears to be strongly turbulent, with large polarization undergoing rapid angular variation, making it a numerical problem with unknown implications. The conventional picture, encoded in a proposed OP discussed later, is that the measured field is that of a uniform bulk polarization, of spin and/or orbital origin, of the electron density in the bulk, which onsets only at, or sometimes below, T_c. Several details of the near-field region, including relativistic and quantum corrections, are necessary to regularize an otherwise divergent muon self-induced magnetic field at the muon site.

IX. SUPERCONDUCTING STATE: A MAGNETIC MOMENT IN A SUPERCONDUCTOR

A. Reported instances of time reversal symmetry breaking at T_c

The *raison d'etre* of this article has been to look more closely at the process of depositing a positive muon into a superconducting metal and interpreting the observations of depolarization, and consistently forming a picture of the symmetry of the order parameter and mechanism of pairing along with relevant properties of the superconducting state. Concerns are the weakness of the experimental signal, and just what changes in the sample arise due to pairing into a coherent condensed phase with a gap opening (sometimes with points or lines of nodes).

There are now more than a dozen superconducting Fermi liquid metals labeled as magnetic, requiring TRSB OPs,[6] all supported by μSR depolarization data. This representative list includes a variety of materials types, each followed by the reported spontaneous field, or by NA if the field was not available.

- skutterudite $PrOs_4Sb_{12}$ (1.2 G)[63]
- non-centrosymmetric $I\bar{4}3m$ Re_6Zr (NA)[64]
- nickel carbide $LaNiC_2$ (0.1 G)[136], (NA)[66], (NA)[67]
- Dirac silicides (Nb,Ta)OsSi (0.83 G, 0.17 G)[68]
- kagome structure antimonide KV_3Sb_5 (0.3 G),[69]
- quasiskutterudite $Lu_3Os_4Ge_{13}$ (1.1 G),[70]
- putative frustrated superconductor Re_2Hf (1.2 G),[71]
- non-centrosymmetric intermetallic La_7Pd_3 (NA)[72]
- rocksalt structure monosilicide ScS (NA)[73]
- topological superconductor $LaNiGa_2$ (0.2 G).[31]

The common feature of all of these experiments is the muon.

References to a few more examples, including sisters of some of the above, can be found in Ghosh *et al.*[33]. Sumiyama *et al.*[66] noted that inferred fields in $LaNiC_2$ are sample dependent; one value of 0.1 G was given by Hillier *et al.*[136]

As mentioned, and acknowledged in several reports, the inferred field borders on the lower limit of detection. Also, reported analysis involving fitting of a few parameters to theoretical functional forms is not uniform. A few examples of the type of theory and forms of depolarization expressions are given in Appendix XIV C 2. What is less obvious in reports, but can be an associated concern, is that the SC state zero field depolarization rate at its maximum at T=0 is a small fraction of the value in the normal state above T_c, which is magnetic noise that remains in the SC state. For example, for Re_6Zr with T_c=6.8 K, the maximum signal at T=0 is 3% above the normal state value, with the associated field value not being provided. For $LaNiGa_2$, the sample case we have chosen for this article, with T_c=2 K, the increase is 6% above the normal state value as $T \to 0$.

A broader picture, briefly. A few μSR studies of *correlated* superconductors can be noted. In the prominent class of heavy fermion superconductors,

- UPt_3 has been reported from zero field depolarization as TRSB, but at the low field limit of detection (0.1 G)[74]
- the well-studied heavy fermion SC system $U_{1-x}Th_xBe_{13}$ reported also from μSR an increased depolarization below T_c for $x = 0.019 - 0.035$ but did not report a value for the inferred TRSB field.[75]

On the other hand, measurements on two cuprates, where there have been theoretical suggestions[59] of orbital loop derived magnetic fields, have shown nothing. For the cuprate high temperature SCs (80-93 K) $YBa_2Cu_3O_7$ and $Bi_2Sr_2CaCu_2O_8$, no additional depolarization was detected below T_c, however their experimental lower limit of detection of a spontaneous field was stated as 0.8 G.[76]

B. Organization of the following sections

A few questions will be addressed in the following sections. For example, given the experimental indication of TRSB, why does the proposed exotic state of, say, $LaNiGa_2$ involve a combination of (i) breaking of U(1) symmetry [given], (ii) avoidance of singlet spin pairing [uncommon], (iii) change of magnetic symmetry [uncommon], (iv) broken orbital/band symmetries at T_c [uncommon], and in $LaNiGa_2$ may do so in (v) a nonunitary manner [uncommon]? One 'given' and four 'uncommons' multiply to a 'highly uncommon' occurrence – a

rare sighting. The topological band character of $LaNiGa_2$ does give a distinction from the other cases listed in Sec. IX A, but most of the above questions extend to other members of this class of *fragile magnetic superconductors*.

A primary question, addressed by several superconductor theory groups more widely is: what type of order parameter is consistent with the measured constraints, and precisely what are the constraints? It has been understood since not long after BCS theory appeared that a magnetic impurity diminishes a singlet order parameter locally and degrades SC properties, that is, a magnetic moment has a detrimental effect on singlet superconductivity locally. The muon is a magnetic impurity. A triplet OP will respond differently from a singlet state, in ways that depend on details of the triplet OP.[58] The following sections deal with the electronic behavior underlying these questions, then addressing them to some extent.

This second partition of this paper began with Sec. IX A providing an introduction to several superconductors reported to show TRSB. Sec. X provides a description of the supercurrent vortex generated by the muon's magnetic field. This discussion is extended in Sec. X C to bring in the effects of flux quantization. The corresponding ("Ampere's law") field at the muon's site is the topic of Sec. IV. The interaction of the muon moment with the opening of the gap, leading to in-gap states, is the topic of Sec. XI. The topic addressed in Sec. XII is the structure of the order parameter, considering possibly singlet, possibly triplet, pairing together with ingredients to satisfy fermion antisymmetry. Section XIV S contains a few observations on the microscopic physics – the SC pairing glue – about which little can be promoted beyond electron-phonon coupling. A summary and some discussion are provided in Sec. XIII.

X. SUPERCURRENT, ITS FIELD, AND FLUX QUANTIZATION

The interaction of the muon with the condensate occurs in selected ways. The dipolar vector potential (and resulting magnetic field) is strongly position dependent, thus stimulating supercurrents. This effect and related quantities are the topic of this section. One of the Londons brothers' equations states the relationship of a dissipationless electronic fluid to a magnetic field. Given the point magnetic moment's magnetic field, the muon is surrounded by a magnetic vortex, described in the following subsection. This circulating current produces a field at the muon's site, which is the topic of Appendix X B. A further effect is that a magnetic impurity such as a muon creates localized states within the gap, so the muon is directly coupled to the gap opening. There is a concern: the London equation supposes a superfluid density in a superconducting state without saying (or knowing) much about (i) superconductivity, viz. the order parameter with its pairing strength and character, and the coherence length distance scale, which governs (together with boundary conditions) the variation of the gap in inhomogeneous situations, or (ii) modern electronic structure theory. The London theory did introduce the field penetration depth, which will appear shortly. The field dependence of the muon varies (strongly) at a smaller length scale, being confined over first or second interatomic distances, where the disturbance of the superconducting state may still not be understood. Specifically, how the OP vanishes as the muon is approached remains an enigma, as it extends consideration below the London and Ginzburg-Landau length scales to the atomic level. The discussion will carry on with the available formalism.

A. Supercurrent

Due to the lack of electrical resistivity, a persistent supercurrent $\vec{J}_s$ arises in response to the total normal state magnetic field $\vec{B}^{tot} = \vec{H}^{\mu} + \vec{B}^{ind}$, following (at least within a quasiclassical Green's function treatment[77,78]) the London equation for an inhomogeneous magnetic field. In the Coulomb (divergenceless) gauge the relation becomes

$$\begin{aligned}\nabla \times \vec{J}^s(\vec{r},T) &= -\frac{4\pi}{\lambda_L^2(T)}[\vec{B}^{\mu}(\vec{r},T) + \vec{B}^{ind}(\vec{r})] \\ &= -\frac{4\pi}{\lambda_L^2(T)}[\vec{\nabla} \times \vec{A}^{\mu}(\vec{r}) + \vec{B}^{ind}(\vec{r})] \quad (11)\end{aligned}$$

for an 'external' field, such as that of the muon. The induced polarization is an 'external' field in this context, but being much smaller than the muon field it can be neglected. Applying the condition that J_s vanishes when $\vec{A} \to 0$, one obtains the remarkably simple solution (since $\vec{A}^{\mu}$ is given)

$$\vec{J}^s(\vec{r},T) = -\frac{4\pi}{\lambda_L^2(T)}\vec{A}^{\mu}(\vec{r}). \quad (12)$$

The $\vec{r}$ dependence is that of $\vec{A}$ while the amplitude dependence is that of $\lambda_L^2(T)^{-2}$, which becomes non-zero below T_c and approaches its T=0 value rapidly below T_c.

The situation is complex. The supercurrent $\vec{J}^s$ seeks to shield the bulk of the SC from the supercurrent-driving $\vec{B}^{\mu}$ field. Given the circular form of $\vec{A}^{\mu}(\vec{r})$, the supercurrent density forms a vortex around the muon, with the field magnitude becoming ever smaller, hence its diameter becoming ever larger, as $|z|$ becomes large. This vortex will be entirely different from the textbook form that enters a Type II superconductor in an applied constant magnetic field. These statements are illuminated in the following subsection. In addition, the near region where the muon's field approaches and then exceeds the critical field of the superconductor, the London superfluid density (see below) vanishes thus the supercurrent density vanishes, applying a boundary condition on the supercurrent density.

The result is that when the field exceeds H_{c2} of the host, a normal electronic state (in a field) will return

inside that radius, with resistance damping the current. For our example $LaNiGa_2$ a rough average of the anisotropic H_{c2} values is ∼0.2 T. Using convenient units for the muon moment μ=0.448 T $\AA^3$, the critical superconducting-normal radius is roughly 1.3 $\AA$. This is the distance by which the supercurrent must have decreased to zero, or perhaps drops rapidly to zero as the order parameter may do.

1. Comments on the superfluid density. Some background is warranted, for this paper but also because this property is measured by another (applied field) μSR technique, separate from the presently discussed zero field measurement. The London brothers derived their penetration depth λ_L as

$$\frac{1}{\lambda_L^2(T)} = 4\pi e^2 \frac{n_s(T)}{m} \tag{13}$$

in terms of a resistance-less superfluid density $n_s(T)$ and electron mass m (band masses were not yet understood). Note that the penetration depth diverges as $T \rightarrow T_c$ from below, as a result of the vanishing n_s. The Gorter-Casimir two fluid model gives the temperature dependence as

$$\frac{\lambda_L^2(0)}{\lambda_L^2(T)} = 1 - \frac{T}{T_c}^{\,p}\,, \tag{14}$$

with exponent p=4. Often experimental data is fit to this expression with p as the fitting parameter, providing some information about the T-dependence of the gap $2\Delta(T)$.

In his classic book Tinkham[79] described n_s as a phenomenological parameter, while Schrieffer (in his classic book[80]) emphasized that only electrons near the Fermi surface experience any dynamical effects due to excitations on the superconductivity energy scale. Phenomenologically, one might expect the "superelectron density" to be $n^{sc} = 2\Delta(T)N(0)$, *i.e.* the number of electrons that have disappeared from the energy region 2Δ centered on E_F into the condensate that provides conductivity at T=0 (there are no excited quasiparticles). Combining expressions from the BCS paper gives roughly this value for the number of paired electrons in the BCS wavefunction. For the parameters of $LaNiGa_2$, this estimate gives $n_s(0) \approx 2\times10^{-3}$ electrons/f.u. Experimentally, the emphasis is on T-dependence; an absolute magnitude is rarely quoted from analysis of experiment.

2. Some background. The zero-frequency normal state electromagnetic (T-independent) penetration depth λ_n in terms of Fermi surface quantities is[81]

$$\frac{c^2}{\lambda_n^2} = \frac{4\pi}{3} e^2 N(0) v_F^2 \equiv \Omega_p^2 \tag{15}$$

in terms of the Fermi level DOS N(0) and velocity v_F. Ω_p is the Drude plasma frequency, which is a property of the normal state Fermi surface, and for conventional intermetallic compounds is a few to several eV. Since Fermi surface properties are a given for any specific metal, one might consider this equation to give its conversion into a length scale.

Ω_p became so named because for the homogeneous electron gas (where the density n determines k_F, E_F, v_F, and any combination), the expression for the conductivity $Omega^2\tau$ (see just below) is nearly the same as measured for monovalent alkali metals Li-Cs with spherical Fermi surfaces. Ω^2 has nearly the same value as the optical plasmon frequency

$$\omega_p^2 = \frac{4\pi}{3} n e^2/m, \tag{16}$$

the position of the peak in the electronic energy loss function and involves excitations of all electrons in the band(s). For some context, for a transport scattering time of τ, the d.c. conductivity is $\sigma(T) = \Omega_p^2\tau(T)/4\pi$, which is the connection for which Ω_p is most often calculated. The connection with the free electron expression then gives the correspondence

$$N(0)v_F^2/3 \rightarrow N(0)v_{x,eff} \leftrightarrow (n/m)_{eff} \tag{17}$$

as an effective value of the density/mass ratio for the normal state: effective density of electrons involved in transport and a band effective mass. (v_F, m_{eff} are anisotropic in general.) For intermetallic Fermi liquid metals $\hbar\Omega_p$ is on the order of a few eV.

Once one makes the association of superconducting electron density n_s as $N(0) \times 2\Delta$, one is left with an anisotropic effective mass expression

$$m_{x,eff} = \frac{6\Delta}{v_{x,eff}^2}. \tag{18}$$

All of these expressions involving, or obtained from, use of n_s are phenomenological, lacking formal justification. The number of superconducting electrons is an evasive quantity.

B. Field at the muon site

The supercurrent J^s produces its magnetic field $\vec{B}^s(\vec{r})$. $\vec{J}^s$ will, from all levels (each contributes a circular sheet of current loops) along the $\hat{z}$ axis, produce a field $\vec{B}^s(\vec{r})$ that strives to cancel $\vec{B}^{tot}$ at a distance beyond the coherence length, that is, in the bulk material. The muon experiences the combined field

$$\vec{B}^{tot}(0) = \vec{B}^{ind}(0) + \vec{B}^{spon}(0) + \vec{B}^s(0), \tag{19}$$

the last two fields arising only below T_c.

We consider the dominant member $\vec{A}^\mu$, which leads to $\vec{B}^{ind}$ and to $\vec{B}^s$. From electrodynamics, the field due to a current, and its value at the muon site, is

$$\begin{aligned}
\vec{B}^s(\vec{r}) &= \frac{1}{c}\int \vec{J}^s(\vec{r}') \times \frac{\vec{r}-\vec{r}'}{|\vec{r}-\vec{r}'|^3} \\
&= -\frac{4\pi c}{\lambda_L^2(T)} \int \vec{A}^\mu(\vec{r}') \times \frac{(\vec{r}-\vec{r}')}{|\vec{r}-\vec{r}'|^3} d^3r', \\
\vec{B}^s(0) &= \frac{4\pi}{\lambda_L^2(T)} \int \vec{A}^\mu(\vec{r}') \times \frac{\vec{r}'}{|\vec{r}'|^3} d^3r'.
\end{aligned} \tag{20}$$

With $\vec{A}^{\mu} = (\vec{\mu}\times\vec{r})_{/}r^3$, $\vec{\mu} = (0,0,\mu)$, the integral for the x or y coordinates gives zero, consistent with the symmetry allowing only a z component. In cylindrical coordinates the integral over ϕ gives 2π, leaving the integral

$$\begin{aligned} B_z^s(0) &= -\frac{2c^2}{\lambda_L^2}\int \rho d\rho\ dz \frac{\rho^2}{(\rho^2+z^2)^3} \\ &= -\frac{4\pi c^2}{\lambda_L^2}\int_{-\infty}^{\infty} dz \int_0^{\infty} \frac{w\ dw}{(w+z^2)^3} \\ &= -\frac{4\pi c^2}{\lambda_L^2}\int_{-\infty}^{\infty} dz[-\frac{1}{4(w+z^2)^2}|_0^{\infty}] \\ &= \frac{2\pi c^2}{\lambda_L^2}\int_0^{\infty}\frac{dz}{z^4}. \end{aligned} \tag{21}$$

This divergent (at z=0) integral reflects the same need for including quantum treatment and high field physics as in the normal state (see Sec. IV) plus the more general limitations that (i) the supercurrent expressions do not apply in the normal state very near the muon position and (ii) the London equation itself becomes questionable on atomic distances. Physically, the result will be nonzero and would be sensitive to any chosen *ad hoc* cutoff at very small $|z|$.

This result returns one to the same (an)isotropy discussion as for the normal state. For the homogeneous electron gas with cylindrical symmetry of the system, the field at the muon site will align with the muon moment, thereby providing no torque and no depolarization. Again, the low symmetry of the muon site will cause the field to deviate from the z direction, thereby providing a mechanism of depolarization for any host.

The conclusion at this point is that there is a nonvanishing depolarizing magnetic field at the muon site that turns on as the material become superconducting. The T-dependence arises from that of $\lambda(T)$:

$$\begin{aligned} \frac{B_z^s(0,T)}{B_z^s(0,T=0)} &= \frac{\lambda_L((0)}{\lambda(T)} \\ &= \sqrt{1-(\frac{T}{T_c})^4)} \approx 2\sqrt{1-\frac{T}{T_c}}, \end{aligned} \tag{22}$$

for T not far below T_c. This increase toward the maximum value at T=0 occurs rapidly below T_c. At $T = 0.75T_c$ the field will already have reached 86% of its value at T=0; most of the T-dependence occurs just below T_c.

C. Flux quantization

Magnetic flux penetrating a type II singlet superconductor ($T<T_c$, $H_{c1}<H<H_{c2}$) consists of roughly evenly distributed vortices containing one flux quantum Φ_o, confined by circulating supercurrents that shield the bulk regions of the SC. Studying magnetic impurities within Ginzburg-Landau theory, Ashcroft and Krusch found[82] that for a δ-function impurity in a Type II SC and within a range of model parameters, a strongly localized magnetic impurity behaves similarly to a quantized flux vortex, the two being related by a "singular" (but treatable) gauge transformation in their model. Local quasiparticle states arising from carrier confinement by a SC vortex have been studied by Gygi and Schlüter,[83–85] and by Su *et al.*[86] for a topological SC. The magnetic field from the muon's moment will likewise be surrounded by supercurrent enclosing a single flux quantum Φ_o vortex, not externally driven but rather arising from the muon itself, as discussed just above.

With no source or sink for the field, the vortex will extend to the sample surface at large $|z|$. Each cross-sectional area at height z will contain a flux quantum confined within a radius that is z-dependent. see Sec. **??** for some explicit values of field versus radius. Supposing there is a uniform 0.2 G field, as reported for $LaNiGa_2$, present in the absence of the muon, at large $|z|$ the vortex radius will be $\sim 10\mu$m, a mesoscopic area within which the SC OP would be reduced toward zero. Quenching of the order parameter by the muon's moment would lead to a gapless system, though likely not evident in current probes. If this scenario were correct, the vortex at the surface might be detectable, very weak and possibly requiring more time than the mean lifetime of the muon.

However, 0.2 G is much less than H_{c1}, in which case the flux might be confined within a bubble within the sample. This lower critical field is given by

$$H_{c1} = \frac{\Phi_0}{4\pi\lambda_L^2}(ln\frac{\lambda}{\xi}+0.50). \tag{23}$$

Both length scales are direction-dependent for $LaNiGa_2$. Using the experimental values in Sec. XIV N, $H_{c1} \approx 100$ G for fields applied along the a and c axes, and roughly twice as large for the b axis. For standard singlet-paired SCs, such a small field, if from an external source, would be entirely excluded, with only the muon's field and that of the supercurrent remaining, both amounting to a local disturbance. If the spontaneous field is persistent and uniform, then triplet pairing scenarios come into play.

XI. KONDO PHYSICS; YSR STATES

A. Magnetic moment coupled to pairing

The Kondo picture of a magnetic impurity in an electron gas addresses the coupling of the spin degree of freedom of a magnetic impurity coupled to itinerant electrons through an on-site interaction $J_K\sum_{j,s}\vec{S}\cdot\vec{s}_{j,s}$ in terms of the exchange parameter J_K and the impurity and electron spin operators $\vec{S},\vec{s}_J,s$. As Cooper pairing begins, an itinerant electron in the area is frustrated between anti-aligning with another electron (for singlet pairing), or with anti-aligning with the impurity spin. The coupling is taken to anti-aligning in sign, which without pairing leads to a collective singlet forming between the impurity and the electrons. This interaction will be discussed in Sec. XI.

A magnetic impurity also imposes a vector potential that couples differently to the conduction electrons – a

magnetic interaction over a region versus an on-site exchange coupling. Research into effects of the electronic exchange interaction has extended over decades. The interaction between the muon magnetic moment and the electronic system involves differences.

Early work addressed data on superconducting samples containing a collection, perhaps a sublattice, of small magnetic particles,[87,88] and effects that arise due to anisotropy and a Type-II state.[89]. A related emphasis was the interaction between a dipole and the superconducting surface.[90] It can be noted that some superconductors with dense lattices of rare earth ions with large moments showed little coupling to itinerant electrons, *i.e.* potential Cooper pairs. High T_c cuprates, viz. $\mathcal{R}Ba_2Cu_3O_{7-\delta}$, $\mathcal{R}$=rare earth (except for Pr), with T_c∼80-100 K, display little evidence of coupling, with the $4f$ moments finally ordering antiferromagnetically only around 1 K. The rare earth $\mathcal{R}$ class $\mathcal{R}Ni_2B_2C$, on the other hand, displays a rich competition between SC and antiferromagnetic order in the 10-20 K range, even showing coexisting superconductivity and magnetic order in the H-T phase diagram.[91]

As noted earlier, the vector potential of a magnetic moment drives circular currents around its axis that form the vortex. In a conventional superconductor, the exchange coupling of the atomic moment interacts with and depresses the OP in its vicinity. Spatial variation of the vector potential drives supercurrents, or as often stated, a magnetic field stimulates supercurrents that oppose the field, as in the Meissner effect.

Check this paragraph. Another issue arises from the $3\mu/r^3$ scaling of the magnetic field near the muon moment. When this field exceeds the critical field, the OP must vanish. The muon then will always exist in a small normal state region of space. This change from near-full OP to a normal region will occur on a very much smaller length scale than ξ (the small length scale in Type II SCs), which brings up the (possibly) unexplored question of how this crossover occurs on the Å scale. However, scanning tunneling microscopy spectra and S-I-S tunneling characteristics demonstrate that a bulk gap extends to very near a surface or interface, where there is an abrupt change from full amplitude OP to vanishing OP. How the increasingly large near-field might affect a muon's detection of relaxation-inducing fields, and indeed the reaction of the OP to such a rapidly varying field, are areas yet to be illuminated.

Neglecting details, the classic picture of a magnetic moment in a metal in the normal state is that of the Kondo effect: if the exchange coupling between the net local moment and the itinerant electrons is antiferromagnetic in sign, many-body screening of the moment ("spin screening") produces an effective local moment-conduction electron singlet that becomes evident in several normal state properties (resistivity, magnetization, heat capacity, some others). The singlet correlations set in and finally saturate at a temperature well below the Kondo temperature T_K where the singlet evolution begins, and at low temperature the material is a strongly enhanced Fermi liquid. Evidence of Kondo screening has not been reported and would not be expected for a sparse concentration of μ^+ moments, especially considering that the muon moment is two orders of magnitude smaller than atomic moments. Several Kondo compounds become superconducting, a topic that is not a part of this paper.

1. *Kondo singlet versus Cooper singlet*

An early approach to this coupled local moment – pairing order parameter issue is embodied in the 1970 results of Zittartz and Müller-Hartman,[92] (ZMH) who extended earlier works at the model Hamiltonian level that had been influential in understanding the normal state Kondo effect. One might anticipate that the opening of the SC gap interrupts the essential low energy Kondo physics, and the quantum aspects of the spin can be treated less explicitly. What is known is that Kondo lattice materials – crystals with a sublattice of magnetic moments – can enter the now well studied Kondo heavy Fermi liquid superconducting phase. Kuster and collaborators[56] have shown how to probe this question for the case of magnetic atoms on surfaces.

Appending the Kondo Hamiltonian with a BCS 'pairing potential' term, ZMH established within this model that as the gap opens, bound states involving the local moment appear within the gap but near the gap edges. The character of these states should include strong local moment character, but only much more recent studies have clarified both their energetic and orbital character.

According to this level of theory, a single muon impurity couples to the electron cloud that is beginning to pair into Cooper singlets, with the outcome being, besides other spectral changes, a pair of magnetic moment-derived localized bound states within the gap, at energies near the gap edges at $\pm\Delta(T)$. This connection provides a mechanism of coupling of the SC order parameter to an impurity spin. As derived in Sec. IV (not considering Kondo coupling), the μ^+ moment creates a strongly spin polarized region around the muon that is changing sign with polar angle θ, with field far greater than the critical field. This electronic magnetization near the muon, having strong polarization (varying with direction) acts to obviate singlet SC pairing in that region (but not necessarily encouraging triplet pairing), thereby reducing the gap magnitude, to the extent that any OP can be treated on the Angström level. The magnetic ion's (muon's) field likely dominates, providing a moment-quasiparticle coupling of a new character. Study of the SC-Kondo model has since that time been addressed by more recent many-body techniques, see for example Sykora and Meng's calculation of the interplay between the Kondo singlet state and the induced YSR states.[93] Some results of the study by Choi and Muzikar[78] of a Kondo impurity in an exotic superconductor are discussed in Appendix XIV L.

2. Yu-Shiba-Rusinov states

A magnetic impurity in a gapped SC interferes with the singlet OP that according to the ZMH-type of model and solution leads to bound YSR (Yu-Shiba-Rusinov[94–97]) states within the SC gap 2Δ but, according to early studies, near the gap edges at $\pm\Delta$. Such states are analogous to shallow donor and acceptor states in semiconductors, and might someday play a similar role in SC electronics. For some time after the Kondo effect was elucidated, it was considered that the SC gap inhibited zero-energy processes (which dominate the Kondo effect) as being frozen out, and the moment could be considered as classical. As theoretical interest and experimental capabilities have progressed, quantum behavior of the impurity spin has become a topic of study, while the internal structure of the state raised interest. This area of study should be regarded as ongoing, with relevance to this article to be determined. The status as of 2006 was reviewed by Balatsky, Vekhter, and Zhu.[34]

Previous studies treated the impurity moment-electron coupling, implicitly (point contact coupling) in early work but increasingly explicitly in more recent studies, as interatomic electronic exchange akin to (but more broadly than) the rules of Goodenough[98], Kanamori,[99], and Anderson[100] between the impurity state mixing with orbitals of itinerant states. This direction of study neglected the smaller effect of the orbital behavior near the dipolar field of the moment. In studying the muonic impurity at the sub-atomic level, both effects become relevant. The environment in μSR studies provides a direct coupling between the muon vector potential (orbital effects) and the SC condensate. Coupling of the muon is of a distinct character due to the fact that the coupling is through the vector potential which reduces the gap, rather than through (say, $3d$) atomic orbitals. Hydrogen interstitials introduce similar formal considerations, but with an order of magnitude smaller effect.

3. μYSR states

As mentioned, the muon is a close cousin of interstitial hydrogen. Given a more-or-less singly occupied $1s$ orbital of the muon, there will be no electronic (spin) moment (which from DFT calculations is magnetically inactive) and a $1s$ orbital has no orbital moment. Regarding this point: it seems that DFT studies of proton and muon interstitials[37,39,42,43] have rarely searched for spin polarized states of the muon. Interest in an "ultra-deep donor" state in ultra-pure semiconductors received a boost from a simple type of correlated electron calculation applied to the H $1S$ orbital in Ge, which identified such a spin-polarized state a few eV (note: not a few meV) below the gap in Ge.[101] Screening in metals alters the physics of such states. Back to the main topic: the muon vector potential field will interact with the OP and it can be expected to give rise to defect states within the gap, which will here be denoted μYSR states.

The induced currents for the bare muon (without the smaller induced electronic magnetic intensity, neglected for now) are, by Eq. 12 and for an isotropic host, circular currents around the $\hat{z}$-axis decreasing as z^{-4} away from the muon. Magnetic field lines do not terminate, so the current vortex must enclose one unit of quantized flux (its increasing magnetic field will put it, in a certain range, in the Type II regime, before destroying pairing when the field exceeds H_{c2}). The radius of the vortex increases in radius in the x-y plane accordingly, see Appendix XIV B for values.

Low symmetry of the muon site will affect analysis. The non-circular environment will allow a non-zero expectation value of the magnetic moment operator, hence non-zero orbital magnetization. Change of direction of the muon spin will result in a change of rotation of the orbital currents, which provides new information but again may complicate analysis.

The study of YSR states has progressed to DFT studies of $3d$ ions. Fe, with its large moment, has been the preferred atom within or on the surface, of conventional SCs such as Pb and Nb, revealing a great amount of detail that can occur in such cases. Some cases are addressed in Appendix XIV M. In-gap states due to a muon, with only the moment's vector potential and with the unpolarized $1s$ orbital not involved, have yet to be studied, although a few groups may soon have the capability (see App. XIV M).

XII. IMPLICATIONS FOR THE PAIRING SYMMETRY

Construction of plausible exotic OPs relies on the guiding principles of antisymmetry of the Cooper pair and the BCS form of the nonlinear gap equation, which becomes linear at T_c. For elements and intermetallic compounds that display conventional Fermi liquid behavior without any unusual magnetic tendencies, superconductivity is initially assumed and then (frequently) verified to be due to phonon-induced pairing of electrons – singlet and s-wave pairing. When properties, in the normal or SC state, are unexpected, an exotic (ı.e. non-BCS) OP is anticipated. μSR is the primary technique providing evidence of TRSB (a spontaneous magnetic field) in nominally conventional metals.

The two central subclasses of OP are (spin) singlet pairing and (spin) triplet pairing, the only two classes to be obtained from two spin-half electrons. These distinctions provide the first line of attack in constructing possible OPs. Beyond that, symmetry in momentum space ('orbital symmetry', beyond s-wave) provides the second consideration. For TRSB, spin (more generally, magnetic) symmetry becomes the issue, along with accompanied symmetry breaking. To complete the antisymmetric character of the Cooper pair, further symmetries are considered as possibilities: space group, inversion, orbitals, bands, etc.

A. Spin singlet scenarios

1. Ubiquitous electron-phonon coupling

I. Generalities. Electron-phonon coupling (EPC) is distinctive given that it (i) is always in play, and (ii) is always attractive for s-wave pairing (the kernel in the gap equation does not change sign), with coupling strength λ moderated by a retarded Coulomb repulsion μ^*, typically falling in the 0.10-0.16 range.[102,103] For low T_c's, say below 5K, it has been difficult but is recently becoming possible, to verify theoretically[2] that SC derives from EPC. The difficulty is that calculating low T_c requires *precise* knowledge of both λ and μ^*, neither of which is normally available. An added complication is that the fundamental Coulomb repulsion is μ, whereas μ^* is a renormalization that depends on the frequency cutoff used in solving the Eliashberg equations.[104]

Taken together (they are each always present), The combination $\lambda_k - \mu^*$ contains some richness, based on the k-dependence of λ_k and the near-independence of μ^* on wavevector (it involves higher energy processes that serve to average out the dependence on k near the Fermi surface). If λ_k is strongly anisotropic, the net interaction $\lambda_k - \mu^*$ can change sign on the Fermi surface, and non-s-wave orbital behaviors may become favored. For $\mu^* \approx$0.10-0.16 and weak but anisotropic λ_k, a change in sign of $\lambda_k - \mu^*$ in the kernel introduces the possibility of a exotic gap symmetry, denoted p-wave, d-wave, or even more involved combinations of symmetries, such as $S{+}id$. While a few p-wave and d-wave SCs have been suggested for quantum materials, some with several types of support, none has been established in the weakly-correlated Fermi liquid metals that are the topic of this article. Simple Fermi liquid SCs, with conventional μ^* and low T_c are commonly and successfully interpreted to arise from EPC, partly due to other experimental information on λ and partly due to the ubiquity of the phonon mechanism.

A pairing strength λ= 0.4-0.5 in an s-p electron compound can account for a T_c up to 5K or so (but is sensitive to μ^*), a range including all TRSB SCs in the class of *fragile magnetic superconductors*. Given the seemingly necessary exotic OP, an additional channel for symmetry-breaking is anticipated. While weak for EPC, this value of coupling may be strong compared to additional candidates, hence alternatives should be complementary to, rather than competitive with, EPC. More visually expressed, they might be simply additional (but "perpendicular") to EPC. Of course, possible phonon coupling to additional degrees of freedom cannot be overlooked.

II. Conventional BCS calculations. Subedi and Singh[105] calculated the phonon spectrum, the Eliashberg spectral function $\alpha^2F(\omega)$, and T_c for $LaNiC_2$, a sister compound to $LaNiGa_2$ with closely related composition, an orthorhombic space group, and similar value of T_c=2.7K. It has a different point group, but one that also has only 1D irreps. The μSR identification as TRSB is based on extraction of a smaller spontaneous field of 0.1 G, a value that is sometimes stated as the lower limit of detectability. The coupling strength is λ=0.52, and using a standard value of the retarded Coulomb repulsion μ^*=0.12, T_c=3K was obtained. This is excellent agreement with experiment, and provides the strength of electron-phonon coupling that must be confronted by other competing pairing mechanisms.

Related calculations on $LaNiGa_2$ were reported by Tütüncü and Srivastava.[106] They assumed the *Cmmm* space group understood at the time to be the structure, rather than the more recently discovered *Cmcm* structure. The electronic structure is similar to the *Cmcm* result, for example the Ni 3d states are filled and lie in the same energy range. The Fermi surfaces for both are large and multisheeted, but different. Based on a limited Q-mesh for the phonons, they obtained $\lambda\approx$0.7, and choosing μ^*=0.17 for their estimate, giving T_c very close to the 2 K experimental value. Calculations using the more recently determined *Cmcm* space group have not been reported.

III. This picture so far. It should be mentioned that quoted calculated values of T_c, when small, are sensitive to (i) the choice of the parameter μ^*, and (ii) a precise, well converged calculation of λ. In any case, the modest values of λ indicate weak coupling. These results for two TRSB superconductors provide a strong indication that the pairing is BCS (spin singlet, phonon mediated), and that other origins of the spontaneous magnetic field should be sought. In this scenario, the reported spontaneous magnetic fields from μSR spectroscopy would be attributed to the field generated by the supercurrents that onset at T_c.

2. Spin singlet pairing more generally

Occam's razor directs one toward the simplest form of OP consistent with observations. We consider first singlet pairing due to phonon glue, which is the presumption underlying experimental identification of materials properties and which lie within familiar ranges for weak coupling SCs . Cooper's demonstration that the Fermi surface is unstable to formation of bound singlet pairs of $(+k,\uparrow;-k,\downarrow)$ character is the underpinning of the theory of superconductivity, subject only to the necessity of a net-attractive effective interaction. Phonons are always present, and they always prefer zero momentum singlet pairs, subject to interruptions from other pairing mechanisms that are usually weak in conventional Fermi liquids. Calculations on $LaNiC_2$[105] and $LaNiGa_2$[106] are discussed in Section XII A 1.

Singlet pairing alone involves only a scalar (in general, complex) OP, the gap Δ_{kn} depending on position on the Fermi surface (wavevector k, band n). The k-dependence can incorporate a component of broken crystal symmetry (p-like, d-like, f-like) plus additional out of phase components of higher symmetry, viz. $s{+}id$. Less fundamentally, in accounting for data on TRSB it has become common to incorporate into the theory an additional degree of freedom whose symmetry can be broken, such as a pair

of similar (but not degenerate) bands, or atomic orbitals on symmetry-related atoms (degenerate by default).

1. An exotic singlet scenario. Addressing the TRSB feature more generally, the Dirac point (DP) degeneracy of $LaNiGa_2$[17,18], pinpointed in Fig. 3, suggests a symmetry-driven fragile platform for a broken symmetry that could account for a small magnetic field in the SC state. The symmetry would be that of the mirror $x \to -x$ operation in the $Cmca$ space group that connects the two DPs. (We choose, as common, the special crystallographic $\vec{b}$ axis as the OP $\hat{z}$-axis, and the Z-T direction as the $\hat{x}$ direction.) The $\vec{\tau}$ space in the current model has not broken any true symmetry in the 'near degenerate FS' picture, and only a nondescript degeneracy in the 'degenerate orbitals on equivalent atoms' picture. The broken symmetry involving the pair of DPs provides an obvious candidate for delicacy toward spontaneous change, closely analogous to the pair of DPs in graphene.[107]

This picture comes with a challenge: the overall odd symmetry of the OP. Singlet spin is odd; the broken DP pair is odd (think of splitting to energies $\pm\eta$). The product of the three OP components being odd requires the third – k-space behavior – to be odd. Yet data shows a gapless SC spectrum, typically associated with an s-like behavior. This hurdle can be surmounted by an OP of $p_x + ip_z$ type, somewhat natural given the $Cmca$ structure:

$$\Delta_k^{orb} = \alpha \sin k_x + i\beta \sin k_z,$$
$$\Delta_k^{orb}[\Delta_k^{orb}]^\dagger = \alpha^2 \sin^2 k_x + \beta^2 \sin^2 k_z, \qquad (24)$$

with non-zero real constants α, β. While there has been substantial theoretical discussion of complex combinations of different character, little has been established about what the origin might be. In very stable crystals, this symmetry breaking can involve simply lowering the symmetry of the electronic state with negligible impact on the lattice symmetry, making XRD an ineffective probe.

The absence of anisotropic pairing states in conventional Fermi liquid metals raises questions about why they are so disfavored. For example, the antisymmetric p-wave state should gain energy due to the two members of the Cooper pair having a reduced short-range Coulomb repulsion. Foulkes and Györffy[108] looked at the scattering vertex function Γ, given schematically by $\Gamma = I - IGG\Gamma$, where I is the irreducible scattering vertex and G is the single particle Green's function. Assuming that I does not depend on relative spin orientations, they compared λ_0 the coupling strength for an s-wave kernel, for its p-wave counterpart λ_1. A key point is that for p-wave, μ^* will be much reduced and might be negligible, so the effective couplings may be similar. They took into consideration the accepted lore that anisotropic pairs are strongly affected by impurity scattering, requiring very clean metals. Reducing $T_{c,1}$ proportional to the transport broadening $\hbar/\tau$, an accepted approximation, they suggested that p-wave pairing might occur in Pd, W, or Rh samples, but requiring residual resistivity ratios between 10^3 to 10^5, representative of extremely pure crystals. This work provided at least the plausibility of p-wave pairing in conventional metals. Other works have suggested that phonon pairing in conjunction with other interactions can generate odd-pairing for certain choices of parameters.[109,110].

3. A degeneracy-inspired singlet order parameter

Supposing a system where TRS is broken already in the normal state, the question of the type of order parameter should not be considered closed. $LaNiGa_2$ has unique degeneracies that make it a special case.[16–20] Due to its non-symmorphic space group and Fermi surface geometry giving rise to a pair of diabolical point degeneracies that are not lifted by SOC, and only separated by the gap-opening SC state, a singlet but exotic order parameter can be constructed, incorporating this unique Fermi surface point degeneracy.

The Cooper pair symmetry, required to satisfy the fermionic antisymmetry under exchange of electron coordinates, allows an uncommon product of odd (spin) × odd (orbital) × odd (other) = odd pair. The nodeless gap is another primary condition. Singlet pairing is odd upon exchange of electron coordinates. By choosing an orbital combination of $p_x + ip_z$ for the OP (somewhat natural for an orthorhombic structure with a special y-axis), the orbital symmetry is odd but a nodeless gap is retained: symbolically, $|p_x+ip_z|^2 = p_x^2+p_z^2$ has no zeroes. However, the Dirac point symmetry $D_a \equiv D_b$ by mirror symmetry can be broken into a non-zero odd combination. Introducing a generalized degree of freedom u_a, u_b on each,viz. perpendicular displacements ξ_a, ξ_b, the space is isomorphic to the spin space of the Cooper pair, with coupled displacement described by a set of vector Pauli matrices denoted τ. The combination $[\xi_a - \xi_b]/\sqrt{2}$ is a DP singlet, which with the above representation would be a twisting of the $a-b$ "bond" in the $k_x - k_z$ plane. This provides a breaking of non-symmorphic symmetry, perhaps electronic rather than structural, and reduces the Dirac point symmetry. With an appropriate coupling term in the OP and BdG Hamiltonian, this transformation could break spin symmetry or stimulate orbital currents. The topological nature of these Dirac points in momentum space might give more exotic properties arising from the symmetry breaking process.

B. Spin triplet pairing

1. Challenges to triplet pairing

A more detailed understanding of the interaction and present interpretation, based on TRSB, of triplet pairing appears to confront a few common expectations and challenges: (i) that low T_c, weak coupling SCs commonly conform to Cooper's (BCS) singlet S=0 and zero momentum pairing instability, (ii) triplet correlations will need

to dominate singlet correlations to break TRS, implying a relatively strong coupling (of unclear origin), (iii) magnetic impurities diminish singlet pairing; triplet states are predicted to be highly sensitive to defects even non-magnetic ones, (iv) there are questions relating to the superconducting state coexisting with an intrinsic magnetic field;[58] (v) only a select few intermetallic compounds of seemingly similar non-magnetic Fermi liquid character are identified as breaking TRS, and all are low T_c materials.

This class of *fragile magnetic superconductors* may be analogous to the situation in EPC, where a small difference in a weak-coupling λ can account for the difference between low T_c SC, or none; a smaller that detectable spontaneous field will result in assignment of a similar SC state to a different class. As mentioned in the Introduction, due to the supercurrent derived magnetic field discussed in Sec. X, all implanted muons should incur additional depolarization below T_c, but with some the field would be enough smaller that it lies below detectability and thus is not included in the class of fragile magnetic superconductors.

Triplet S=1 pairing in this class has the sole justification that it accounts for the signal of TRS breaking, as long as remaining symmetry restrictions can be addressed. For triplet pairing, equal S_z=$\pm$ 1 occupations provide a degeneracy from which symmetry can be broken (very slightly) by some small perturbation. As mentioned, many properties of this class do not seem consistent with triplet pairing. It is also a challenge to identify a mechanism to justify equal spin pairing, one that overrides Cooper's strong favoring of both singlet pairing and zero momentum pairs. Some generalities of triplet OPs, of which the INT model[32,33] discussed below is one, are provided in Appendix XIV O.

2. The INT model

Weng *et al.* described[32], and Ghosh *et al.* refined[33] Internally (antisymmetric) Nonunitary Triplet pairing (INT) spin-triplet picture for $LaNiC_2$ and $LaNiGa_2$ in which there is parallel-spin pairing (the S_z=0 channel is neglected). For the magnetization, $|\uparrow\uparrow>$ ($S_z = +1$) occupation exceeds (slightly) that of $|\downarrow\downarrow>$ ($S_z = -1$). Without going into further details (see Appendix XIV O), this one-parameter model is based on an electronic quasi-degeneracy – nearly-degenerate FSs – or alternatively on an active atomic orbital on symmetry-related atoms; either could account for the necessary additional symmetry to be broken. From small structure in $\lambda_L(T)$ and $c_v(T)$ they argued that a "two gap" (or "two band") character might be responsible. (Data for $c_v(T)$ obtained on single crystals[17] since these papers were published are consistent with a single, somewhat anisotropic, gap.)

This viewpoint can be supported more naturally by the observation just above that pair of DPs in $LaNiGa_2$, discovered in electronic structure calculations[18] after its correct space group was revealed by single crystal XRD[17] and confirmed by ARPES data, provide an exact (but material dependent) degeneracy that would be susceptible to instability by spontaneous crystal symmetry breaking. The remainder of the analysis carries through: triplet pairing, symmetric k-dependence, odd symmetry in the orbital space.

C. Orbital magnetism scenario

Spontaneous orbital magnetism in crystalline solids, if it would arise in zero field, is generally expected to be much smaller than spin magnetization. Given the reported field values of 0.1-1 G, the orbital magnetization would need to be that of the spin magnetization discussed earlier, of the order of $10^{-3}\mu_B$/f.u.[45] Orbital currents have been discussed mostly in the context of quantum (strongly correlated) materials, and not yet observed. Several independent searches in the layered cuprates have placed stringent limits on the magnitude of such currents, however they remain of strong theoretical interest.

As mentioned in Sec. X, an orbital supercurrent is driven by the muon moment, leading to a vortex extending (more or less, depending on local symmetry of lack thereof) along the axis of the moment. This supercurrent primarily sustains the vortex, producing a field at the muon site and also in the neighboring environment, but in a roughly circular region. In a susceptible system a vortex might trigger an orbital current state in the bulk.

Weak spontaneous fields that are proposed theoretically are not pictured in terms of large cyclotron orbits such as arise from strong applied fields, but rather from small currents circulating on the nanoscopic scale. It is challenging to reconcile singlet pairing with an intrinsic internal field: its perfect diamagnetism would strive to compensate somehow or expel the spontaneous field – but the spontaneous field OP is proposed (at least for simplicity) to be uniform. This issue is beyond the scope of this paper.

First, the formulation of a microscopic theory of orbital moments, which possess and angular momentum, in a periodic solid is far from obvious. Robbins *et al.*[111] have applied developments that occurred in the theory of polarization in crystals to address this challenge for the normal state, then extended the theory of the orbital moment in a superconductor to the formulation and application of a modern DFT-based band structure code (viz. BdG formulation for a SC) to explore such effects in real materials.

This work required a careful formulation of orbital momentum because in the usual angular momentum operator $\vec{L} = \vec{r} \times \vec{p}$, the position operator $\vec{r}$ is tricky to handle in an extended, periodic system, and the orbital moment will be a periodic quantity. Assuming a chiral, p-wave OP for Sr_2RuO_4, Robbins *et al.* derive an orbital moment of $3{\times}10^{-4}\mu_B$ per f.u., which they suggest accounts for a field of 0.3G, *i.e.* again not far from the measurement limit. The formalism they develop can be expected to be of great use in modeling and understanding orbital mo-

ments in superconductors. The proposal by Robbins *et al.* of orbital currents is discussed in Appendix XIV S 2, see also the specific proposal by Ghosh *et al.*[45] of TRSB loop supercurrent order.

D. FFLO possibility.

This possibility has hardly been discussed in the literature, and upon further study might be found to be untenable. As discussed in Sec. XIV S and Appendix XIV O, TRSB is conventionally typified in language and formalism as spin-triplet pairing. In this picture, the small observed magnetic field implies a very small difference in the numbers of $|\uparrow\uparrow>$ and $|\downarrow\downarrow>$ pairs. Another spin-based scenario (*i.e.* without orbital polarization), given the extremely small observed magnetic field, is that it might qualify as an FFLO-like state within singlet pairing, with a minor difference in spin-up and spin-down polarization. This slight spin polarization results in slightly different up and down Fermi surfaces, which might readily be displaced to provide the nesting that the FFLO picture engenders: a polarization that varies slowly in space, with variation on the length scale of $2\pi/Q$, where Q is the net momentum of a pair.

An idealized FFLO state[112,113] has net momentum $\vec{Q}$ singlet pairs $(k, -k+Q)$, disrupting the simple BCS case of direct pairing across the Fermi surface $(k, -k)$. The gap function varies (again, idealistically for flat nesting Fermi surfaces) in sinusoidal $\vec{Q} \cdot \vec{r}$ fashion. This faces the challenge that each muon seems to experience a single environment as the origin of depolarization, whereas the phase of the FFLO gap would lead to the muons in a given experiment sampling varying magnitudes of the magnetic field. A resolution of this issue is that the variation could occur as $\Delta e^{iQ\cdot r}$, *i.e.* spatial variation of the phase of the complex FFLO OP, but with constant magnitude.

A related possibility is that the muon perturbs pairing in the following way. The charge density in the muon's environment differs from that of the periodic crystal due to the muon's own "1s" charge and to the change in density to displaced neighboring atoms. This can be pictured as this region of disruption perturbing the Fermi surface locally. The muon's magnetic field has broken spin symmetry already, so the disrupted (or broken) pairs would naturally result in unequal spin-up and spin-down carriers, leading to a local magnetic field.

XIII. DISCUSSION AND SUMMARY OF THE PAPER

μSR studies have provided muon depolarization evidence, with magnitude sometimes (but sometimes not) having T-dependence much like the superconducting gap, that is taken as evidence of TRSB, in as many as ten weakly correlated, conventional metals mentioned herein. These differences may be ascribed to the magnitude of the signal approaching the limit of the μSR experiment. Assuming as has been common that this is not a self-induced field, this assignment places them in one of the most unusual classes of superconductors with exotic order parameters, referred to here as *fragile magnetic superconductors*. Perplexingly, the superconducting properties are consistent with singlet pairing, while triplet pairing can produce very different coherence lengths and critical fields,[58] and likely would show very different h- and T-dependencies of the magnetization. The superconducting properties of radiation damaged (disordered) $LaNiGa_2$ are typical of BCS SCs – modest change in properties[21] – while triplet pairing is predicted to be highly sensitive to disorder.

There are few other experiments that can supplement, or confirm, the current understanding, viz. circular Kerr rotation and small angle neutron scattering. In preceding theoretical work, the vector potential of the muon magnetic moment has been mentioned occasionally but its effects not pursued. In this paper the consequences of the muon's vector potential, both spin and orbital, have been introduced and given analysis in some respects, leaving more difficult formal and numerical aspects for further work.

A. Normal state

When the polarized muon in injected into a crystal, it comes to rest in an interstitial position, avoiding the positively charged ion cores but choosing favorable interactions with negatively charged electrons. At this point time-reversal symmetry is broken, most strongly in the immediate environment of the muon – which is also the only position the crystal is sampled, the muon position. Not only does this override the claim of (highly exotic) *time-reversal symmetry breaking*, it biases the system magnetically with respect to the muon polarization direction – which is also the key aspect that the measurement takes advantage of.

Already in the normal state, where nothing is obtained from the limited information that can be gained from a single muon with its 2.2 μs mean lifetime, the near region of the muon becomes impacted by the muon's magnetic field, which has a r^{-3} divergence for electron density approaching the muon. The muon field has a value much larger than or equal to that of the inferred spontaneous magnetic field out to interatomic distances, and – more concerning – diverges to and beyond tesla strengths near the muon. Its field produces spin and orbital polarization in the region, as well as charge currents characteristic of a spatially varying magnetic field. This polarization creates a magnetic moment at the muon's position. In initial spherical approximation (muon in a homogeneous electron gas) the induced field at the muon's site is zero by symmetry. The low site symmetry of the muon will lead to a non-zero field.

The full, seemingly straightforward, integral for the field at the muon site contains by a badly divergent r^{-4}

factor in the integrand. Incorporating broken spatial symmetry by the position of the muon (anisotropy), and three difficult to quantify quantum manybody effects – saturation of the (non-linear) susceptibility, quantum uncertainty of the muon position, parallel-spin electron pair correlations – the field at the muon becomes non-zero but with a magnitude that will require challenging formal and numerical work to specify.

Faced with the identical divergence in their study of nuclear magnetic resonance, Abragam and Bleaney[114] reverted to a relativistic Dirac formalism, and arrived at a regularized result (somewhat akin to changing the order of integration) that is still based on a one-electron wavefunction picture. The same issue would appear in proton NMR, but being an order of magnitude smaller.

As mentioned, already in the normal state there is a magnetic field at the muon's site. It produces no observable effect because (1) the field is nearly collinear with the muon's moment (spin) and produces negligible torque on the moment, and (2) the field would be part of the background of depolarizing electronic and nuclear fields, which would suffer little change upon entering the superconducting state. In short: the muon lives in a singular, perhaps turbulent, small volume, an environment of its own making, and never experiencing the superconducting state locally.

B. Superconducting state

Entering the superconducting state, the environment changes in a few ways. The induced B^{μ}-field due to electron spin polarization might remain, or it might be opposed by the opening of the SC gap, vying for Fermi surface electrons. The muon's magnetic field (together with that of the polarized electrons, which is relatively small, but keep in mind the inferred fields are near the lower limit of detection) leads to the onset of supercurrents, perhaps in competition of the order parameter as well as the conventional electromagnetic fields. These supercurrents strive to protect the bulk of the superconductor from the muon's field – an internal Meissner-like effect. Near the muon, the system will be non-superconducting, as magnetic field of the magnetic moment of the muon exceeds far beyond the critical field of the superconductor. This gaplessness near the muon may be undetectable with known probes.

Secondly, resistance-less current flow will allow the (super)current flow implied by London's and Maxwell's equations (which in the normal state decay due to resistance). Superconducting quantization of the magnetic flux leads to a flux vortex circulating around the axis of the muon moment, narrow at the 'equator' centered on the muon where the field is strongest, growing large in area for large $|z|$. The driving force for the supercurrent is to enforce an internal Meissner effect, protecting the bulk of the superconductor from the muon's magnetic field. This orbital supercurrent will create a field acting back on the muon site, with onset below T_c just as the onset of the gap appears.

The field in the midst of opening of the gap will drive creation of (one or more) Yu-Shiba-Rusinov states (μYSR states) localized with magnetic character, within the gap. Such states have been studied for magnetic ion moment impurities in a solid, where coupling is through well studied atomic orbital related exchange; study of muon magnetic moment driven local states remains for the future.

Either the emergence of supercurrents, or the establishment of YSR states, both arising below T_c, may provide the mechanism for coupling of the gap opening. These questions, outlined in the previous sections, remain as important tasks for future study.

C. Compilation of loose ends

This set of notes addresses only the class of apparently normal Fermi liquid superconductors, a handful that have been identified by μSR depolarization data as TRSB, against a few which have been checked, with no additional depolarization in the SC state being detected. This class comprises the class of *fragile magnetic superconductors.* Polar Kerr rotation experiments have identified TRSB signals in oxide superconductors (Sr_2RuO_4, YBCO) and ferromagnetic/SC superlattices, again with the signals near the limit of detection – a fraction of one μradian.[151] The source of this inferred TRSB is mentioned in relation to magnetic fields but without specific discussion. Only the simpler class of Fermi liquids is addressed here.

Several items contribute to a set of loose ends left for study.

- Time reversal symmetry broken already in the normal state, most strongly near the muon site where the measurement originates, by implantation of the polarized muon. Polarization of the nearby electronic system, and the additional magnetic field that it produces, arises as a consequence of the muon's magnetic field.

- The diverging magnetic field and increasing disturbance approaching the muon position causes an unquantified modification of the (spin) distribution and the (orbital current) magnetization of the region, involving parallel spin correlation, the saturating magnetic susceptibility, and the quantum uncertainty of the muon's position. Magnitudes of the effects will be challenging to obtain. The field at the muon site would however become part of the background from nuclear and electron magnetic moments.

- As often noted, the inferred spontaneous magnetic field is near the lower limit of detection. All host materials will also give rise to fields at the muon site, but below the limit of sensitivity.

- The measured parameters of the superconducting phase are typical of seemingly similar non-TRSB

compounds: coherence lengths, critical fields, penetration depths, magnetic susceptibility, specific heat jump at T_c. In a triplet SC, these properties depend on the character of the order parameter, and they can be dramatically different.

- In two cases ($LaNiC_2$ and $LaNiGa_3$), the electron-phonon coupling strength and singlet T_c has been calculated, obtaining consistency with the experimental value and providing singlet phonon-coupled superconductivity as the likely pairing mechanism.
- In the SC state, the muon moment should create and sustain a single quantum of flux entered on the muon and extending as a vortex. The associated supercurrents give rise to a magnetic field at the muon site that "turns on" below T_c. The effect of this field on depolarization depends on the degree of anisotropy of the environment of the muon.
- A magnetic impurity (viz. muon) is expected to creates localized "μYSR" states within the SC gap, providing a coupling between the muon and the SC order parameter that remains to be elucidated.
- The type of order parameter, currently the INT model in $LaNiGa_2$ and another material or two, may not be as constrained by experimental facts as originally expected, given the unsettled items discussed here.

XIV. APPENDICES

A. The fundamental Hamiltonian

1. Electrons and a muon in a static lattice

With the muon producing a vector potential $\vec{A}^{\mu}$ in an electron gas, and allowing for a spontaneous vector field $\vec{A}^{spon}$ appearing below T_c, the non-relativistic Hamiltonian for the muon and the conduction electrons is (leaving the subscript e off electron operators)

$$\begin{aligned} H^{orb} &= \frac{[p_{\mu} + \frac{e}{c}\vec{A}^{spon}(\vec{r}_{\mu})]^2}{2m_{\mu}} + \sum_{j,s} \frac{[p_{j,s} - \frac{e}{c}\vec{A}(\vec{r}_{j,s})]^2}{2m} \\ &\quad - \sum_{j,s} \frac{e^2}{|\vec{r}_{j,s} - \vec{r}_{\mu}|} + V^{e-ion} + V^{e-e} \\ &\quad + H^{\mu-ion} + T^{ion} + V^{ion-ion} \\ \vec{A}(\vec{r}) &= \vec{A}^{\mu}(\vec{r}) + \vec{A}^{spon}(\vec{r}) \\ \vec{A}^{\mu}(\vec{r}) &= \nabla \times \frac{\vec{\mu}}{r} = \frac{\vec{\mu} \times \vec{r}}{r^3}. \end{aligned} \tag{25}$$

Several terms are abbreviated with self-evident notation. In an applied field the corresponding vector potential A^{ext} would be included in each vector potential term. The electronic terms are to be treated with DFT methods, and the ion kinetic energy T^{ion} vanishes for static atoms. Treating the vector potential in density functional terms requires current density functional theory (CDFT)[115], which has not been implemented in current codes. Nuclear vector potentials are not displayed here, nor are those of the itinerant electrons which without polarization are presumed to average out, randomly or statistically. Each vector potential field is evaluated at the position of the respective moment. The first term is for the muon, the second is the kinetic energy for all electrons. The muon does not experience its own field. The curl operators provide the magnetic fields that couple to the moments.

Moving to Dirac's relativistic treatment of the kinetic energy operator results in expressions that involve the particle (muon and electrons) spin moments that couple to magnetic fields (other than their own), external or from other particles. The spin-related terms are

$$\begin{aligned} H^{spin} &= -\mu_B \sum_j \vec{\sigma}_j \cdot \nabla \times (\vec{A}^{\mu} + \vec{A}^{ind} + \vec{A}^{spon}) \\ &\quad + \ \vec{\mu} \cdot \nabla \times (\vec{A}^{ind} + \vec{A}^{spon}), \end{aligned} \tag{26}$$

where $\vec{\sigma}_j$ is the Pauli spin matrix of the j-th electron.

The quadratic term in the kinetic energy operator has the form

$$\begin{aligned} H^{(2)} &= \frac{e^2}{2mc^2}\vec{A}^2 = \frac{\mu_B^2\mu^2}{\hbar^2}\frac{(x^2+y^2)}{r^6} \\ &= \frac{\mu_B\mu^2}{\hbar^2}[\frac{\rho^2}{(\rho^2+z^2)^3}]. \end{aligned} \tag{27}$$

The last expression is written in the natural cylindrical coordinates ρ and z, with absence of the polar angle ϕ

reflecting the circular symmetry. This term falls off as r^{-4}; on the other hand, it diverges with the same power as r approaches the muon position, becoming worse as z approaches zero. With the factor $2mc^2$ in the denominator it is unlikely to contribute to low energy physics. It will not be necessary in this paper to be more strict about the formalism of the Hamiltonian.

The electronic system is first treated, as in Sec. III A, in the jellium picture of constant density: electron-electron repulsion is compensated by attraction to a smoothed version of the positive ion cores. Extension to band electrons is no problem for our considerations except for complicating equations and subsequent calculations (not done in this paper). The electronic part of this Hamiltonian can be transformed to occupation of states k, s within the Fermi surface, since we deal with systems very near the electronic ground state. The muon, located at the origin of coordinates in most equations, breaks translational invariance.

2. The muon magnetic operator

The linear-in-field term involving the muon in the Hamiltonian simplifies readily. For each electron j, s, and dropping this subscript for simplicity, ($\vec{A}^\mu$ is evaluated at $\vec{r}_{j,s}$; $\vec{p} = -i\hbar\nabla$)

$$\begin{aligned} H_B^\mu &= -\frac{e/c}{2m}[\vec{p}\cdot\vec{A}_\mu + \vec{A}_\mu\cdot\vec{p}] \\ &= \frac{2\mu_B}{\hbar}\vec{A}_\mu\cdot\vec{p}, \end{aligned} \tag{28}$$

using the definition of the Bohr magneton $\mu_B = e\hbar/(2mc)$ and noting that in the Coulomb (divergenceless) gauge $[\vec{p}\cdot\vec{A}^\mu]$ vanishes identically. Then the magnetic part of the Hamiltonian becomes (for each electron)

$$\begin{aligned} H_B^\mu &= \frac{2\mu_B}{\hbar}\vec{A}^\mu\cdot\vec{p} \\ &= \frac{2\mu_B}{\hbar}(-i\hbar)\frac{\mu}{r_3}(-y,x,0)\cdot(\partial_x,\partial_y,\partial_z) \\ &= -\frac{i\mu_B\mu}{r^3}(-y\partial_x + x\partial_y) \\ &= \frac{\mu}{r^3}\mu_B\frac{L_z}{\hbar} \to \frac{\mu\mu_B}{\hbar} < \frac{L_z}{r^3} > . \end{aligned} \tag{29}$$

This expression contains the μ/r^3 factor of $\vec{B}^\mu$ (Sec. III) leading to a troublesome radial integral to quantify the perturbation. $\vec{L}$ is the electronic orbital angular momentum operator relative to the muon at the origin. The Hamiltonian thus favors the development of an electronic angular momentum with respect to the muon position. This may produce an orbital magnetic moment, allowed by the broken TRS due to the muon magnetic moment.

The vector potential accompanying the μ^+ magnetic moment, which does not affect the muon that creates it, is conventionally treated in the Coulomb gauge $\vec{\nabla}\cdot\vec{A} = 0$, as

$$\vec{A}_\mu(\vec{r}) = \nabla\times\frac{\vec{\mu}}{r} = \frac{\vec{M}\times\hat{r}}{r^2} = \frac{M}{r^3}(-y,x,0), \tag{30}$$

a toroidal vortex field that displays a singularity at the muon site. We consider the ground state: the muon sits in a stable quadratic potential in its harmonic oscillator ground state with its spin along the z-axis, and the electrons are in, or very near, their ground state.

The dipole magnetic field, from above, is (neglecting the Fermi contact δ-function term[52])

$$\begin{aligned} \vec{B}_\mu(\vec{r}) &= \nabla\times\vec{A}(\vec{r}) \\ &= \frac{3\hat{r}(\hat{r}\cdot\vec{M}) - \vec{M}}{r^3} \\ &= M\frac{3\hat{r}(z/r) - \hat{z}}{r^3} \\ &= \frac{M}{r^3}(3\frac{xz}{r^2}, 3\frac{yz}{r^2}, 3\frac{z^2}{r^2} - 1). \end{aligned} \tag{31}$$

Treated as a perturbation, the first order change in energy of an electron in state $\eta_{n\ell m_\ell}(\vec{r})$ in a spherical potential is

$$\begin{aligned} \Delta E &= < \eta_{n\ell m_\ell}|\frac{\mu}{r^3}\mu_B\frac{L_z}{\hbar}|\eta_{n\ell m_\ell} > \\ &= \mu\mu_B m_\ell < n\ell m_\ell|\frac{1}{r^3}|n\ell m_\ell > . \end{aligned} \tag{32}$$

This expression as written is indeterminate for s orbitals: the orbital is finite at the origin so the integral is $\int r^2dr/r^3$, thus a logarithmically divergent result if the dr integral is done first. The $m_\ell = 0$ for s orbitals would give a zero result if the angular integral were to be done first and the environment has circular symmetry. For higher ℓ states $p, d, f, ...$, the wavefunction is proportional to r^ℓ, thus giving an extra $r^{2\ell}$ factor in the integrand near the origin and a finite integral. Since small quantities are the topic here, one can note that a similar question arises in a relativistic treatment (Dirac equation), where the $p_{1/2}$ orbital is non-zero at the origin.

A workaround for this indeterminate integral was given by Abragam and Bleaney.[114] Reverting to the relativistic Dirac equation, the integrand for the matrix element (evaluated with the large component of the wavefunction $\gamma(\vec{r})$) was manipulated using the expression $\vec{A} = \nabla\times(\vec{\mu}/r)$. The perturbation term is

$$i\frac{\beta}{\hbar}\vec{\sigma}\cdot < \gamma|[\vec{A}\times\vec{p} + \vec{p}\times\vec{A}]|\gamma > \tag{33}$$

where β is the 4×4 β-matrix. The gradient operator operates on the function γ, and $\gamma^*\nabla\gamma$ is one half of the density gradient $\nabla\gamma^*\gamma$. Thus the derivative operator that had non-relativistically resulted in a r^{-3} factor in the denominator has been transferred to the gradient of the (large component) spin current

$$\vec{J}_{spin} = \nabla\times|\gamma(\vec{r})|^2\vec{\sigma}, \tag{34}$$

leaving only a r^{-2} factor in the denominator of the integrand, which is regularized by the r^2dr volume factor. Their interpretation is that the key is to replace the usual expression of the vector potential by the differential form

$$\vec{A} = \nabla\times\frac{\vec{\mu}}{r}. \tag{35}$$

The ground state orbital (above denoted by γ) is quite asymmetric for a general non-symmetric position of the muon, and will include $p, d, ...$ symmetry contributions in a spherical expansion. The $s_{1/2} - p_{1/2}$ contribution to the gradient of the spin density will be regularized in the same manner as the diagonal s treated just above, and higher-ℓ contributions will approach zero in a way that the integrals are straightforward and finite.

A textbook comment about the dynamics: semiclassically, an electron on the Fermi surface (of a HEG) at point $\vec{r}$ relative to the dipole will experience, in addition to the local spin polarization, a force

$$F_k = -ev\vec{_k} \times \vec{B}(r) \to -ev_F\hat{k} \times \vec{B}(r). \qquad (36)$$

This force produces a circulation of currents around the field direction, with any net current being, by symmetry, collinear with the moment ($\hat{z}$) direction in the homogeneous limit. In intermetallic crystals the circulation is individually around the various Fermi surfaces, with consequences that modern codes can provide. In the very near field region, both the spin polarization and the orbital motions due to the muon's strong dipole field will be non-linear and difficult (i.e. require numerical treatment) to fathom, and to quantify.

B. Distance, moment, and magnetic field scales

To internalize distance and field scales, one can reference them to those of a positron or electron. The field strength along the z-axis is $2\mu_B/a_B^3$=25 T. The Bohr radius a_B is the distance scale of the $1s$ orbital of muon (or proton). For μ^+ with mass $207m_e$, the free-space field has magnitude 12.6 T/207=600 G. For comparison, inferred spontaneous magnetic fields at the muon site identified from μSR data lie three orders of magnitude smaller, at the 0.2 G scale.[63,64,66,68–73] The r^{-3} dependence gives the muon's field the value of 0.2 G around $r = 10a_B \approx$5-6 Å. The inverse cube dependence means that the field dies quickly beyond a_B but increases very rapidly for smaller r. At $a_B/10$, the field is 60 T. The electron density near the muon site is already at a very large field. The field strength at the critical field H_{c2} on the order of 0.2 T of $LaNiGa_2$ at a distance of 1.3 $\mathring{A}$. (The conversion in appropriate units here is $\mu = 0.448G\mathring{A}^3$, where μ is the moment of the muon.)

The magnetic flux quantum is $\Phi_o = 2.07 \times 10^{-15}$ Wb (Weber) in SI units, and in the cgs-gaussian units used in this paper, its value is

$$\Phi_o = 2.07 \times 10^{-15} T\ m^2 = 2.07 \times 10^9 G\ \mathring{A}^2 = 2.07 \times 10^3 T\ nm^2. \qquad (37)$$

To tie the unit magnetic flux strength to area scales, a selection of $\Phi_o/area$ versus *uniform field* B for given radius values follow.

$$\begin{aligned}
\Phi_o &= 2.07 \times 10^9\ G\ \mathring{A}^2 \\
\Phi_o/m^2 &= 2.07 \times 10^{-15}\ T \\
\Phi_o/\mathring{A}^2 &= 2.07 \times 10^5\ T \\
\Phi_o/\mu m^2 &= 2.07 \times 10^{-3} T = 20.7\ G \\
\Phi_o/(10\mu m)^2 &= 0.2\ G, \text{the spontaneous field} \\
\Phi_o/\pi\xi^2 &= 1.4T \quad (\xi \sim\ 35\ nm \text{ for } LaNiGa_2).
\end{aligned}$$

Thus one flux quantum spread uniformly over an area of one square μm corresponds to a field of 2.07×10^{-3} T = 20.7 G. For the field of 0.2 G reported for $LaNiGa_2$, the area enclosing one flux quantum is a circle of radius ∼10μm.

C. The μSR experiment

1. *The setup*

Overviews and reviews of the experiment and analysis were referenced in Sec. I. A synopsis is given here. The μ^+ ion, an elementary particle, decays after production with a half-life of τ_μ=2.2μs, producing a positron (conserving charge) and two neutrinos (one anti-electron type, one muon type, conserving lepton number). Positron emission occurs symmetrically around the direction of the muon spin, but with varying energy of the positron. The mass of the muon provides ∼100 MeV of energy for the decay products, of which the positron gets (presumably randomly) 25-50 MeV kinetic energy (its mass of 0.5 MeV can be neglected). At the lower end of emission energy, 25 MeV, emission is practically isotropic – at any angle with respect to the muon spin. Toward the higher range of energy 50 MeV, the angular dispersion of emission becomes strongly weighted toward the forward direction (the direction of the μ^+ spin at the time of decay), although with little variation within a cone of 40° of forward. These two distributions are pictured in Fig. 4. The spin-half moment has the largest quantum uncertainty of its direction (a mathematical concept, if not a physical one, since only s_z is specified). Thus $\vec{s}$ lies off-vertical by $\sin(s_z/|\vec{s}|) = \sin^{-1}(1/\sqrt{3})$=35° with random polar angle, a variation that must contribute to the distribution that varies little within the ∼±40° forward cone and increases as depolarization occurs.

Measurements of energies and angles by a battery of detectors enables quantification of the rate of depolarization of the muon spin before decay. Typical solid state processes are orders of magnitude quicker than the μ^+ lifetime, thus allowing accumulation of data representative of the muon within an electronic system in its thermodynamic state at temperature T and time t after deposition.

In a μSR experiment, a spin-polarized (aligned) beam of μ^+ particles is deposited into the sample, coming to rest at an isolated interstitial position in the sample without losing its (known) polarization. The direction of the muon spin defines our z direction. The muon's spin is

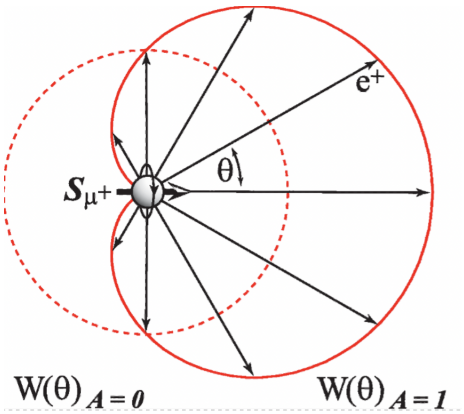

FIG. 4. Angular distribution of the direction of emission of the positron upon muon decay into a positron and two neutrinos, given by $W(\theta) \propto 1 + A\cos\theta$. The factor A depends on the energy of the emitted positron. Two positron energies are pictured: dashed line, 25 MeV near minimum, $A \approx 0$; full red line, 50 MeV near maximum, $A \approx 1$. The arrow denotes the muon spin direction upon decay. For reference: the rest mass of the muon is 207×0.511 MeV $\sim$ 100 MeV, which is what is available for the decay products. See text for further discussion.

associated with a point magnetic dipole μ at the muon site, in a favorable interstitial position (away from positive atomic cores), in metals typically not pictured as being bonded with an atom.

It is like the much studied proton interstitial; Takada *et al.*[116] have studied the model of a proton in an electron gas from high density, where the system becomes like a proton mixing with and screened by electrons, to the low density regime where the proton attracts an extra electron to become an H^- ion favored by the filling of the $1s$ shell. Returning to the muon, the difference in mass affects the size of its magnetic moment, which is an order of magnitude larger than that of the proton. We confine our interest to intermetallic metals with typical metallic densities; semimetals and insulators require their own treatment. Relevant units and magnitudes are presented in Appendix XIV B.

2. *The data and analysis*

Typically presented from zero-field studies is the rate of depolarization $\sigma(T)$. Above T_c there is a background temperature independent depolarization from small quasi-static nuclear moment fields and from larger fluctuating electronic fields at a continuum of distances and with random directions of moments. These are presumed to average to some constant rate above T_c that is uninteresting. Below T_c in materials identified with TRSB, the rate increases with decreasing temperature to a value as $T \to 0$ that can be $\sim$10% above the normal state value but sometimes is only 3% enhanced. $\sigma(T=0) - \sigma(T)$ is interpreted in terms of depolarization arising from a field at the muon site, presumed to be that of a uniform magnetic spontaneously appearing field.

The key result in zero-field experiments is the time development (relaxation) of the muon moment polarization, followed by the process of muon decay. Theories of the depolarization process have been presented at a few levels, of which three are mentioned here. Often the 1967 Kubo-Toyabe functional form,[117] which takes into account a stochastic depolarization field and anisotropy, is adopted as a first step in the process to fit the depolarization data and extract materials properties. The Kubo-Toyabe form gives the polarization distribution G^{KT} versus time as

$$G_z^{KT}(t) = \frac{1}{3} + \frac{2}{3}(-\sigma^2 t^2)e^{-\sigma^2 t^2/2}, \tag{38}$$

where $\sigma = \gamma\Delta$ in terms of the isotropic Gaussian distribution width and the muon gyromagnetic ratio $\gamma = 2\pi \times 13.55$ KHz/G. This form is used to fit data in many μSR papers.

Kornilov and Pomjakushin[118] in 1991 extended the theory to include include a randomly-directed field with δ-function strength H_o (apparently modeling a polycrystalline host) as well as the Gaussian distribution. The analytic expression they obtained is

$$G_z^{KP}(t) = \frac{1}{3} + \frac{2}{3}[1 + (\sigma^2 t/\omega)^2]e^{-\sigma^2 t^2/2} \times [\cos\omega t + \tan^{-1}(\sigma^2 t/\omega)], \tag{39}$$

where $\omega = \gamma H_o$ in terms of the δ-function field H_o. This formula introduces a frequency $\omega = \gamma H_o$, and plots of the difference from G_z^{KT} versus σt were presented.

A recent (2020) description has been given by Takahashi and Tanimura[119] that is said to consist of a more fully quantum derivation and includes the thermal bath of vibrations and spins, hence giving a T-dependent expression resulting from their hierarchical equation of motion method. The result requires numerical solution and fitting of several parameters, hence the identification of a specific field value from experimental data is less direct.

The calculation of depolarization while the muon is in place is the first step, the second is the decay. (i) The decay energy E_μ of the position varies from roughly 25 MeV to 50 MeV (1/4 to 1/2 of the muon rest mass energy). (ii) The direction of emission of the positron, often described as primarily forward in the angular distribution of the muon polarization at the time of decay, is more interesting, being rather strongly E_μ- dependent. Defining the energy parameter $\zeta = E_\mu/m_\mu c^2$, denoting the fractional polarization at time of decay as P_μ, and using θ and the angle between spin at decay relative to the initial polarization, the decay distribution from the Standard Model (SM) of particles is?

$$\frac{d^2\Gamma}{d\zeta d\cos\theta} \propto \zeta^2\Big[(3-3\zeta) + \frac{2}{3}\rho(4\zeta-3) + 3\eta\zeta_o\frac{1-\zeta)}{\zeta} + +P_\mu\xi\cos\theta[(1-\zeta) + \frac{2}{3}\delta(4\zeta-3)]\Big] \tag{40}$$

in terms of the SM parameters are $\rho = \delta = \frac{3}{4}, \xi = 1, \eta = 0$ as calculated my Michel. $x_o = m_p/E_{max}$ is a small

constant, $E_{max} \sim m_\mu c^2/2$. There is not good reason to try to understand this distribution, the point is that it is a SM result and there has not yet been any known violation of the SM.

With suitable detectors, the experiment averages over the positron energy, giving the simple result

$$\frac{d\Gamma}{d\cos\theta} \sim 1 - \frac{1}{3} P_\mu \cos\theta. \tag{41}$$

Presumably this distribution is convoluted appropriately with the thermal distributions above to obtain the expression from which a spontaneous field can be extracted; general publications to not go into that much detail.

3. Experimental data of interest; $LaNiGa_2$ example

There are approaching ten superconductors currently labeled as exotic, including several (see references in the previous subsections) with proposed TRSB OPs supported primarily by μSR data. That the muon disturbs the sample[43] has been incorporated into the theoretical picture: once μ^+ comes to rest in the sample, it is much like an interstitial proton, which has been heavily studied in the context of ionic conductors, hydrogen storage applications, etc. The character and degree of lattice disturbance has not yet been calculated for SCs with exotic OPs. The most evident model – of a point charge in an electron gas – has received separate study. In a metal, the point charge attracts a local charge density that in first approximation is like the H $1s$ density, since screening is mild at distances less than one bohr.

A crystal, which is of interest here, is more involved. It has been established that the proton or μ^+ can cause relaxation of neighboring atoms by a few tenths of an Angström[43], *i.e.* the sample has been disturbed locally.

The proton is the lightest of possible interstitial nuclei in a crystal. Anharmonicity of its vibrations due to its small mass has been studied in several cases, viz. the impact of H in superconductors such as PdH_x with its surprisingly high $T_c \sim 10$K (for Pd) and its inverse isotope shift of T_c.[120] A related complication lies in the quantum uncertainty of its position at an interstitial site.[43] While there is an instructive history of these effects in the literature, the present description considers both effects in the more extreme case of a μ^+ particle in a crystal.

The proton is not the lightest particle probe of condensed matter. Before returning to the μ^+ particle, we mention the positron e^+. Upon insertion, it comes to rest due to strong Coulomb interactions, but resides in (at low temperature) the ground state positron extended Bloch orbital, where it annihilates with an electron e^-, from which positron emission tomography (PET scans) has emerged.

With 207 times larger mass, the μ^+ elementary particle rapidly comes to a stop in a crystal and finds the preferable interstitial site,[43] The weakness of the confining potential in the interstitial site allows large quantum uncertainty in the position of the muon,[43] making quantum behavior important to include in the interpretation of μ-based studies. This effect, and that of anharmonicity more generally, can be handled reasonably by modern DFT methods.[39,121]

D. Symmetry of the dipolar field

The point dipole of the muon corresponds to an axial vector potential, given here in the Coulomb gauge, and corresponding magnetic field, for $\vec{\mu}=\mu\hat{z}$,

$$\begin{aligned}
\vec{A}^\mu(\vec{r}) &= \frac{\vec{\mu}\times\hat{r}}{r^2} = \frac{\mu}{r^3}(-y,x,0) \\
\vec{B}^\mu_{tot}(\vec{r}) &= \nabla\times\vec{A}_\mu(\vec{r}) = \frac{3\hat{r}(\hat{r}\cdot\vec{\mu})-\vec{\mu}}{r^3} + \frac{8\pi}{3}\mu\delta(\vec{r}) \\
&= \vec{B}^\mu_{dip} + \vec{B}^\mu_{con}
\end{aligned} \tag{42}$$

with dipole and contact terms.

The magnetic field $\vec{B}_\mu(\vec{r}) = \nabla\times\vec{A}_\mu(\vec{r})$ is given by the textbook expression with the moment taken as the $\hat{z}$ direction

$$\begin{aligned}
\vec{B}^\mu(\vec{r}) &= \frac{3\hat{r}(\hat{r}\cdot\vec{\mu})-\vec{\mu}}{r^3} \\
&= \mu\frac{3\hat{r}(z/r)-\hat{z}}{r^3} \\
&= \frac{\mu}{r^3}(3\frac{xz}{r^2}, 3\frac{yz}{r^2}, 3\frac{z^2}{r^2}-1) \\
&= \frac{3\mu}{r^3}(\sin\theta\cos\theta\cos\phi, \sin\theta\cos\theta\sin\phi, \\
&\qquad \cos^2\theta - \frac{1}{3} \\
&= \frac{\mu}{r^3}[2\cos\theta\ \hat{r} + \sin\theta\ \hat{\theta}] \\
&\equiv \frac{3\mu}{r^3} f(\theta,\phi),
\end{aligned} \tag{43}$$

where $|f(\theta,\phi)| \leq 1$ is the angular variation. The δ-function term (Fermi contact term) of the dipole field $(8\pi/3)\mu\hat{z}\delta(\vec{r})$ is, with relativistic extensions finite, and small for small Z.[52] These different forms of the common point dipole expression, including the one in polar coordinates, are useful for following symmetry considerations. Units are cgs-gaussian as used in Jackson's classic textbook on classical electrodynamics.[122]

The system symmetry of the dipolar magnetic field $\vec{B}(x,y,z)$ includes the following:

- for $x \to -x$ the x-component changes sign, and analogously for the y-component (cylindrical symmetry),
- the cylindrical symmetry gives

$$\sqrt{B_x^{\mu\,2} + B_y^{\mu\,2}} = 3\mu|\sin\theta\cos\theta|/r^3 \tag{44}$$

independent of ϕ. Only the z-component is non-zero along the axis and in the x-y plane

- the z-component is invariant under z-reflection, the x and y components reverse under z-reflection
- altogether, there is inversion symmetry: $B^\mu(-\vec{r}) = B^\mu(\vec{r})$.

A consequence is that the HEG+μ^+ system, introduced in Sec. III A, has this same axial symmetry.

E. Field at μ^+ site due to magnetic polarization

Each volume element of electron moment $\vec{M}^{ind}(\vec{r})\Delta V$ will produce the same form of dipole field $\vec{B}^{\mu}(\vec{r}')\Delta V$ from the magnetization from $\vec{r}'$ via $\chi_p \vec{H}^{\mu}(\vec{r})$ as given by the dipole expression , except that the original origin $\vec{0}$ will be assumed by $\vec{r}$ and the position of a given field point will be $\vec{r'}$.

Then

$$\vec{\mathcal{B}}(\vec{r}') = \int d^3r \frac{3\widehat{(r'-r)}\vec{M}^{ind}(\vec{r})\cdot\widehat{(r'-r)} - \vec{M}^{ind}(\vec{r}'-\vec{r})}{|r'-r|^3}.$$

Simplification occurs because we are only interested in the field at the muon site, *i.e.* at $\vec{r'} \to 0$, so $\widehat{\vec{r'}-\vec{r}} \to -\hat{r}$. Note: $\hat{z} = (0,0,1)$ is a direction and remains unchanged. Then

$$\begin{aligned}\vec{\mathcal{B}}(0) &= \int d^3r \frac{3(-\hat{r})\vec{M}^{ind}(\vec{r})\cdot(-\hat{r}) - \vec{M}^{ind}(\vec{r})}{r^3} \\ &= \int d^3r \frac{3\hat{r}\vec{M}^{ind}(\vec{r})\cdot\hat{r} - \vec{M}^{ind}(\vec{r})}{r^3}. \end{aligned} \tag{45}$$

F. The small-r region in more detail

As mentioned, the (so far) divergent B field at the muon site will enforce full electronic spin polarization $P(r) \to P(0) = 1$

$$P(r) = \frac{n_\uparrow(r) - m_\downarrow(r)}{n_\uparrow(r) + m_\downarrow(r)}, \tag{46}$$

for which the longitudinal magnetic susceptibility vanishes. Likely the decay from full polarization $P(0) = 1$, hence the onset of susceptibility, will be at least as slow as r^2, and this will regularize the infrared divergence.

Accurate solution to this problem, even at the homogeneous electron gas level, seems non-trivial given the Fermi repulsion between electrons: two electrons of the same spin cannot exist at the same place; the pair distribution function of parallel spin electrons vanishes at zero separation in any electronic system. The B-field growing as r^{-3} and the Coulomb attraction as $-r^{-1}$, along with the Fermi repulsion, a 2-body (many-body) effect, likely makes this a numerical many-electron problem, viz. Gutzwiller-Hartree-Fock or better. [The vector potential $\vec{A}(\vec{r}) = \vec{M} \times \hat{r}/r^2$ that appears in the Hamiltonian has a weaker singularity at the origin. However, the kinetic energy term $-\frac{\hbar^2}{2m}(\vec{p} - \frac{e}{c}\vec{A})^2$ brings in a $1/r^3$ magnetic field energy term and other complexities].

In cylindrical coordinates the azimuthal angle ϕ separates out due to the cylindrical symmetry, but one is left with coupled 2nd order differential equations in the radial ρ and axial z coordinates, definitely a numerical problem. Note: this problem seems to be an analytic one for the H atom (or muonic atom), since the orbitals are analytic functions, and it's a one-electron problem.

G. Induced magnetization; resulting B field

We only need the z-component of the field, since the cylindrical symmetry allows no x- or y-component. The dot product in the above expression is

$$\begin{aligned}\vec{M}^{ind}(\vec{r})\cdot\hat{r} &= \chi_p(r)\vec{B}_\mu(\vec{r})\cdot\hat{r} \\ &= \chi_p(r)\frac{\mu}{r^3}(3\frac{xz}{r^2}, 3\frac{yz}{r^2}, 3\frac{z^2}{r^2} - 1)\cdot(x,y,z)/r \\ &= \chi_p(r)\frac{\mu}{r^3}\left[(3\frac{x^2}{r^2} + 3\frac{y^2}{r^2}) + (3\frac{z^2}{r^2} - 1)\right]\frac{z}{r} \\ &= \chi_p(r)\frac{\mu}{r^3}\frac{z}{r}[2] = \chi_p(r)\frac{2\mu}{r^3}\frac{z}{r} = \chi_p(r)\frac{2\mu\cos\theta}{r^3}.3\frac{z}{r}(\vec{M}^{ind}(\vec{r}\end{aligned}$$

This term is non-negative, being large along the $\hat{z}$-axis and zero in the x-y plane. It is worthy of note that the x and y dependence has dropped out of the dot product of two vectors depending (apparently) independently on $\vec{r}$. It is due, again apparently, to the symmetries of each.

After subtracting off the $M_z^{ind}(\vec{r})$ term in the dipolar field that is large along the $\hat{z}$-axis negative in the x-y plane, the z-component of $\vec{B}(0)$ involves some cancellation: the 'incoming' dipolar field from the muon is interfered with by the 'outgoing' dipolar fields from each point $\vec{r}$. The result becomes

$$\begin{aligned}B_z(0) &= \int d^3r\chi_p(r)\left[\frac{3z}{r}\,(\frac{2\mu}{r^3}\frac{z}{r}) - \frac{\mu}{r^3}(3\frac{z^2}{r^2} - 1)\right]/r^3 \\ &= \mu\int d^3r\chi_p(r)\left[6\frac{z^2}{r^2} - (3\frac{z^2}{r^2} - 1)\right]/r^6 \\ &= \mu\int r^2\ dr\ d\nu\ d\phi\chi_p(r)\left[3\frac{z^2}{r^2} + 1)\right]/r^6 \\ &= 8\pi\mu\ \int \chi_p(r)\frac{dr}{r^4}, \end{aligned} \tag{47}$$

leaving, at this level of discussion, a divergent field at the muon site. Because the z-component within the integrand is non-negative there is no cancellation within the r integral. The strong small-r divergence is startling, but at small r non-linear response (substituting for χ_p) and quantum effects require reconsideration. Discussion of the resolution of this unphysical result is given in Sec. V.

It is interesting to look at the angular dependence of $\vec{B}(\vec{r})^2$, which is proportional to the energy density of the field. Using Eq. 43,

$$[\vec{B}^{ind}]^2 = \frac{\mu^2}{r^6}(1 + 6\cos^2\theta). \tag{48}$$

which at a fixed value of r has a maximum along the poles and a minimum in the x-y plane.

H. Operator representation for induced B-field

The magnetic field of the muon, with magnetization $\vec{M}^{\mu}(\vec{r}) = \vec{\mu}_\mu\delta(\vec{r})$, gives rise to the well known dipolar

magnetic field in Appendix XIV D. The linear relationship suggests the definition of an integral "dipolar operator" $\mathcal{D}(\vec{r}-\vec{r'})$ by

$$\vec{B}(\vec{r}) = \int d\vec{r'}\mathcal{D}(\vec{r},\vec{r'})\vec{M}(\vec{r'}) = \int d\vec{r'}\frac{3\ \widehat{\vec{r}-\vec{r'}}[\widehat{\vec{r}-\vec{r'}}\cdot\vec{M}(\vec{r'})]-\vec{M}(\vec{r'})}{|\vec{r}-\vec{r'}|^3}, \quad (49)$$

which gives the magnetic field $\vec{B}(\vec{r'})$ due to any magnetization field $\vec{M}(\vec{r})$. Applying this to the z-oriented μ^+ point magnetic moment gives Eq. 43 and is visualized in Fig. 1.

The field

$$\vec{B}^\mu(\vec{r}) = \int d\vec{r'}\mathcal{D}(\vec{r},\vec{r'})\vec{\mu}\delta(\vec{r'}); \quad \vec{B}^\mu = \mathcal{D}\vec{M}_\mu, \quad (50)$$

polarizes the electron density according to the susceptibility χ_p, $\vec{M}^{ind}(\vec{r}) = \chi_p(n(\vec{r}))\vec{B}_\mu(\vec{r})$ [in operator notation $M^{ind} = \chi_p B^\mu$]. This electronic magnetization (excess of $\uparrow$ moments over $\downarrow$ gives rise to its own magnetic field which becomes, in terms of the dipole operator

$$\begin{aligned}\vec{B}^{ind} &= \mathcal{D}\vec{M}^{ind} = \mathcal{D}\chi_p\vec{B}^\mu = \mathcal{D}\chi_p\mathcal{D}\vec{M}^\mu;\\ \vec{B}^{ind}(\vec{r}) &= \int d^3r' \int d^3r''\mathcal{D}(\vec{r},\vec{r'}) \\ &\quad \times \ \chi_p(n(\vec{r'}))\mathcal{D}(\vec{r'},\vec{r''})\vec{M}^\mu(\vec{r''})\\ \vec{B}^{ind} &= \mathcal{D}\chi_p\mathcal{D}\vec{M}^\mu. \end{aligned} \quad (51)$$

There are two important simplifications. First, we want only the on-site $\vec{r}=0$ field. Second, the original field arose from the point muon $\vec{r'}=0$, which removes the second integral. In addition, $n(\vec{r})$ varies smoothly by a factor of two or less in an interstitial site in a metallic compound, and $\chi_p(n)$ is a regular and moderately varying function of n,[50] so we pull a representative value $\bar{\chi}_p$ out of the integral. This leaves

$$\vec{B}^{ind}(0) = \bar{\chi}_p \int d^3r'\mathcal{D}(0,\vec{r'})\mathcal{D}(\vec{r'},0)\vec{\mu}. \quad (52)$$

This integral has the look of $\bar{\chi}_p < \mathcal{D}^2 > \vec{\mu}$, and indeed $calD(-\vec{r}) = \mathcal{D}(\vec{r})$ bears out this positive integrand. Note that the last part $\mathcal{D}(\vec{r'})\vec{\mu}$ is $\vec{B}^\mu$, whose integral vanishes by the symmetries listed in Appendix **??**.

The magnetization $M^{ind}(\vec{r})$ is operated on by the dipolar operator $\mathcal{D}(0,\vec{r'})$T Simplifying the integration variable to cylindrical coordinates with z-component of $\hat{r} = z/r$):

$$\begin{aligned}\vec{B}^{ind}(0) &= \bar{\chi}_p \int d^3r \frac{1}{r^3}[3\hat{r}\cdot[\frac{3\hat{r}(\hat{r}\cdot(\vec{\mu})-\vec{\mu}]}{r^3}] \\ &\quad -[\frac{3\hat{r}(\hat{r}\cdot\vec{\mu})-\vec{\mu}}{r^3}]\\ &= \mu\bar{\chi}_p\int\frac{d^3r}{r^6}3\hat{r}[3\frac{z}{r}-\frac{z}{r}]-[3\hat{r}\frac{z}{r}-1]. \end{aligned} \quad (53)$$

The z-component is

$$\begin{aligned}B_z^{ind} &= \mu\bar{\chi}_p\int\frac{d^3r}{r^6}[9\frac{z^2}{r^2}-3\frac{z^2}{r^2}]-[3\frac{z^2}{r^2}-1]\\ &= \mu\bar{\chi}_p\int_0^\infty\frac{2\pi\ r^2dr}{r^6}\int_{-1}^{+1}d\nu\ (3\nu^2+1), \end{aligned} \quad (54)$$

using spherical coordinates. This procedure reproduces the more direct result of Appendix XIV G, a divergent integral that must be regularized by quantum or relativistic effects.

I. Quantum fluctuation of the muon

The infrared divergence of the integral Eq. 54 is daunting and unphysical. Additional factors must be entering the physics. An obvious one is zero-point uncertainty of the muon.

An obvious issue is zero-point uncertainty (ZPU) of the muon position, often inaccurately called zero-point motion. While the harmonic oscillator ground state (harmonic phonon)already contains an uncertainty, interstitial protons in crystals are known to encounter anharmonicity, and the order of magnitude lighter muon will be even more anharmonic with larger ZPU. This effect has been calculated to impact the ground state interstitial position of the muon.[43] Obviously this effect cannot be treated in a HEG model, but the physics is reasonably clear.

Relative to the equilibrium (stable) position of the muon, the quadratic (harmonic oscillator [HO]) potential felt by the muon will lead to the HO ground state wave function $\psi(r) = C\ exp(-\alpha r^2/2)$ where α is an inverse mean square displacement and C is a normalization constant. The expectation value in this state will be

$$\int d^3r\psi(r)\frac{8\pi\mu}{r^4}\psi(r) \propto \int r^2\frac{e^{-\alpha r^2}dr}{r^4} \sim \int\frac{dr}{r^2}, \quad (55)$$

i.e. the divergence is reduced by the small phase space at small r but is still 'infrared' divergent. Anisotropy of the HO potential will not reduce this remaining infrared divergence, which appears to require an additional r^2 factor within the integral.

J. Pair correlation

As mentioned, the (so far) divergent B field at the muon site will, at the simplest level, enforce full electronic spin polarization $P(r) \to P(0) = 1$

$$P(r) = \frac{n_\uparrow(r)-n_\downarrow(r)}{n_\uparrow(r)+n_\downarrow(r)}, \quad (56)$$

near the muon site, an upper limit at and beyond which the longitudinal magnetic susceptibility χ_p vanishes: a fully polarized system cannot be further polarized. From variational[53,54] and quantum[55] Monte Carlo calculations

on correlated wave functions (Gutzwiller-Slater determinants) the decay from full polarization $P(0) = 1$, hence the onset of (some reduced) susceptibility, will arise as phase space reduction will regularize the infrared divergence, as we now describe.

Accurate solution to this problem, even at the homogeneous electron gas level, becomes non-trivial given the Fermi repulsion between electrons: two electrons of the same spin cannot exist at the same place; the pair distribution function $g_{\uparrow\uparrow}(r, r')$ of parallel spin electrons vanishes at zero separation in any electronic system. The B-field growing as r^{-3} and the Coulomb force as r^{-2}, along with the Fermi repulsion, a 2-body (many-body) effect, makes this a numerical many-electron problem, to be treated at the Gutzwiller-Hartree-Fock level or better. This effect does however provide the needed additional $r^2\ dr$ term that regularizes the integral.

In cylindrical coordinates the polar angle ϕ separates out due to the cylindrical symmetry, but one is left for relevant quantities with coupled 2nd order differential equations in the radial ρ and axial z coordinates, a numerical task.

K. μ^+ coupling to conduction electrons

The perturbation in charge, hence in atomic displacements, due to muon implantation are thought to be conventional, like that of a proton. Crucial to μSR is that the muon enters with its magnetic moment and its accompanying magnetic field. The total field, including the induced magnetization, was discussed in the main text. In the SC phase, supercurrents respond to the (inhomogeneous) magnetic field.

For simplicity let us consider the effect of the bare muonic field; the paramagnetic response to the density is very much the same shape, thus is a minor enhancement. The first-order in field term in the Hamiltonian is, after minor algebra, for electron i,

$$\begin{aligned} H^{mag} &= \frac{1}{2m}\{\vec{p}_i - \frac{e}{c}\vec{A}^\mu\}^2 = \frac{\vec{p}_i^2}{2m} \\ &- \frac{e}{2mc}(\vec{p}_i\cdot\vec{A}^\mu + \vec{A}\cdot\vec{p}_i) + \frac{e^2}{2mc^2}\vec{A}^2 \\ &= \frac{p_i^2}{2m} - \frac{e}{2mc}2\vec{A}^\mu\cdot\vec{p}_i + \frac{e^2}{2mc^2}\vec{A}^2 \\ &\approx \frac{p_i^2}{2m} - 2\mu_B\frac{\mu}{r^3}\vec{L}_{i,z} \\ &\sim \frac{p_i^2}{2m} - 2\ell_{i,z}\mu_B|\vec{B}^\mu(r)|. \end{aligned} \tag{57}$$

In the Coulomb (divergenceless) gauge ($\vec{p}_i\cdot\vec{A}$)=0, and the Bohr magneton $\mu_B = \frac{e\hbar}{2mc}$ has been introduced. $\ell_{i,z}$ is the $\hat{z}$ component of the angular momentum of electron i in units of $\hbar$.

In the electronic many-body ground state Ψ first order perturbation theory result is

$$\begin{aligned} \mathcal{E}^{mag} &= \int \Psi^*(r,\{r_j\})[-2\mu_B\frac{\mu}{r^3}\vec{L}_{i,z}]\Psi(r,\{r_j\}d^3r\{d^3r_j\} \\ &= -2\mu_B\frac{\mu}{\hbar} < \frac{L_z}{r^3} >_\Psi \end{aligned} \tag{58}$$

for each electron r_i. Recalling that the electron density at the muon site is finite, and the volume element is $4\pi r^2 dr$, this integral is logarithmically IR divergent unless (1) the expectation value of L_z is identically zero, or (2) higher ℓ contribution enter due to low symmetry. However, the muon environment is not spherically symmetric, so the integral does not vanish by symmetry. While opposite spin electrons may contribute opposing contributions to the integral, earlier sections have verified that the electronic density near the muon is highly polarized, so there is no precise up-down cancellation. Without any precise cancellation within the integrand and with a finite density at the muon site, the divergent integral requires more attention. The conclusion is that there is a non=zero energy from this muon-electron interaction.

In a crystal the angular momentum, formally defined as $\vec{L} = \vec{r}\times\vec{p}$, must be handled carefully.[111] The last line introduces the magnitude of the muon magnetic field for estimation of magnitudes. More significant is that the angular variation of the field, and the fact that the field lines return to their origin, guarantee that the field has no net direction – the integral of the field vanishes ($\vec{B}^\mu(-\vec{r}) = -\vec{B}^\mu(\vec{r})$). This raises a question about whether field effects will be first order or second order.

The effects on the Fermi surface states will be governed by first order matrix elements with conduction band itinerant states expanded in an angular momentum $[L \equiv (\ell, m)]$ expansion

$$\Psi_{k,n}(\vec{r}) = \sum_L b_L^{k,n} R_L^{k,n}(r) Y_L(\hat{r}) \tag{59}$$

with the origin at the muon site (not the host atom site) being midway between two or a few more atoms. These expansions near the muon site will involve *s-p* atomic orbital tails overlapping the region of the muon magnetic field.

The magnetic field perturbation matrix between perturbed Bloch states is

$$H'_{km,k'm'} = \vec{\mu}\cdot < \Psi_{k,m}|\vec{B}^{tot}|\Psi_{k',m'} > . \tag{60}$$

The perturbed Bloch states incorporate the muon density, so while translational symmetry is broken, states can still be labeled by the underlying Bloch basis, perhaps augmented by local functions if the muon energy lies within a band gap in which case localization requires a separate index. Each of the three functions can be expanded in an angular momentum representation around the muon, but the degree of various L, L', L'' contributions will be strongly dependent on the geometry, and on the direction of the muon moment, with no universal guidelines being apparent.

L. Kondo impurity in an exotic superconductor

This appendix follows from Sec. XIV S, providing an example of a Kondo impurity within an exotic OP in a spherical model. The question of impurity-induced magnetic fields in unconventional SCs was addressed by Choi and Muzikar,[78] taking an OP of the ^3He A-phase as an example: $\Delta(\hat{k}) = \Delta_o(\hat{k}_x + i\hat{k}_y)$. This OP describes an internal orbital momentum of the pair characterized by symmetry as 'ferromagnetic,' and the resulting supercurrents produce a magnetic field at the impurity site. Taking parameters thought at that early time to be characteristic of $YBa_2Cu_3O_7$, but with sizable uncertainty, they estimated a field of the order of 10 G well below T_c.

The Choi-Muzikar approximation for the on-site magnetic field is

$$B(0) = -\hat{z}\beta(T)(ek_F^2)(\frac{T_c}{T_F})^2\frac{v_F}{c}(\sigma k_F^2). \qquad (61)$$

Here $\beta(T)$ is a numerical factor that varies between zero and unity, ek_F^2 is a field value expected to be of order 10^2 T,[78] T_F is the Fermi temperature of the order of 5×10^4K for a large multisheeted Fermi surface metal ($E_F \sim 4-5$ eV), $v_F \sim c/300$ for good metals, and σ is the impurity cross-section for which σk_F^2 is expected to be of the order of unity. For these parameters the field is of the order of 10^{-3}G (give or take a couple of orders of magnitude, considering that their spherical energy band picture, with $1/T_F$ instead of $N(0)$, etc.), so this is a very rough estimate. T_F is a substitute for a bandwidth and in certain materials could be an order of magnitude smaller, which would make the estimate a factor of 10^2 larger. Broadly speaking, the strength of the field is expected to be small but it is not well constrained by this expression. A more general treatment of supercurrents in SCs has been given by Koizumi and Ishikawa[123] that gives a vivid impression of the complexity of the problem, but should be useful for further considerations.

M. YSR states in real materials

Computational developments in treating defects (large unit cells in DFT) and in modeling the Bogoliubov-de Gennes band structure of real superconductors has greatly extended the understanding of the spectra and energetics of YSR states in actual materials. Extending scanning tunneling methods to the study of magnetic atoms or molecules on superconductor surfaces has provided direct evidence of the behavior caused by YSR states.

The extension of the multiple scattering method (KKR: Korringa, Kohn, Rostoker) to handle very large unit cells opened up the study of truly isolated impurities. Similar extensions of band theory to the superconducting state – the gap, Bogoliubov-de Gennes quasiparticle theory – for actual materials has played an important role in furthering understanding.[124] These methods have enabled the study of YSR states, with real atomic moments in (or on) materials being studied in the labs. The chosen SCs include the second discovered SC – Pb – and the best elemental SC – Nb – and an unconventional SC, NbSe. Fe, with its large and very well studied moment, provides the preferred magnetic atom (or molecule). Rare earth atoms, with their larger moments, also invite attention. At present, applications incorporate phenomenological attractive pair potentials to simulate the SC state of the host.

DFT methods and applications to the nominally nonmagnetic N impurity in Nb have been described by Saunderson *et all.*[124]. The effect on the gap and the excitation spectrum above the gap was the aim of this study. Park *et al.*[125] studied the spectrum, including a zero bias peak, for a magnetic impurity (Mn, Fe, Co) in the s-wave SC Pb (T_c=7K). The atomic $3d$ series embedded in Pb was studied by Ruessmann *et al.*[126], who obtained strong magnetic-SC coupling and orbital splitting of a number of gap states (or resonances), sometimes extending across most of the gap. Spin-orbit coupling was shown to have a strong effect on the spectrum, as SOC splittings are much larger than the gap of ∼2.5 meV. For the Fe impurity the gap is essentially closed, *i.e.* SC order is effectively quenched in the vicinity of the impurity. Topological SC was brought into study by Chiu and Wang,[127] who analyzed the system Fe on Fe(Te,Se) with topological Z_2 bands. Their study indicated that the topological character of the bulk becomes reflected in new behavior of the surface YSR states.

Several groups have reported spectroscopic studies, including YSR states, on SC surfaces decorated with magnetic entities.[139–142] The orbital structure of YSR states relating to Cr atoms on SC Pb(111) was reported by Choi *et al.*[139], who found that the Cr-derived YSR resonances extended across much of the gap but left a pseudogap of low DOS around mid-gap (Δ = 2.7 meV). Xia *et al.*[141] Kondo molecular magnet Tb_2Pc3 on Pb(111) surface. **To be completed.**

N. $LaNiGa_2$ material parameters, energy scales

We choose as a representative case the topological superconductor $LaNiGa_2$ (orthorhombic, $Cmcm$), with the characteristic measured quantities from the Supplemental Information of Badger *et al.*[17], giving values for single crystal samples. This list is followed by calculated or estimated energies mostly from Quan *et al.*[18]. When three numbers are given, they refer to the a, b, c lattice direction anisotropic values, and T=0 values are given for the T-dependent properties. KWR is the Kadawaki-Woods ratio.

- T_c=2 K; kT_c=0.17 meV, a relevant energy scale
- λ_{GL}= 174, 509, 189 nm
- ξ_{GL} = 51.5, 17.6, 47.3 nm
- κ = 3.38, 28.9, 4.00
- γ=14.1 mJ/mole-K^2 (specific heat constant)
- $\Delta C(T_c)/\gamma T_c$=1.33; BCS value 1.43
- ρ_o=5.2 $\mu\Omega$ cm

- $H_p(0)$=3.66 T, the (extrapolated) Pauli limiting field
- H_{c2} Helfand-Werthamer: 0.275, 0.094, 0.253 T
- H_c thermodynamic critical field: 23 mT
- KWR: A/γ_n^2=1.28 ($[\mu\Omega$ cm/K$^2]/[$mJ/mol K$^2]^{-2}$)

The following list gives material properties and representative energies for $LaNiGa_2$, using conventional notation. The notation $\delta\mathcal{E}$ is the energy difference (gain by order) between symmetric and broken symmetry phases.
- N(0)=3.25 states/eV-f.u.-both spins
- γ_o=7.66 mJ/mole-K^2
- el-ph $\lambda = \frac{\gamma}{\gamma_o} - 1 = 0.84$
- $\Delta_o \approx$1.5 kT$_c$=0.25 meV; $2\Delta_o$=0.5 meV
- $\Delta\mathcal{E}_{sc} = \frac{1}{2}N(0)\Delta_o^2$=0.1 μeV
- B^{int}=0.2 G from μSR data; $\mu_B B^{int}\approx 8\times10^{-}9$ eV
- m^{int}=$0.012\mu_B$/f.u.=$3\times10^{-3}\mu_B$/atom
- exchange splitting of bands $=\frac{m}{N_\uparrow(0)}$ ≈4 meV
- $\Delta\mathcal{E}_{mag}=\frac{1}{4}I_{st}m^2=6\mu$ eV (Stoner $I_{st}\approx 0.5$ eV)

Sometimes useful is averaging over the orthorhombic directions (for making estimates or comparing with cubic materials): ξ_{GL}∼35 nm, λ_{GL}∼300 nm, κ∼4-29 (a moderately to strongly Type II superconductor), H$_{c2}$∼m 0.1-0.26 mT.

O. The triplet order parameter

TRSB OPs, *i.e.* emergence of a magnetic polarization, is conventionally represented by a spin-triplet SC OP of the form[6]

$$\Delta_k = \vec{d}_k \cdot \vec{\sigma}\ i\sigma_y, \tag{62}$$

where $\vec{d}$ is the complex triplet spin 3-vector whose k- and band n-dependence is neglected until required by data, and $\vec{\sigma}$ is the vector of Pauli matrices for spin. Using triplet spin notation,

$$\begin{aligned}\Delta_{\uparrow\uparrow} &= -d_x + id_y,\\ \Delta_{\downarrow\downarrow} &= \ d_x + id_y\\ \Delta_{\uparrow\downarrow} &= \ d_z = \Delta_{\downarrow\uparrow}.\end{aligned} \tag{63}$$

and rotation of spins results in transformation of Δ as a vector. (The vector $\vec{d}$ has nothing to do with a singlet d-wave OP.)

This straightforward extension to triplet OP is not sufficient to account for the symmetries of $LaNiGa_2$ (as for $LaNiC_2$, with its symmorphic but noncentrosymmetric space group). The orthorhombic D_{2h} point group has only one-dimensional irreducible representations, providing no underlying structural symmetry to be broken. This lack can be addressed by including a more microscopic degree of freedom, with the chosen one being a pair of atomic orbitals on symmetry related sites. The language of bands is more often used, and may be more appropriate for $LaNiGa_2$ due to the band degeneracies

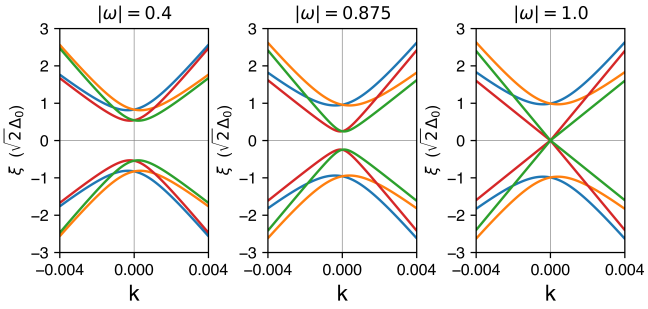

FIG. 5. Sketch of the quasiparticle (Bogoliubov-de Gennes) band structure along one dispersive band direction of the triplet, topological superconductivity model for $LaNiGa_2$. Graphs are shown for Three values of the "triplet strength" ω are displayed. For ω=1, the non-symmorphic band sticking at the zone boundary, hence two nodes, persists into the superconducting state. In the nonunitary regime $\omega < 1$ the degeneracy is broken, giving a gap to quasiparticle excitation.

across the plane of degeneracies provided by the nonsymmorphic crystal structure. The two-dimensional orbital/band symmetry, to be broken below T$_c$, is by denoted at Pauli matrices $\vec{\tau}$ in that space. The order parameter then becomes, in most general form,

$$\Delta_k = \vec{d}_k \cdot \vec{\sigma}\ (i\sigma_y) \otimes \vec{t}_k \cdot \vec{\tau}\ (i\tau_y). \tag{64}$$

In the simplest case the k and orbital dependence can be neglected and $\vec{t}_k \cdot \vec{\tau}$ replaced by τ_0 (the identity). This simplest form, with no $\vec{t}_k \cdot \vec{\tau}$ in the OP but simply $i\tau_y$, is the one currently in use for $LaNiGa_2$, which we follow below for the moment.

Once included in the Bogoliubov-de Gennes matrix for quasiparticles, the eigenvalues E_k are

$$E_k = \pm\sqrt{\varepsilon_k^2 + \vec{d}\cdot\vec{d}^* \pm |\vec{d}\times\vec{d}^*|} \tag{65}$$

where ε_k is the normal state band energy, and each has double Kramers degeneracy. The cross product is imaginary or zero. A nonzero value of $|\vec{d}\times\vec{d}^*|$ results in a "non-unitary" state for which there are eight distinct bands, without degeneracies. This requires an intrinsically complex $\vec{d}$; a zero value of the cross product (viz. from a purely real or purely imaginary $\vec{d}$) corresponds to a unitary state.

The non-unitary state corresponds to quasiparticles with two dispersion curves (split degeneracies), hence two separate energy gaps, prompting this peculiar feature to be one focus of experimentalists. Unitary states have an interpretation, generalized from singlet pairing, of equal amplitudes of $|\uparrow\uparrow>$ and $|\downarrow\downarrow>$ pairing, while the nonunitary state has unequal pairing hence magnetic polarization. Figure 5 provides a schematic close-up view of the the quasiparticle bands around the gap, for three values of the nonunitarity $\omega = |\vec{d}\times\vec{d}^*|$ in terms of normalized polarization vectors $\vec{d}$.

1. Nonunitarity more generally

The symmetry classification and properties of triplet OPs, generalized from the spherically symmetric case of ^3He to crystal symmetry, was presented by Blount in 1985.[134] For nonunitary consequences of crystal symmetry, an overview appeared by Ramires,[14] after extensions of the theory and some proposed examples from experiment. Briefly (possibly over simplified): the triplet OP is characterized by a complex vector $\vec{d}_k$ in complex 3D space; the OP may have more or fewer arguments or subscripts. Sigrist and Euda[6] expressed the general criterion of unitarity as

$$\Delta_k \Delta_k^\dagger \propto \sigma_o. \tag{66}$$

That is, if the generalized magnitude of Δ_k is proportional to the identity matrix, the phase is unitary. Here this means that if $i\vec{d}_k^* \times \vec{d}_k$ is non-zero (*i.e.* if they are 'non-parallel' in their complex vector space), then the OP is non-unitary. This indicates that the phase in not invariant under TRS. This results in a non-vanishing spin average of $\Delta_k^\dagger \vec{\sigma} \Delta_k$. Only vanishing an average over the Fermi surface is required for unitarity.[6] In that case the order parameter gives rise to a magnetic moment, which then couples to an external magnetic field. to In Eq. 65 the dot product gives the unitary contribution to the gap, while the cross product, if nonzero, adds on a nonunitary lifting of degeneracy and two-gap character of the spectrum.

Alternatively, if the cross product is zero (as when the two vectors are collinear, as they are when purely real or purely imaginary) the OP is unitary. Thus nonunitarity is associated with a phase difference between different components of $\vec{d}$. In the formulation of Ramires and coauthors, their time-reversal operator is defined by

$$\vec{q}_{TRO} \cdot \sigma = 2i(\vec{d}_k \times \vec{d}_k^*) \cdot \vec{\sigma}. \tag{67}$$

If nonunitary ($\vec{q}_{TRO}$ is non-zero), there is a non-zero expectation value of magnetization – TRS has been broken. Additional details, related to SOC (with or without), and effects of distinct point groups, are available in Ramires' paper.[14]

An aside. For the nonunitary possibility, having one of the gaps be zero has been discussed. This gapless state may persist on an area of the Fermi surface, where a degeneracy survives superconducting pairing. The original reports on ambient pressure UTe_2, T_c=1.6K, indicated that a residual specific heat coefficient γ within the SC state suggested that half of the FS carriers were not gapped,[128] leaving what has become known as a Bogoliubov Fermi surface. Note however that in this report no other broken symmetry was detected at the SC transition. More recent samples have changed this picture, and adding pressure and doping directions into the phase diagram has revealed great complexity, related to a nearby magnetic critical point. In any case, a zero gap surface (not points or lines) is conceivable, perhaps by requiring the terms involving $\vec{d}$ in the above BdG expression to vanish (viz. for only some of several Fermi surfaces, or of some parts of them).

For a general function of $\vec{d}_{kn}$ with six real functions of $\vec{k}$ (periodic and respecting symmetries), and on band n, with one of them fixed by a normalization, three conditions – vanishing of the vector $\vec{d} \times \vec{d}^*$, nonunitarity – leaves a 'tuned' condition where two of the remaining degrees of freedom conspire to provide a two-dimensional surface where a zero-gap degeneracy survives. Using some historical terminology, this is a positive condition but with zero probability of occurrence (subspace of zero measure), although nature might oblige by constraining certain components.

P. The order parameter for $LaNiGa_2$

1. Basics of pairing

As a brief review: fermionic antisymmetry upon interchange of the two members of a Cooper pair require, for pair spin S and orbital momentum L, either BCS pairing – S=0 (antisymmetric), L=0 (symmetric, commonly satisfied by pairing $k, -k$ states), or S=1, L=odd, also $k, -k$ pairs. ^{3}He provides examples of triplet S=1 OPs. The magnetic character of the TRSB signals appears to arise from equal spin pairing ($S_z = \uparrow\uparrow = +1$ and $S_z \downarrow\downarrow = -1$), with the unusual $S_z = 0$ channel neglected as it is evidently irrelevant due to its nonmagnetic character.

In a crystal the orbital characterization L (no longer a quantum number in a crystal) gives way to the angular variation of the gap on the FS, which due to periodicity gives rise to the variation with respect to k_x, k_y, k_z involving sinusoidal functions that incorporate both point group aspects and lattice periodicity.

When properties do not fit into the basic BCS picture – spin singlet pairing, crystal-symmetric gap function – an initial issue is 'what other broken symmetries' (beyond $U(1)$ pairing)? In the normal state the standard symmetry group is $U(1) \otimes \mathcal{G} \otimes \mathcal{S} \otimes \mathcal{T}$ in terms of the space group $\mathcal{G}$, spin rotation symmetry $\mathcal{S}$, and time reversal $\mathcal{T}$. Other broken symmetries may arise, viz. charge density waves, so that coupled spin-translation symmetry of the normal state must be included. At T_c, pairing breaks $U(1)$ symmetry. If the magnetization causing the spontaneous field is spin in origin, $\mathcal{S}$ is broken. If it is orbital (currents) in nature, then crystal symmetry $\mathcal{G}$ is broken. Both will be accompanied with breaking of time reversal symmetry $\mathcal{T}$, which in non-relativistic systems is not broken without an accompanied symmetry-lowering.

2. Electronic structure, Dirac points in $LaNiGa_2$

The work in the previous appendix was published before the correct $Cmcm$ space group was discovered. If there is triplet pairing, there are aspects of the current picture that may be improved on. Regarding Weng *et*

al.[32]: degeneracies of the same orbitals on symmetry-related atoms are a given; justification is needed to promote this as intimate involvement in TRSB, and why TRSB is observed only in selected materials of the weakly correlated Fermi liquid class.

Regarding Ghosh *et al.*'s supposition[33] of Hund's rule coupling in this compound: without the μSR results the standard interpretation of the band structure of $LaNiGa_2$ would be that the $3d$ bands of Ni are narrow and confined between -2.5 eV and -1 eV below the Fermi level – they are filled and inert. There is some $3d$ character at E_F, but it is due to minor mixing with neighbor atom p orbitals, or the tails of such orbitals that leak into the Ni volume and are expanded in $L = 2$ symmetry. In either case, any atomic Ni $3d$ character is minor and ambiguous, because it is occurring in the interstitial region where atomic orbital tails are not well defined; the key evaluation is that the $3d$ bands are fully occupied, with no propensity toward moment formation. The extremely small spin polarization calculated in their DFT+Hund's $3d$ interaction must be sensitive to the amount of $3d$ character, which as noted above may be subjective.

A prominent missing element is that the *Cmcm* symmetry is not fully accounted for. The non-symmorphic space group provides a BZ face of degeneracies, and after SOC is included, two diabolical k-points remain along the Z-T line, shown for $LaNiGa_2$ in Fig. 3. They are 3D Dirac points DPs) that will possess a non-zero topological index.[148] These points, symmetrically located across the Z point, mark where two Fermi surfaces touch even after consideration of SOC. Elsewhere, SOC lifts band crossing to anticrossing, thus eliminating constant energy surface touching and the topological index. Below T_c, the touching FSs will separate as the gap opens; elsewhere in the BZ the gap will open between BdG hole and electron quasiparticle bands in a conventional manner.

This pair of degenerate diabolical points presents an ideal platform for the τ-space pair that complete the required form of OP required by symmetry. Whereas the spin $\vec{d}_k$ vector is active over all of the FS and carries a k dependence (even if negligible upon first pass), the $\vec{\tau}$-space vector $\vec{t}$ is specific to the diabolical points, labeled as (Dirac) D^+ and D^-, quite analogous to graphene but in 3D. The plus/minus designations refer only to the direction of the DP along the T-Z-T line, which are degenerate in the normal state. At T=0 (but in the [unstable] normal state) the Fermi level (E_F=0) falls precisely at $\pm K_D$, insensitive to the precise value of E_F through off-stoichiometry or doping. At finite T electrons are excited above, leaving holes below, according to the Fermi-Dirac distribution.

3. *Properties of $LaNiGa_2$*

The normal state. The relevant properties of $LaNiGa_2$ are: (i) non-symmorphic orthorhombic *Cmcm* space group, (ii) normal Fermi liquid transport, (iii) no magnetic activity, from susceptibility[17] and NMR,[19] (iv) fully gapped SC state (specific heat $c_v(T)$, penetration depth $\lambda_L(T)$, critical field), (v) ARPES data supports the band touching on the BZ face of degeneracies, (vi) an inferred magnetic field of 0.2G arising below Tc with T-dependence similar to that of the BCS gap. The specific heat $c_v(T)$, earlier fit by a four-parameter two-gap model,[32] is, for the single crystal data,[17] equally well fit by a single gap allowing for some variance over the Fermi surface, due to some unclear behavior in the lower range of measurement. The Kadawaki-Woods ratio of 1.28 (quadratic coefficient of resistivity divided by the specific heat coefficient: A/γ) is typical of conventional Fermi liquids, and not of strongly correlated metals. The normal state behavior is that of a conventional Fermi liquid. It is only the spontaneous magnetic field below T_c that requires further consideration.

Inferred structure of the gap. The shape of c_v(T) has acquired importance in designing a viable OP. As mentioned, It was found by Ghosh *et al.*[33], for data on polycrystal samples, that a two band model with four parameters fit the data better near the lower end of the measured temperature range than does a single gap expression. Single crystal data[17] could fit the data well down to T/T_c= 0.3, below which the data began to differ somewhat from the single-gap exponential form (the data terminates at T/T_c=0.15, providing only a limited region of temperature for analysis).

Topological character of the Dirac points. The topological character of $LaNiGa_2$ enters the picture: even after including SOC (a relatively large energy compared to others: Δ_o, k_BT_c, phonon energies, etc.) which splits other band crossings, the symmetry of the line Z-T precludes spin-orbit splitting, and two degenerate bands at E_F on the face of degeneracies cross the Z-T line and remain degenerate after including SOC. SOC is essential to include because the SC gap $2\Delta(0)$ ≈0.5 meV is 30-50 times smaller than the SOC-induced splitting of band crossings, and shifting Fermi surface bands more generally. This leaves the normal state with two three-dimensional Dirac points (symmetry related) (call them $\pm K_D$) along the Z-T line.

For completeness, it can be noted that: (i) isolated spin-degenerate bands (hence FS states) become mixed spin-up and spin-down bands but remain doubly degenerate; they can still be regarded as 'spin-up' and 'spin-down' according to their majority character, and they are only shifted by SOC and remain isolated; (ii) crossing bands without special symmetry properties anticross, opening a local band gap where the two spin directions are more strongly mixed; (iii) band crossings occur *precisely* at the Fermi surface with zero probability, unless some symmetry positions the crossing *precisely* at the FS. This rare property occurs along the degenerate BZ faces in non-symmorphic crystals because the band crossing (or touching, if you want) happens along the entire Z-T symmetry line, making it invulnerable to the position of the Fermi level. Thus for $LaNiGa_2$, the normal state FSs remain disjoint and doubly degenerate *except* at the two Dirac points, which are fourfold degenerate

and topological, and provide a unique spectrum of the BdG quasiparticle bands, which revert to the usual BdG bands anywhere else on the five Fermi surfaces.

The electronic excitation spectrum. The density of states from the near-region of $\pm K_D$, relative to the Fermi energy is

$$N(\varepsilon) \propto \frac{\varepsilon^2}{v^3}, \tag{68}$$

where the effective velocity is roughly equal to the root mean square of the velocities along the three crystal axes. This quadratic dependence on ε leaves a dearth of states near E_F around the $\pm K_D$ points – effectively a local pseudogap on the touching Fermi surfaces, for many purposes. Pairing will shift all bands slightly (some fraction of the gap, see below), but pairing will destroy the final band degeneracy with the minimum gap $2\Delta_k(T)$ lying at $\pm K_D$. These points will impact of the low temperature thermodynamics, including $c_v(T)$.

The quasiparticle spectrum. The BdG quasiparticles near these points, in the proposed INT model[32,33] with a triplet OP, will have dispersion relations

$$\xi_k = \pm\sqrt{(\vec{v}_k \cdot \vec{k})^2 + \vec{d}\cdot\vec{d}^* \pm |\vec{d}\times\vec{d}^*|}, \tag{69}$$

where $\vec{k}$ is measured from K_D and $\vec{v}_k$ describes the anisotropic velocities around K_D. If the cross product vanishes, double degeneracy is retained, which is the unitary case. If the product does not vanish, this degeneracy is lifted. The spectrum of this non-unitary case is often called a two-gap spectrum. Examples of BdG bands, unitary and nonunitary and schematic for $LaNiGa_2$, are presented in Fig. 5.

If the material involves transition metal atoms (especially in ionic materials), or $4f$ or $5f$ atoms, the appearance of some sort of magnetic order is not so unexpected, and there are various examples, viz. in heavy fermion superconductors.[15] There are numerous examples of proposed breaking of the space group symmetry, viz. d-wave character of the order parameter in some cuprates, and others for more enigmatic (viz. uranium) compounds.[41]

4. Constructing an exotic order parameter

In conventional s-p metals (standard non-magnetic Fermi liquids), spin polarization (TRSB) leading to an internal magnetic field, costs energy which occurs without obvious compensating gain in energy, and it is less clear how to recover that energy cost from violation of singlet pairing to parallel spin (triplet) pairing, which is commonly assumed to provide the magnetic signal as reported from several μSR (muon spin resonance, rotation, or relaxation) experiments. An example that will be referred to in this paper is $LaNiGa_2$, which has recently been synthesized and characterized in single crystal form[17] with a space group ($Cmcm$) distinct from that reported on powder samples four decades earlier ($Cmmm$).[30]

μSR experiments have detected spin relaxation characteristic of a small ($\sim$0.2 G) magnetic field[31] at the position of the muon, with onset at the superconducting transition at T_c=2K: TRSB coupled to Cooper pairing. Full consideration of the properties of $LaNiGa_2$ have previously led it to be an example of the small class of probable superexotic SCs, being unique due to displaying triplet pairing, two orbital character,[32] and a nonunitary spectrum of quasiparticles.[33] Density functional theory (DFT) calculations on the $Cmcm$ structure revealed a planar zone boundary degeneracy that requires consideration. Though important in the big picture, these complexities will be a lesser topic here.

5. The INT model for the $LaNiGa_2$ order parameter

The present picture has arisen from a progression from Hillier *et al.*[31], to that of Weng *et al.*[32], then to the more 'quantitative theory' of Ghosh *et al.*[33]. These groups were not yet aware that the space group is $Cmcm$, so they built on the reported[30] $Cmmm$ structure. For the form of the required TRSB order parameter there may be little difference, because the point groups of both $Cmmm$ and $Cmcm$ (D_{2h}) have only one-dimensional (hence, nondegenerate) irreducible representations, hence no degeneracy to be split.[147] The non-symmorphic space group of $Cmcm$ does however provide a striking new degeneracy: a 3D Dirac point electronic structure (even after including SOC) with topological character. This distinction invites a reinterpretation of the source of symmetry breaking, in addition to the breaking of $U(1)$ and time reversal symmetries (see below).

Hillier *et al.* reported TRSB and suggested that nonunitarity seemed to be required by symmetry. They did no modeling of the order parameter, but reported the necessary form of the Ginzburg-Landau free energy functional that is required for TRS breaking (a triplet OP coupled to the magnetization). Weng *et al.* reported more data (penetration depth, specific heat, H_{c2}),[32] noting the nodeless gap, and suggested that the additional broken symmetry that seemed necessary might be due to the degeneracy of orbitals on two symmetry-related atoms, with symmetry also broken at T_c. They described a triplet picture in which the $S_{\uparrow\uparrow}$ occupation differs slightly from that of $S_{\downarrow\downarrow}$, based partly on a picture of active atomic orbitals. From small structure in $\lambda_L(T)$ and $c_v(T)$ they argued that a 'two gap' (or 'two band', or 'two orbital') character might be responsible.

The SC order parameter, which is constructed in the simplest form that can account for data current available, is given in the 4×4 space as Eq. 64 with the vector $\vec{t}_k$ left as the τ-space identity,

$$\Delta_k = \vec{d}_k \cdot \vec{\sigma}\ (i\sigma_y) \otimes (i\tau_y). \tag{70}$$

According to Weng *et al.*[32], the k dependence of $\vec{d}$ is odd with the four possible choices having $\vec{d}_k$ lie in the $(1, i, 0)$ direction. A concern is: odd in k, viz. $\sin k_x$ etc. has nodes, whereas $LaNiGa_2$ is fully gapped. The normal

state is required to incorporate the symmetries that are broken by the OP, to account for data. The observation of broken TRS necessitates another degenerate degree of freedom, most readily available from the crystal structure. The point group D_{2h} of $Cmcm$ $LaNiGa_2$, with eight elements, has only one-dimensional (non-degenerate) irreducible representations, which provides no degeneracy.

Ghosh *et al.* argued that, because the $Cmmm$ Fermi surface displayed a region where two sheets that are roughly parallel, certain atomic orbitals might lie at the root of broken symmetry. They chose the d_{z^2} and d_{xy} orbitals on the Ni atoms (which are layered in the x-y plane. Introducing a Hund's-like attractive interaction encouraging parallel spins on the Ni atoms, they treated a parallel-spin-pairing OP picture that involved incorporation of a full DFT calculation including all of the Fermi surfaces of $LaNiGa_2$. Adjusting the attractive interaction parameter to reproduce T_c=2 K, their model predicted a small magnetization and resulting spontaneous field of 0.3 G, effectively the same as experiment. The interested person should consult the original three papers discussed here for the many details that are addressed.

Q. Spin and magnetic aspects of pairing

1. Singlet spin scenario

Occam's razor points toward the simplest and most studied of SC in standard Fermi liquids. We assume first singlet pairing due to phonon glue. Cooper's demonstration that the Fermi surface is unstable to formation of bound pairs of $(+\vec{k}\uparrow;-\vec{k}\downarrow)$ states focused on the zero total momentum $\vec{K} = 0$, $S = 0$ character of the pair. This simplest SC unit is the underpinning of the theory of superconductivity, subject only to the necessity of an net-attractive effective interaction. Phonons are always present, and they always prefer $\vec{K} = 0, S = 0$ pairing, subject to interruptions from other pairing mechanisms, which are weak in conventional Fermi liquids. The corresponding calculations for $LaNiC_2$ and $LaNiGa_2$ are described in Sec. XII A 1, and give strong evidence this conventional mechanism accounts for the superconductivity, thus other origins of the spontaneous magnetic field should be sought.

Cmcm symmetry of $LaNiGa_2$. The Dirac point degeneracy along $Z - T$, surviving after SOC has split all other band degeneracies, suggests a specific mechanism for broken symmetry that may account for a small magnetic field in the SC state: the mirror $x \to -x$ operation that connects the two DPs. [We choose, as common, the special $\vec{b}$ axis as the OP $\hat{z}$-axis, and the Z-T direction as the $\hat{x}$ direction.] The $\vec{\tau}$ space in the current model has not not broken any symmetry in the 'near degenerate FS' picture, and only a nondescript and ubiquitous degeneracy in the 'degenerate orbitals on equivalent atoms' picture. The broken symmetry between the pair of DPs provides an obvious candidate for delicacy toward spontaneous behavior, closely analogous to the pair of DPs in graphene.

This picture comes with a challenge: the overall odd symmetry of the OP upon exchange of the two electrons' coordinates. Singlet spin is odd; the broken PD pair is odd (think of splitting to energies $\pm\delta$). The produce of the three OP components being odd requires the third – k-space behavior – to be odd. Yet data shows a gapless SC spectrum, typically associated with an s-like behavior. This hurdle can be surmounted by an OP of $p_x + ip_y$ type:

$$\Delta_k^{orb} = \alpha \sin k_x + i\beta \sin k_y,$$
$$\Delta_k^{orb}[\Delta_k^{orb}]^\dagger = \alpha^2 \sin^2 k_x + \beta^2 \sin^2 k_y, \qquad (71)$$

with non-zero real constants α, β. While there has been substantial theoretical discussion of complex combinations of different character, little has been established about what the origin might be. In very stable crystals, this symmetry breaking can involve simply lowering the symmetry of the electronic state with negligible impact on the lattice symmetry, making XRD an ineffective method for study.

2. Triplet spin scenario

Weng *et al.*[32] and Ghosh *et al.*[33] described a spin-based spin-triplet picture (above) in which there is only parallel-spin pairing. For the magnetization, $S_{\uparrow\uparrow}$ occupation exceeds (very) slightly from the $S_{\downarrow\downarrow}$. Without details, this picture is based either on nearly-degenerate FSs, or on an active atomic orbital on symmetry-related atoms, that might account for the necessary additional symmetry to be broken. From small structure in $\lambda_L(T)$ and $c_v(T)$ they argued that a "two gap" (or "two band") character might be responsible.

This viewpoint can be supported much more reasonably by the observation just above that the DPs provide an unusual, perhaps unique, degeneracy that may be susceptible to instability. The remainder of the analysis carries through: triplet pairing, symmetric k-dependence, odd symmetry in the orbital space.

3. Orbital moment scenario

Spontaneous orbital magnetism in crystalline solids, if it would arise in zero field, is expected to be much smaller than spin magnetization. Given the field values of 0.1-0.3 G, the orbital magnetization would need to be that of the spin magnetization discussed earlier, of the order of $10^{-2}\mu_B$/f.u. Orbital currents have been discussed mostly in the context of quantum (strongly correlated) materials. Searches especially in the layered cuprates have placed stringent limits on the magnitude of such currents.

In such an event, the orbital current would need to couple to the $U(1)$ OP. As mentioned in Sec. **??**, an orbital supercurrent is driven by the muon moment, leading to a vortex extending (more or less, depending on local symmetry of lack thereof) along the axis of the moment. This

supercurrent primarily sustains the vortex, producing a field at the muon site and also in the neighboring environment, but in a roughly circular region rather than the periodic orbital currents required to provide a (nearly) uniform periodic magnetic field.

R. Energetics relating to the superconducting state

Straightforward spin polarization, whatever might be its origin, allows estimation of energy gain versus energy loss. Quan *et al.* have provided these estimates, with the conclusion that costs are larger than gains, although all are extremely small for a 2K superconductor and a magnetization of $10^{-2}\mu_B$/atom. There could be energy gains from the unknown mechanism, and associated Hamiltonian, coupling spin to pairing.

S. Options for a mechanism for TRSB

The topic of the pairing mechanism – the bosonic glue binding a Cooper pair – in an exotic superconductor is a challenging one. A burning question based on the present interpretation of data – time-reversal symmetry breaking – is how a tiny field of 0.1-1 G can be produced. The direct approach is to consider the field as due to spin, or alternatively, to orbital polarization. The ever-present electron-phonon coupling was discussed in Sec. XII so nothing more will be added here.

1. Coulomb interaction: charge or spin

Examples of other pairing glues discussed for decades include spin-fluctuations and non-magnetic electron-electron polarizations – excitons, d-mons, acoustic plasmons, perhaps a few more. Susceptibility data for these conventional metals rules out a spin-fluctuation mechanism, *i.e.* dynamic local moments, in many of the materials, where the susceptibility $\chi(T)$ is typical of conventional Fermi liquid superconductors. Likewise, as conventional metals the other possible mechanisms mentioned above are highly unlikely. The very fragile magnetism (tiny magnetic moment that is inferred) provides an imposing challenge for any proposed order parameter.

Most other candidates are also unlikely in multicomponent compounds with several large Fermi surfaces and strong metallic screening. The remaining possibility is that there is some more subtle combination of electron and phonon origin that can coexist with the usual phonon mechanism to break $U(1)$, time reversal symmetry, and perhaps some other underlying symmetry. This scenario would be, in Ginzburg-Landau language, be a secondary OP that couples to phonons and causes emergence of some type of magnetic character.

The inherent energy gain from Cooper $S = 0$ pair formation may be superseded by $S = 1$ triplet pairing. In quantum materials with partially filled d or f shells, Hund's rule (parallel spin) pairing is discussed. The candidates are however nowhere near a Stoner instability, which is invoked to provide a tendency toward equal-spin pairing. 'In intermetallic compounds with no magnetic tendencies, it becomes difficult to follow this line of argument. Nevertheless, the apparent emergence of a spontaneous magnetic field has pointed the construction of possible order parameters in this direction. From this viewpoint, one needs not only parallel-spin pairing but a mechanism that provides a very small but nonzero imbalance between up-up and down-down pairing.

2. Orbital polarization

The other path toward a magnetic order parameter is kinetic – the orbital character of the pair – rather than spin in origin. Orbital motion of charges produce magnetic fields. One suggestion to account for small magnetic order has been an emergence of supercurrent loops alongside pairing below T_c, carrying orbital angular momentum and producing magnetism. Such orbital loops have been proposed for quantum materials with strong local correlation effects, without confirmation.

The orbital loop triplet picture of Ghosh, Annett, and Quintanilla[45] provides a detailed example but carries requirements: (i) on-site intra-orbital singlet pairing, and (ii) at least two distinct but symmetry related sites within the unit cell to host the intra-orbital pairing. Like many scenarios for exotic OPs, the point group must have at least one degenerate irreducible representation (irrep), to host the symmetry-breaking. The local intra-orbital pairing includes the critical aspect of singlet pairing that is a foundational aspect of BCS pairing, while differing by being real space, versus momentum space (k,-k), pairing.

The crystal symmetry irrep condition provided a hurdle, as the point group D_{2h} of $Cmcm$ had only one-dimensional irreps. Since SOC in $LaNiGa_2$ is weak[18] for these purposes, the applicable lattice+spin group is $D_{2h} \otimes SO(3)$, which has three-dimensional irreps, and the four possible TRSB SC instabilities are all purely triplet.[31,136,137]. Another feature is that all four are nonunitary indicating equal-spin pairing requiring an additional OP of magnetic character.

This is not yet a solution, as each of the triplets is point-nodal, inconsistent with the observed fully gapped character of $LaNiGa_2$. Triplet pairing is however different from singlet, in that an on-site interaction (presumably locally attractive $-U$, as in negative U models) is less repulsive than for singlet pairs. Their model took the form of OP $\Delta^{n,m}_{\alpha,\beta}(\vec{k})$ in orbitals n, m (on the same site) and spin α, β spaces. For different orbitals A and B, their proposed coupling incorporated the off-diagonal pairing OP $\Delta_{\uparrow\uparrow} < c^\dagger_{A,\uparrow} c^\dagger_{B,\uparrow} >$ and magnetization $\Phi_{A,\sigma} < c^\dagger_{A,\sigma} c_{A,\sigma} >$ (together with their index- rotated and complex conjugated partners). Their suggestion was that the d-orbital material Re_6X, X=Ti, Zr, Hf, (symmorphic, space group $I\bar{4}3m$ and with identified TRSB, provides a reasonable candidate.

[1] W. Lang, Inhomogeneous superconductors, arXiv:2310.18232.

[2] W. E. Pickett, Room Temperature Superconductivity: the Roles of Theory and Materials Design, Rev. Mod. Phys. **95**, 021001 (2023).

[3] G. R. Stewart, Heavy Fermion Systems, Rev. Mod. Phys. **56**, 755 (1984).

[4] R. E. Rudd and W. E. Pickett, Single Spin Superconductivity: Formulation and Ginzburg-Landau Theory, Phys. Rev. B **57**, 557 (1998).

[5] J. F. Annett, Symmetry of the order parameter for high-temperature superconductivity, Adv. Phys. **39**, 83 (1990).

[6] M Sigrist and K. Ueda, Phenomenological theory of unconventional superconductivity, Rev. Mod. Phys. **63**, 239 (1991).

[7] J. F. Annett, Unconventional superconductivity, Contemp. Phys. **36**, 423 (1995).

[8] T. Tsuneto, *Superconductivity and Superfluidity*, (Cambridge University, Cambridge, U.K., 1998).

[9] V. P. Mineev and K. V. Samokhin, *Introduction to Unconventional Superconductivity.* (Gordon and Breach, Amsterdam, 1999).

[10] M. Sigrist, Introduction to unconventional superconductivity, AIP Conf. Proc. **789**, 165 (2005).

[11] M. Sigrist, Introduction to unconventional superconductivity in non-centrosymmetric metals, AIP Conf. Proc. **1162**, 55 (2009).

[12] A. P. Mackenzie and Y. Maeno, The superconductivity of Sr_2RuO_4 and the physics of spin-triplet pairing, Rev. Mod. Phys. **75**, 657 (2003).

[13] K. I. Wysokinski, Time Reversal Symmetry Breaking Superconductors: Sr_2RuO_4 and Beyond, Condens. Matter **4**, 47 (2019).

[14] A. Ramires, Nonunitary superconductivity in complex quantum materials, J. Phys.: Condens. Matt. **34**, 304001 (2022).

[15] R. H. Heffner, Muon studies of heavy fermions, J. Magn. Magn. Compds. **108**, 23 (1992).

[16] M. Staab, R. Prater, S. Sreedhar, J. Byland, E. Mann, D. Zackaria, Y. Shi, H. J. Bowman, A. L. Stephens, M.-C. Jung, A. Botana, W. E. Pickett, V. Taufour, and I. Vishik, Symmetry Enforced Fermi Surface Degeneracies Observed in Time-Reversal Symmetry-Breaking Superconductor $LaNiGa_2$, arXiv:2312.11464.

[17] J. R. Badger *et al.*, Dirac lines and loop at the Fermi level in the Time-Reversal Symmetry Breaking Superconductor $LaNiGa_2$, Commun. Phys. **5**, 22 (2022).

[18] Y. Quan, V. Taufour, and W. E. Pickett, Nonsymmorphic Band Sticking in a Topological Superconductor, Phys. Rev B **105**, 064517 (2022).

[19] P. Sherpa, I. Vinograd, Y. Shi, S. A. Sreedhar, C. Chaffey, T. Kissikov, M.-C. Jung, A. S. Botana, A. P. Dioguardi, R. Yamamoto, M. Hirata, G. Conti, S. Nemsak, J. R. Badger, P. Klavins, I. Vishik, V. Taufour, and N. J. Curro, Absence of strong magnetic fluctuations or interactions in the normal state of $LaNiGa_2$, arXiv:2311.06988.

[20] S. Sundar, M. Yakovlev, N. Azari, M. Abedi, D. M. Broun, H. U. Ozdemir, S. R. Dunsiger, D. Zackaria, H. Bowman, P. Klavins, V. Taufour, J. E. Sonier, Gap structure of the non-symmorphic superconductor $LaNiGa_2$ probed by μSR, arXiv:2311.00069.

[21] S. Ghimire, K. R. Joshi, E. H. Krenkel, M. A. Tanatar, Y. Shi, M. Konczykowski, R. Grasset, V. Taufour, P. P. Orth, M. S. Scheurer, and R. Prozorov, Electron irradiation reveals robust fully gapped superconductivity in $LaNiGa_2$, Phys. Rev. B **109**, 024515 (2024).

[22] A. Schenck, *Muon spin rotation spectroscopy: principles and applications in solid state physics,* (Adam Hilger Ltd., Bristol, U.K., 1985).

[23] C.P. Slichter, *Principles of Magnetic Resonance*, (Springer-Verlag, 1980).

[24] J.H. Brewer and P.W. Percival, eds., *Muon Spin Rotation II: Proceedings of 2nd Int. Topical Meeting on Muon Spin Rotation, Vancouver, 1980* (North-Holland, Amsterdam, 1981).

[25] J.H. Brewer, R.F. Kiefl and P.W. Percival, eds., *Muon Spin Rotation VI: Proceedings of 6th Int. Topical Meeting on Muon Spin Rotation/Relaxation/Resonance, Wailea, Maui, 1993* (North-Holland, Amsterdam, 1994).

[26] S. J. Blundell, Spin-polarized muons in condensed matter, Contemp. Phys. **40**, 175 (1999); https://doi.org/10.1080/001075199181521.

[27] S.L. Lee, S.H. Kilcoyne, and R. Cywinski, eds., "Muon Science: Muons in physics, chemistry and materials ", *Proceedings of the 51st Scottish Summer School in Physics, NATO Advanced Study Institute* (Institute of Physics Publishing, London 1999.)

[28] A. Yaouanc and P. Dalmas de Réotier, *Muon Spin Rotation, Relaxation, and Resonance: Applications to Condensed Matter*, Intl. Series of Monographs on Physics 147, 1-504 (Oxford University Press, 2011).

[29] S. J. Blundell, R. de Renzi, T. Lancaster, and F. L. Pratt, *Muon Spectroscopy – An Introduction* (Oxford University Press, Oxford, U.K., 2021).

[30] Y. Yarmolyuk and Y. Grin, Crystal structure of the $RNiGa_2$ compounds (R=La, Ce, Pr, Nd, Sm, Gd), Dopovidi Akademii nauk Ukrainskoi RSR, Seriya A: Fiziko-Mathematichni ta Tekhnichni Nauki **44**, 71 (1982).

[31] A. D. Hillier, J. Quintanilla, B. Mazidian, J. F. Annett, and R. Cywinski, Nonunitary triplet coupling in the centrosymmetric superconductor $LaNiGa_2$, Phys. Rev. Lett. **109**, 097001 (2012).

[32] Z. F. Weng *et al.*, Two-Gap Superconductivity in $LaNiGa_2$ with Nonunitary Triplet Pairing and Even Parity Gap Symmetry, Phys. Rev. Lett. **117**, 027001 (2016).

[33] S. K. Ghosh, G. Csire, P. Whittlesea, J. F. Annett, M. Gradhand, B. Újfalussy, and J. Quintanilla, Quantitative theory of triplet pairing in the unconventional superconductor $LaNiGa_2$, Phys. Rev. B **101**, 100506(R) (2020).

[34] A. Balatsky, I Vekhter, and J.-X. Zhu, Impurity-induced states in conventional and unconventional superconductors, Rev. Mod. Phys. **78**, 373 (2006).

[35] J. Bardeen, L. N. Cooper, and J. R. Schrieffer, Theory of Superconductivity, Phys. Rev. **108**, 1175 (1957).

[36] A. D. Hillier *et al.*, Muon spin spectroscopy, Nat. Rev. - Methods Primers **2-4** (2022). https://doi.org/10.1038/s43586-021-00089-0

[37] S. J. Blundell and T. Lancaster, DFT plus : Density functional theory for muon site determination Appl. Phys. Rev. **10**, 021316 (2023).

[38] B. M. Huddart, A. Hernandez-Melian, T. J. Hicken, M. Gomilsek, Z. Hawkhead, S. J. Clark, F. L. Pratt, T. Lancaster, MuFinder: A Program to determine and analyze muon stopping sites, Comp. Phys. Commun. **280**, 108488

(2022).
[39] M. Gomilsek, F. Pratt, S. Cottrell, S. Clark, and T. Lancaster, Many-body quantum muon effects and quadrupolar coupling in solids, Commun. Phys. **6**, 142 (2023).
[40] B. M. Andersen, A. Kreisel, and P. J. Hirschfeld, Spontaneous time-reversal symmetry breaking by disorder in superconductors, arXiv::2312.08099.
[41] S. Sundar *et al.*, Ubiquitous Spin Freezing in the Superconducting State of UTe_2, arXiv:2207.13725.
[42] B. M. Huddart, I. J. Onuorah, M. M. Isah, P. Bonfà, S. J. Blundell, S. J. Clark, R. De Renzi, and T. Lancaster, Intrinsic Nature of Spontaneous Magnetic Fields in Superconductors with Time-Reversal Symmetry Breaking, Phys. Rev. Lett. **127**, 237002 (2021).
[43] F. Bernardini, P. Bonfa, S. Massidda, and R. De Renzi, *Ab initio* strategy for muon site assignment in wide band gap fluorides, Phys. Rev. B **87**, 115148 (2013).
[44] S. K. Ghosh, M. Smidman, T. Shang, J. F Annett, A. D. Hillier, J. Quintanilla, and H. Yuan, Recent progress on superconductors with time-reversal symmetry breaking, J. Phys.: Condens. Matt. **33**, 033001 (2021).
[45] S. K. Ghosh, J. F. Annett, and J. Quintanilla, Time-reversal symmetry breaking in superconductors through loop supercurrent order, New. J. Phys. **23**, 083018 (2021).
[46] M. Sato and Y. Ando, Topological Superconductors: A Review, Rep. Prog. Phys. **80**, 076501 (2017).
[47] S. Sautbekov, The vector potential of a magnetic dipole, J. Magn. Magn. Matls. **484**, 403 (2019).
[48] J. D. Jackson, The Nature of Intrinsic Magnetic Dipole Moments, CERN document 77-17 (1977).
[49] A. I. Duff and J. F. Annett, Variational QMC of a hydrogen atom in jellium with comparison to LSDA and self-interaction corrected LSDA solutions, Phys. Rev. B **76**, 115113 (2007).
[50] J. F. Janak, Uniform susceptibilities of metallic elements, Phys. Rev. B **16**, 255 (1977).
[51] R. M. Martin, *Electronic Structure Basic Theory and Practical Methods* (Cambridge University Press, 2004).
[52] J. Autschbach, Perspective: Relativistic Effects, J. Chem. Phys. **136**, 150902 (2012).
[53] W. E. Pickett and J. Q. Broughton, Variational Monte Carlo study of the partially polarized electron gas, Phys. Rev. B**48**, 14859 (1993).
[54] G. Ortiz and P. Ballone, Correlation energy, structure factor, radial distribution function, and momentum distribution of the spin-polarized uniform electron gas, Phys. Rev. B**50**, 1391 (1994).
[55] G. G. Spink, R. J. Needs, and N. D. Drummond, Quantum Monte Carlo study of the three-dimensional spin-polarized homogeneous electron gas, Phys. Rev. B **88**, 085121 (2013).
[56] F. Küster, A. M. Montero, F. S. M. Guimaraes, S. Brinker, S. Lounis, S. S. P. Parkin, and P. Sessi, Correlating Josephson supercurrents and Shiba states in quantum spins unconventionally coupled to superconductors, Nat. Comm. **12**, 1108 (2021).
[57] "Zero point motion" of a quantum particle is often counter-intuitive. Such effects are properly interpreted as quantum 'uncertainty' in position rather than classical motion. The most common textbook examples are (1) zero point uncertainty of atomic position does not scatter electrons at T→0; perfect metals have zero resistivity at T=0, and (2) quantum uncertainty does not give width to x-ray diffraction peaks at T=0, only the amplitude is reduced.
[58] B. Rosenstein, B. Ya. Shapiro, and I. Shapiro, Ginzburg-Landau theory of the triplet superconductivity in 3D Dirac semi-metal, arXiv:1501.07910.
[59] C. M. Varma, Non-Fermi-liquid states and pairing instability of a general model of copper oxide metals, Phys. Rev. B **55**, 14554 (1997).
[60] C. Nayak, Density-wave states of nonzero angular momentum, Phys. Rev. B **62**, 4880 (2000).
[61] M. Klug, J. Kang, R. M. Fernandes, and J. Schmalian, Orbital loop currents in iron-based superconductors, Phys. Rev. B **97**, 155130 (2018).
[62] Y. Hu, S. Yamane, G. Mattoni, K. Yada, K. Obata, Y. Li, Y. Yao, Z. Wang, J. Wang, C. Farhang, J. Xia, Y. Maeno, and S. Yonezawa, Time-reversal symmetry breaking in charge density wave of CsV_3Sb_5 detected by polar Kerr effect, arXiv:2208.08036.
[63] Y. Aoki, A. Tsuchiya, T. Kanayama, S. R. Saha, H. Sugawara, H. Sato, W. Higemoto, A. Koda, K. Ohishi, K. Nishiyama, and R. Kadono, Phys. Rev. Lett. **91**, 067003 (2003).
[64] R.P. Singh, A.D. Hillier, B. Mazidian, J. Quintanilla, J.F. Annett, D. McK. Paul, G. Balakrishnan, and M.R. Lees, Detection of Time-Reversal Symmetry Breaking in the Noncentrosymmetric Superconductor Re6Zr Using Muon-Spin Spectroscopy, Phys. Rev. Lett. **112**, 107002 (2014).
[65] A. D. Hillier, J. Quintanilla, and R. Cywinski, Evidence for Time-Reversal Symmetry Breaking in the i Noncentrosymmetric Superconductor $LaNiC_2$, Phys. Rev. Lett. **102**, 117007 (2009); *erratum*, **105**, 229901 (2010).
[66] A. Sumiyama,D. Kawakatsu, J. Gouchi, A. Yamaguchi, G. Motoyama, Y. Hirose, R. Settai and Y. Onuki, Spontaneous magnetization of non-centrosymmetric superconductor $LaNiC_2$, J. Phys. Soc. Japan **84**, 013702 (2015).
[67] S. Sundar *et al.*, Two-gap time reversal symmetry breaking superconductivity in noncentrosymmetric $LaNiC_2$, Phys. Rev. B **103**, 014511 (2021).
[68] S. K. Ghosh, P. K. Biswas, C. Xu, B. Li, J. Z. Zhao, A. D. Hillier, and X. Xu, Time-reversal symmetry breaking superconductivity in three-dimensional Dirac semimetallic silicides, Phys. Rev. Research **4**, L012031 (2022).
[69] C. Mielke III *et al.*, Time-reversal symmetry-breaking charge order in a kagome superconductor, Nature **602**, 245 (2022). This compound, KV_3Sb_5, shows charge order below 80 K and a more complex temperature dependence of the magnetic signal below T_c.
[70] A. Kataria, J. A. T. Verezhak, O. Prakash, R. K. Kushwaha, A. Thamizhavel, S. Ramakrishnan, M. S. Scheurer, A. D. Hillier, and R. P. Singh, Time-reversal symmetry breaking in the superconducting low carrier density quasiskutterudite $Lu_3Os_4Ge_{13}$, Phys. Rev. B **107**, L100506 (2023).
[71] M. Mandal, A. Kataria, C. Patra, D. Singh, P. K. Biswas, A. D. Hillier, T. Das, and R. P. Singh, Time-reversal symmetry breaking in frustrated superconductor Re_2Hf, Phys. Rev. B **105**,094513 (2022).
[72] D. A. Mayoh, A. D. Hillier, B. Balakrishnam, and M. R. Lees, Evidence for the coexistence of time-reversal symmetry breaking and Bardeen-Cooper-Schrieffer-like superconductivity in La_7Pd_3, Phys. Rev. B **103**, 024507 (2021).
[73] Arushi, R. K. Kushwaha, D. Singh, A. D. Hillier, M. S. Scheurer, and R. P. Singh, Time-reversal symmetry breaking in the superconducting state of ScS, Phys. Rev. B **106**, L020504 (2022).
[74] T. M. Luke, A. Keren, L. P. Le, W. D. Wu, Y. J. Uemura, D. A. Bonn, L. Taillefer, and J. D. Garrett, Muon spin relaxation in UPt_3, Phys. Rev. Lett. **71**, 1466 (1993).

[75] R. H. Heffner *et al.*, New Phase Diagram for (U,Th)Be_{13}: A Muon-Spin-Resonance and H_{c1} Study, Phys. Rev. Lett. **65**, 2816 (1990).

[76] R. F. Kiefl *et al.*, Search for Anomalous Internal Magnetic Fields in High-T_c Superconductors as Evidence for Broken Time-Reversal Symmetry, Phys. Rev. Lett. **64**, 2082 (1990).

[77] D. Rainer and M. Vuorio, Small objects in superfluid ^{3}He, J. Phys. C **10**, 3093 (1977).

[78] C. H. Choi and P. Muzikar, Impurity-induced magnetic fields in unconventional superconductors, Phys. Rev. B **39**, 9664 (1989).

[79] M. Tinkham, *Introduction to Superconductivity*, 2nd Ed. (Dover Publ. Inc., Mineola, N.Y., 1996).

[80] J. R. Schrieffer, *Theory of Superconductivity* (W. A. Benjamin Inc., New York,, 1964).

[81] P.B. Allen, W.E. Pickett, and H. Krakauer, Anisotropic Normal State Transport Properties Predicted and Analyzed for High T_c Oxide Superconductors, Phys. Rev. B **37**, 7482 (1988).

[82] J. Ashcroft and S. Krusch, Vortices and magnetic impurities, Phys. Rev. D **101**, 025004 (2020).

[83] F. Gygi and M. Schlüter, Electronic tunneling into an isolated vortex in a clean type-II superconductor, Phys. Rev. B **41**, 822(R) (1990).

[84] F. Gygi and M. Schlüter, Angular band structure of a vortex line in a type-II superconductor, Phys. Rev. Lett. **65**, 1820 (1990).

[85] F. Gygi and M. Schlüter, Self-consistent electronic structure of a vortex line in a type-II superconductor, Phys. Rev. B **43**, 7609 (1991).

[86] W. Su, R. Wang, C. Chen, and X. Wang, Unique quantum impurity states driven by a vortex in a topological superconductor, arXiv:2206.04862 (2022).

[87] J. Pinel, C. Lebeau, and J. Rosenblatt, Behaviour of a type I superconductor in the presence of magnetic dipoles, Solid State Commun. **9**, 725 (1971).

[88] J. Pinel and C. Lebeau, Effect of magnetic dipoles on order parameter of superconductor, Phys. Lett. A **58**, 477 (1976).

[89] S. N. Burmistrov and L. B. Dubovskii, Magnetic Dipole Interaction in an Anisotropic Type-II Superconductor, J. Supercond. **4**, 207 (1991).

[90] Z. J. Yang, Surface effect of a superconductor on a magnetic dipole, Physica C **234**, 263 (1994).

[91] U. Yaron, P. L. Gammel, A. P. Ramirez, D. A. Huse, D. J. Bishop, A. I. Goldman, C. Stassis, P. C. Canfield, K. Mortensen, and M. R. Eskildsen, Microscopic coexistence of magnetism and superconductivity in $ErNi_2B_2$2C, Nature **382**, 236 (1996).

[92] J. Zittartz and E. Müller-Hartmann, Theory of Magnetic Impurities in Superconductors I. Exact Solutions of the Nagaoka Equations, Z. Physik **232**, 11 (1970).

[93] S. Sykora and T. Meng, Renormalization approach to the superconducting Kondo model, arXiv:2109.11995 (2022).

[94] L. Yu, Bound state in superconductors with paramagnetic impurities, Acta Phys. Sin. **21**, 75 (1965).

[95] H. Shiba, Classical spins in superconductors, Prog. Theor. Phys. **40**, 435 (1965); Prog. Theor. Phys. **50**, 50 (1973).

[96] A. I. Rusinov, On the theory of gapless superconductivity in alloys containing paramagnetic impurities, Zh. Eksp. Teor. Fiz. Pisma Red. **9**, 146 (1968); [JETP Lett. **9**, 85 1969].

[97] A. I. Rusinov, Superconductivity near a paramagnetic impurity, Zh. Eksp. Teor. Fiz. **56**, 2047 (1969); [Sov. Phys. JETP **29**, 1101 (1969)].

[98] J. B. Goodenough, Theory of the Role of Covalence in the Perovskite-Type Manganites [La, M(II)]MnO_3, Phys. Rev. **100**, 564 (1955).

[99] J. Kanamori, Superexchange interaction and symmetry properties of electron orbitals, J. Phys. Chem. Solids, **10**, 87 (1959).

[100] P. W. Anderson, Antiferromagnetism: Theory of Superexchange Interaction, Phys. Rev. **79**, 350 (1950).

[101] W. E. Pickett, M. L. Cohen, and C. Kittel, Theory of the hydrogen interstitial impurity in germanium, Phys. Rev. B **20**, 5050 (1979).

[102] N. N. Bogoliubov, V. V. Tolmachev, and D. V. Shirkov, *A New Method in the Theory of Superconductivity*, (1958) (translation: Consultants Bureau, Inc., New York, 1959).

[103] P. Morel and P. w. Anderson, Calculation of the Superconducting State Parameters with Retarded Electron-Phonon Interaction, Phys. Rev. *125*, 1263 (1962).

[104] P. B. Allen and R. C. Dynes, Transition temperature of strong-coupled superconductors reanalyzed, Phys. Rev. B **12**, 905 (1975).

[105] A. Subedi and D. J. Singh, Electron-phonon superconductivity in noncentrosymmetric $LaNiC_2$: First-principles calculations, Phys. Rev. B **80**, 092506 (2009).

[106] X. Tütüncü and G. Srivastava, Origin of superconductivity in layered centrosymmetric $LaNiGa_2$, Appl. Phys. Lett. **104**, 022603 (2014).

[107] A. H. Castro Neto, F. Guinea, N. M. R. Peres, K. S. Novoselov, and A. K. Geim, The electronic properties of graphene, Rev. Mod. Phys. **81**, 109 (2009).

[108] I. F. Foulkes and B. L. Györffy, *p*-wave pairing in metals, Phys. Rev. B **15**, 1395 (1977).

[109] I. Schnell, I. I. Mazin, and A. Y. Liu, Unconventional superconducting pairing symmetry induced by phonons, Phys. Rev. B **74**, 184503 (2006).

[110] P. M. R. Brydon, S. Das Sarma, H.-Y. Hui, and J. D. Sau, Odd-parity superconductivity from phonon-mediated pairing: Application to $Cu_xBi_2Se_3$, Phys. Rev. B **90**, 184512 (2014).

[111] J. Robbins, J. F. Annett, and M. Gradhand, Theory of the orbital moment in a superconductor, Phys. Rev. B **101**, 134505 (2020).

[112] P. Fulde and R. A. Farrell, Superconductivity in a Strong Spin-Exchange Field, Phys. Rev. **135**, A550 (1964).

[113] A. I. Larkin and Yu. N.Ovchinnikov, Zh. Eksp. Teor. Fiz. **47**, 1136 (1964); translated in Inhomogeneous State of Superconductors, Sov. Phys. JETP. **20**, 762 (1965).

[114] A. Abragam and B. Bleaney, *Electron paramagnetic resonance of transition ions,* (Oxford University Press, Oxford U.K., 2012).

[115] G. Vignale, M. Rasolt, and D. J. W. Geldart, Magnetic Fields and Density Functional Theory, Adv. Quant. Chem **21**, 235 (1990).

[116] Y. Takada, R. Maezono, and K. Yoshizawa, Emergence of a Kondo singlet state with the Kondo temperature well beyond 1,000K in the proton-embedded electron gas: Novel route to high-T_c superconductivity, arXiv:1507.06432.

[117] R. Kubo and T. Toyabe, *Magnetic resonance and relaxation*, ed. R. Blink, (North Holland, Amsterdam, 1967), p.810.

[118] E. I. Kornilov and V. Yu. Pomjakushin, On a generalization of the Kubo-Toyabe formula, Phys. Lett. A **153**, 364 (1991).

[119] H. Takahashi and Y. Tanimura, Open Quantum Dynam-

ics Theory of Spin Relaxation: Application to μSR and Low-Field NMR Spectroscopies, J. Phys. Soc. Japan **89**, 064710 (2020); arXiv:2004.06994 (2020).

[120] A. Meninno and I. Errea, *Ab initio* study of metastable occupation of tetrahedral sites in palladium hydrides and its impact on superconductivity, arXiv:2209.14773, and references therein.

[121] I. Errea, M. Calandra, and F. Mauri, First-Principles Theory of Anharmonicity and the Inverse Isotope Effect in Superconducting Palladium-Hydride Compounds, Phys. Rev. Lett. **111**, 177002 (2013).

[122] J. D. Jackson, *Classical Electrodynamics* (John Wiley & Sons, New York, 1962).

[123] H. Koizumi and A. Ishikawa, Theory of supercurrent in superconductors, Intl. J. Mod. Phys. B **34**, 2030001 (2020).

[124] T. G. Saunderson, Z. Gÿorgypál, J. F. Annett, G. Csire, B. Üjfalussy, and M. Gradhand, Real-space multiple scattering theory for superconductors with impurities, Phys. Rev. B **102**, 245106 (2020)

[125] K. Park, B. Nyari,, A. Laszloffy, L. Szunyogh, and B. Ujfalussy, Spin-polarized zero-bias peak from a single magnetic impurity at an *s*-wave superconductor: first-principles study, arXiv:2109.05511 (2021).

[126] P. Rüssmann, 2 D. A. Silva, M. Hemmati, I. Klepetsanis, B. Trauzettel, P. Mavropoulos, and S. Blügel, Density-functional description of materials for topological qubits and superconducting spintronics, arXiv:2308.07383 (2023).

[127] C.-K. Chiu and Z. Wang, Yu-Shiba-Rusinov states in a superconductor with topological Z_2 bands, arXiv:2109.15227.

[128] S. Ran, C. Eckberg, Q.-P. Ding, Y. Furukawa, T. Metz, S. R. Saha, I.-L. Liu, M. Zic, H. Kim, J. Paglione, and N. P. Butch, Nearly ferromagnetic spin-triplet superconductivity, Science **365**, 684 (2019).

[129] E. I. Blount and C. M. Varma, Electromagnetic Effects near the Superconductor-to-Ferromagnet Transition, Phys. Rev. Lett. **42**, 1079 (1979).

[130] R. M. Valladares, A. J. Fisher, and W. Hayes, Path-integral simulations of zero-point effects for implanted muons in benzene, Chem. Phys. Lett. **242**, 1 (1995).

[131] E. L. Silva, A. G. Marinopoulos, R. C. Vilo, R. B. L. Vieira, H. V. Alberto, J. Piroto Duarte, and J. M. Gil, Hydrogen impurity in yttria: Ab initio and SR perspectives, Phys. Rev. B **85**, 165211 (2012).

[132] M. Manninen and P. F. Meier, Screening of impurities in semiconductors: Muonium in germanium, silicon, and diamond, Phys. Rev. B **26**, 6690 (1982).

[133] The expectation in such a system is that a finite concentration of magnetic impurities would lead to an impurity band that would widen and merge into states beyond the gap, in which case the interpretation would be a narrowing of the gap due to the impurities, and a concomitant decrease of T_c with the concentration of magnetic impurities, as is commonly observed.

[134] E. I. Blount, Symmetry properties of triplet superconductors, Phys. Rev. B **32**, 2935 (1985).

[135] Z.-Q. Bao, X. C. Xie, and Q.-F. Sun, Ginzburg-Landau-type theory of spin superconductivity, Nature Commun. **4**, 2951 (2013).

[136] A. D. Hillier, J. Quintanella, and R. Cywinski, Evidence for time-reversal symmetry breaking in the noncentrosymmetric superconductor $LaNiC_2$, Phys. Rev. Lett. **102**, 117007 (2009).

[137] J. Quintanella, A. D. Hillier, J. F. Annett, and R. Cywinski, Relativistic analysis of the pairing symmetry of the noncentrosymmetric superconductor $LaNiC_2$, Phys. Rev. B **82**, 174511 (2010).

[138] E. Morenzoni *et al.*, Muon Spin Rotation and Relaxation Experiments on Thin Films, Hyperfine Int. **133**, 179 (2001).

[139] D.-J. Choi, C. Rubio-Verd, J. de Bruijckere, M. M. Ugeda, N. Lorente, and J. I. Pascual, Mapping the orbital structure of impurity bound states in a superconductor, Nat. Comm. **8**, 15175 (2017).

[140] F. von Oppen and K. J. Franke, Yu-Shiba-Rusinov states in real metals, Phys. Rev. B **103**, 205424 (2021).

[141] H.-N. Xia, E. Minamitani, R. Zitko, Z.-Y. Liu, X. Liao, M. Cai, Z.-H. Ling, W.-H. Zhang, S. Klyatskaya, M. Ruben, and Y.-S. Fu, Spin-orbital Yu-Shiba-Rusinov states in single Kondo molecular magnet, Nature Commun. **13**, 6388 (2022).

[142] T. G. Saunderson, J. F. Annett, B. Csire, and M. Gradhand, Full orbital decomposition of Yu-Shiba-Rusinov states based on first principles, Phys. Rev. B **105**, 014424 (2022).

[143] S. H. Ji *et al.*, High-resolution scanning tunneling spectroscopy of magnetic impurity induced bound states in the superconducting gap of Pb thin films, Phys. Rev. Lett. **100**, 226801 (2008).

[144] J. Senkpiel, C. Rubio-Verdu, M. Etzkorn, R. Drost, L. M. Schoop, S. Dambach, C. Padurariu, B. Kubala, J. Ankerhold, C. R. Ast, and K. Kern, Robustness of Yu-Shiba-Rusinov resonances in presence of a complex superconducting order parameter, Phys. Rev. B **100**, 014502 (2019).

[145] S. Karan, H. Huang, A. Ivanovic, C. Padurariu, B. Kubala, K. Kern, J. Ankerhold, and C. R. Ast, Tracking a Spin-Polarized Superconducting Bound State across a Quantum Phase Transition, arXiv:2304.02955.

[146] NbYSR

[147] M. Sigrist, Broken time reversal symmetry in unconventional superconductors, Physica C **341-348**, 695 (2000).

[148] B.-J. Yang and N. Nagaosa, Classification of stable three-dimensional Dirac semimetals with nontrivial topology, Nat. Commun. **5**, 4898 (2014).

[149] A. B. Shick, V. Janis, V. Drchal, and W. E. Pickett, Spin and Orbital Magnetic State of UGe_2 Under Pressure, Phys. Rev. B **70**, 134506 (2004).

[150] A. B. Shick, S.-I. Fujimori, and W. E. Pickett, UTe_2: a Nearly Insulating Half-filled j=5/2 5f3 Heavy Fermion Metal, Phys. Rev. B **103**, 125136 (2021).

[151] A. Kapitulnik, J. Xia, E. Schemm, and A. Palevski, Polar Kerr effect as probe for time-reversal symmetry breaking in unconventional superconductors, New J. Phys. **11**, 055060 (2009).